KWAME NKRUMAH UNIVERSITY OF SCIENCE AND TECHNOLOGY, KUMASI

ANALYSIS OF MIMO ANTENNA CONFIGURATION EFFECTS ON WiMAX NETWORK DEPLOYMENT IN GHANA

BY

ERIC TUTU TCHAO

A THESIS SUBMITTED TO THE DEPARTMENT OF ELECTRICAL ENGINEERING, KWAME NKRUMAH UNIVERSITY OF SCIENCE AND TECHNOLOGY IN PARTIAL FUFILLMENT OF THE REQUIREMENT FOR THE DEGREE OF DOCTOR OF PHILOSOPHY IN TELECOMMUNICATIONS ENGINEERING

MAY 2015

DECLARATION

I hereby declare that this submission is my own work towards the award of the Ph.D degree and that, to the best of my knowledge, it contains no material previously published by another person nor material which had been accepted for the award of any other degree of the university, except where due acknowledgment had been made in the text.

Eric Tutu Tchao ....

Candidate Signature Date

Certified by:

Nana Kwasi Diawuo (Ph.D) ....

Internal Examiner Signature Date

Certified by:

Prof. P. Y. Okyere ....

Head of Department Signature Date

DEDICATION

To my Beloved Parents and the rest of my family.

ABSTRACT

Worldwide Interoperability for Microwave Access (WiMAX) technology has gained growing interest due to its applications and advantages. It is fast emerging as a last-mile problem solution for broadband access technology. This thesis presents operational scenarios for the deployment of a Fourth Generation (4G) WiMAX system in a typical Sub-Saharan African environment. The work in this research has been specified based on real world conditions considering the regulatory rules stipulated by the National Communication Authority for radio frequency spectrum utilization in the 2.6GHz licensed band in Ghana. Appropriate propagation models and network planning tools have been used to design the optimized final radio network plan for the various Multi-Input Multi-Output (MIMO) configurations.

A parameter called Interference to Noise Ratio (INR) was introduced to optimize the BER performance of the deployed 2x2 MIMO configuration in the presence of multiple interferers. The INR parameter was used to fit the BER results and then subsequently optimize the 2x2 MIMO configuration performance in the striped case to create a wide virtual bandwidth. The fitting INR parameter helped to improve the BER performance once the threshold INR was exceeded. This result extends the principle of successive decoding to MIMO systems affected by partial band interference under the assumption of a common receive correlation matrix. Unsuppressed sidelobe emissions also distort the performance of MIMO antenna systems used in deploying multicarrier networks. In order to accurately evaluate the performance of the MIMO antenna configurations used in the network deployment scenario, a mathematical model for estimating the effective beamwidth and sidelobe suppression factors for MIMO antenna systems used in multicarrier deployment scenarios was developed. The derived step function can be used to minimize the effect of antenna sidelobe emission in a realistic deployment scenario and also as an operational guideline tool to model added isolation factors. This function may provide a means to determine practical antenna sidelobe suppression factors in subsequent WiMAX deployments.

Coverage, capacity, and interference predictions have been performed using MATLAB, 4-NEC 2 and Genex-U-Net for the predefined areas of Accra and Tema, Ghana. Simulation results for different downlink/uplink ratios with different frequency reuse schemes and antenna configurations have been presented. A total of 11 base stations have been suggested to provide coverage of -92dBm using 32 sectors adaptive 4x4 MIMO antenna configuration to provide a 3dB gain over the deployed adaptive 2x2 MIMO system thereby reducing deployment cost. Finally, based on the high system performance of the evaluated network, secure communication models and network architectures have been proposed in three case study areas.

Keywords: Performance Evaluation; Capacity Simulation; Interference Modeling; WiMAX Radio Planning; Successive Cancellation Technique.

ACKNOWLEDGMENT

I would like to express my utmost gratitude and thanks to God almighty for His protection during the course of this hectic programme. I am very grateful to the Vice Chancellor, Professor W.O. Ellis, for giving me the opportunity to pursue the degree in the first place and supporting me during the period. I am eternally grateful to my supervisors, Professor Willie Ofosu, Dr. Kwasi Diawuo and Rev. Dr. J. K. Oppong, for their support and patience over the course of the programme. They provided me with the necessary guidance and the criticisms to put me on the right track. They taught me how to elevate the quality of my work and I cannot forget the hard deadlines they set for me to produce results. Once again, thank you very much.

I would also like to thank Prof. P. Y. Okyere and Mr. Okrah for their encouragement and support. Special thanks to Professor Amanquah of the Department of Computer Science at Ashesi University, Mr Francis Boaten of DiscoveryTel Ghana, and Mr Samuel Nkrumah of Huawei Technologies S.A for the many insightful discussions we had during the course of the PhD programme. I am grateful to Mr. Affum, Mr. Agyekum, Mr. Griffith Selorm Klogo, Mr Eliel Keelson, Mr Henry Abu Diawuo and Mr. Obed Fosu(Makosa) for their time and contributions. Last, and certainly not the least, I would like to express my thanks to my parents, siblings and Miss Selorm Aggor for their unlimited support and unconditional love — without you, none of this would have happened.

CONTENTS

LIST OF ABBREVIATION

3G .... Third Generations

3GPP .... Third Generation Partnership Project

4G .... Fourth Generations

ASN .... Access Service Network

B3G .... Beyond Third Generation

BER .... Bit Error rate

BS .... Base Station

CAPEX .... Capital Expenditure

CINR .... Carrier Interference plus Noise Ratio

CDMA .... Code Division Multiple Access

CPE .... Customer Premise Equipment

CSN .... Connectivity Service Network

DSL .... Digital Subscriber Line

ERP .... Effective Radiated Power

FDD .... Frequency Domain Duplexing

FDM .... Frequency Division Multiplexing

FFR .... Fractional Frequency Reuse

G.SHDSL .... Generalised High-Bitrate Digital subscriber Line

IDFT .... Inverse Discrete Fourier Transform

ISI .... Inter Symbol Interference

LTE .... Long Term Evolution

MAC .... Media Access Control

MAI .... Multiple Access Interference

MDAs .... Ministries, Department and Agencies

MIMO .... Multi Input Multiple Output

NIST .... National Institute of Standards and Technology

NRM .... Network Reference Model

NWG .... Network Working Group

OFDM .... Orthogonal Frequency Division Multplexing

OFDMA .... Orthogonal Frequency Division Multiple Access

OPEX .... Operational Expenditure

PDAs .... Personal Digital Assistants

PHY .... Physical Layer

PMP .... Point-to-Multi Point

PUSc .... Partial Usage Sub-Channelization

RRC .... Radio Resource Control

RSS .... Received Signal Strength

RTWP .... Received Total Wideband Power

SLL .... Sidelobe Level

SINR .... Signal to Noise plus Interference Ratio

SISO .... Single Input Single Output

SS ....Subscriber Station

TCP/IP ....Transmission Control Protocol/Internet Protocol

TDD .... Time Division Duplexing

TDMA .... Time Division Multiple Access

VoIP .... Voice over Internet Protocol

WiFi ....Wireless Fidelity

WiMAX ....Worldwide Interoperability for Microwave Access

WWAN .... Wireless Wide Area Networks

WirelessMAN .... Wireless Metropolitan Area Network

WISP .... Wireless Internet Service Provider

LIST OF TABLES

LIST OF FIGURES

CHAPTER 1

INTRODUCTION

1.1 OVERVIEW OF WiMAX NETWORKS

Broadband internet access is the backbone of any Information Communication Technology (ICT) system. Broadband based ICT systems helps to build an inclusive and knowledge-based society. In a knowledge-based society, people can create and efficiently share information. A knowledge-based society also helps individuals and nation states to achieve their full potential in promoting sustainable development. This in the long run helps to improve the quality of life of citizens [1]. However, broadband internet is quite expensive in many Sub Saharan African countries and as such there is a need to find an affordable technology which would provide a platform for the least privileged to have access to broadband internet access.

There are several broadband technologies available on the market. However WiMAX, which is defined as Worldwide Interoperability for Microwave Access, offers a platform which provides increased coverage and low-cost services [2]. WiMAX is a broadband internet access technology that provides wireless transmission of data using different transmission modes. The transmission mode ranges from stationary point-to-multipoint links to portable, nomadic and fully mobile internet access. This makes WiMAX a superior broadband technology in terms of coverage and network capacity [3]. The standard is defined by IEEE (Institute of Electrical and Electronic Engineers) 802.16x. WiMAX is commonly referred to as Broadband Wireless Access (BWA) by many technology industry experts. The IEEE's 802.16x family has been commercialized by the industry alliance called the WiMAX Forum [4].

WiMAX has proven to be an efficient and capable end-to-end technology that provides low deployment cost and last mile solution for enabling broadband wireless access to areas which are underserved by fixed broadband infrastructure. The IEEE 802.16 technology provides coverage of up to 48km compared to other technologies; Generalised High-Bitrate Digital subscriber Line (G.SHDSL) can cover 7 km; Wireless Fidelity (WiFi) can only cover 3km in Line of sight (LoS) deployment scenario. The unique characteristics of WiMAX allow the Base Stations to provide a collision-free Media Access Control (MAC) Uplink/downlink (UL/DL) channels and simultaneously handle thousands of Customer Premise Equipment [5]. Because of its ability to efficiently provide handover schemes and power control mechanism, it is able to support a variety of services ranging from data, legacy voice, Voice over Internet Protocol (VoIP), and Transmission Control Protocol/Internet Protocol (TCP/IP) to applications with different Quality of Service (QoS) classes. These numerous varieties of services are provided with different level of guarantees [6].

Due to the numerous advantages outlined above, the frequency bands of 2.6GHz and 3.5GHz have been allocated for fixed and mobile WiMAX deployments in Ghana. The allocated bands have been prepared for auction to bring broadband internet access to the least privileged and areas that are undeserved by the current broadband technologies [7]. When WiMAX is fully deployed in Ghana, Telecom companies will be able to leverage the superior performance of WiMAX and its open standards to provide applications and services which will cater for the increasing demand for a reliable and a high data services. Mobile broadband subscribers in Ghana will be able to enjoy services such as streaming media on the internet, live video conferencing and mobile television on their computers as well as handsets and personal digital assistants (PDAs) in the comfort of their homes.

Through field measurements and evaluations done in many countries in Europe, Asia, and in countries such as the United States, superior performance as promised by the BWA technology, such as high network capacity, greater coverage and improved quality of service with different levels of guarantees have been confirmed in [8–12]. However in many African countries, WiMAX networks have recently been deployed and there is little or no information about the performance of WiMAX in Ghana and other Sub-Saharan African countries.

In this research, we will evaluate the performance of Multi-Input Multi-Output (MIMO) configurations used in deploying a Fourth Generation WiMAX (4G-WiMAX) network in Ghana which has environmental conditions similar to many Sub Saharan African countries. Based on the field measurement results, the MIMO antenna configurations used in deploying the network under study will be optimized to enable the deployed WiMAX network meet the user demand.

1.2 PROBLEM STATEMENT AND MOTIVATION FOR THE STUDY

The objective of using appropriate technology to bridge the widening digital divide has been very difficult to implement in many developing African nations. This is mainly because the basic elements necessary for communication infrastructure investments are unavailable [13]. This has led to low concentration of mobile and fixed communication infrastructure in many African countries. According to a World Bank report released in 2005, Africa has the lowest internet users when compared to the global internet users' statistics [14]. The limited communication infrastructures that exist deteriorate faster because of the undue pressure put on them. Sections of telecommunications infrastructures in many countries in Sub-Saharan Africa have been damaged beyond repair due to inadequate funding, poor maintenance and repair culture [15]. At 2008, the broadband internet penetration rate was less than 6 percent in many Sub-Saharan African countries. Countries that were more advanced in ICT, such as South Africa, Mauritius, Kenya and Nigeria had recorded a penetration rate of 8 percent [16].

Currently, the exponential growth in technology has impacted development programs of African nations. This has translated to two activities; (i) specific nations acquiring the technologies needed for their development, and (ii) providing the necessary skills to the cadre of technicians, technologists, and engineers to not only deploy the technologies, but as well to operate and maintain them. Deployment of the technologies requires an appreciation of the environment in which the technologies will be used, and this in turn entails a good understanding of the ambient conditions and how these will impact the operational conditions of the deployed technologies. This is particularly necessary for wireless applications. Broadband internet penetration in Ghana as at December 2011 was 5.2 percent [17]. Fortunately exponential growth of broadband technology has provided many developing countries avenues to adopt the appropriate technology for development.

WiMAX, being one of these technologies, offers the platform to provide broadband internet access to Ghana and most countries in Sub-Saharan Africa as a whole, to help bridge this widening digital divide. Since 4G-WiMAX is a relatively new technology to Sub-Saharan Africa, there are bound to be problems in its initial deployment. Regulators and network operators will be interested in configuration optimization techniques which could minimize inter-network interference challenges in newly deployed networks [18].

Moreover it has been realized in evaluation of WiMAX networks deployment done in many countries abroad that factors, such as environmental/propagation conditions, spectral availability, system capacity, user mobility, noise and interference, limit the performance of wireless systems [19]. Wireless systems, by virtue of their communications channel being shared, are more prone to interference from neighbouring systems than wired systems. In any deployed wireless communication system there are many forms of interference that antenna configurations can be subjected to. Examples of these interference include co-channel interference, adjacent-channel interference, and multiple access interference [20]. In many deployed WiMAX networks, sector antennas are used.

The main reason for using sector antenna is to concentrate the emitted radio waves in a specified direction. The radiation in that directional field is called the main antenna lobe. However unwanted radiation outside the main lobe is also produced. These are known as sidelobes. The main lobe is aimed within a specific cell, but the sidelobes, and particularly the upper sidelobes, due to their angle above the main lobe can end up in neighbouring cells. These unwanted and unsuppressed emissions from the sidelobes are a major source of interference in newly deployed networks as discussed in [21].There is therefore a need to analyze the effect of antenna radiation patterns on network coverage. In Ghana radio frequency planning and coordination is generally poor. As such the unwanted emissions from the sectored antennas are likely to play a major role in the successful deployment of WiMAX networks. Of particular interest in this thesis will be the modeling of acceptable sidelobes suppression factors particular to the network under study to enhance the performance of Multi-Input Multi-Output (MIMO) systems.

Furthermore, there is also the need to provide an unbiased evaluation of WiMAX networks in a typical Sub-Saharan environment to evaluate the network performance of WiMAX technology. This will equip network operators and other internet service providers with the requisite knowledge to efficiently deploy these broadband wireless technologies in areas that are not easily accessible by other technologies. Currently, there are about thirty one (31) WiMAX sites in Ghana [22]. These deployed sites form part of a long term plan of providing broadband access to key sectors of the Ghanaian economy with WiMAX technology. Since WiMAX network would be used to plan the nation's critical network infrastructure, understanding the performance comparison of the deployed WiMAX network with other 4G technologies is important because differences in performance levels might result in redeployment of the network's BS with other technologies.

Moreover, the current cost of doing business in the Ghanaian telecommunication sector would be a major concern to regulators and industry stakeholders who would want to roll out broadband wireless services. The increase in expenditure in initial technology deployment and constant reduction in the profit margin after some few years of network deployments calls for network design optimization techniques. The network optimization techniques will be of immense benefit to radio planners and as such the various parameters used in planning a wireless network need to be evaluated to determine which design configuration minimizes cost without compromising performance.

1.3 RESEARCH OBJECTIVES

Over the past 20 years, communications have been developed rapidly from analog to digital, voice to data, narrowband to broadband and single mode to multimode with the aim of providing broader bandwidth and more diverse services. A wide range of smart terminals have emerged and mobile internet services are changing from day to day. Explosive growth in data traffic has put much pressure on network operators [23]. To that effect, a 4G-WiMAX network has been deployed in Ghana to meet the ever-increasing user demand for broadband wireless service. Scientific research methods will be used in this research to study the performance of the WiMAX network. These methods will be discussed in Chapter Three.
The general objective of this research is to evaluate the network performance of MIMO antenna configurations used in deploying a WiMAX network in Ghana. The four specific research objectives for this thesis have been outlined below:

- To provide coverage and capacity estimation for the deployed WiMAX network. These results will serve as a model for planning future network expansions.

- To provide analytical expressions and simulation results for modeling the effect of unsuppressed sidelobes emissions on the MIMO antenna configurations used for deploying the network under study. In order to effectively model the effect of interference in the network, the output of the MIMO system is analyzed. This analysis will deal with the role the antenna radiation pattern plays in producing same type interference in the network. The analysis will form the basis for choosing the appropriate sidelobes suppression values to minimize the effect of interference in the network. The derived sidelobes suppression values will be used in simulating the initial radio and optimized network plan.

- To provide indicative performance comparison of measured values in outdoor environments with the simulated results. An urban Sub-Saharan African environment will be considered in this thesis. The channel model for this environment will be modeled using the stochastic distribution of customer premise equipment in the Accra and Tema networks.

- To identify key sectors of the Ghanaian economy which can benefit from WiMAX networks deployment and design secure communication architectures for implementation.

1.4 SIGNIFICANCE OF THE STUDY

WiMAX offers a cost effective broadband access with higher degree of coverage compared to previous generations of wireless technologies in environments where it was difficult to deploy communication infrastructure due to the terrain profiles and lack of investment [10]. The coverage planning of WiMAX systems is based on precise positioning of Base Station (BS) tower and is evaluated based on signal power measurements. The accurate placement of BS with appropriate configurations provides maximum promised coverage as well as achieving Capital Expenditure (CAPEX) and Operational Expenditure (OPEX) [24]. Research on the network design for deploying high capacity WiMAX networks in environments similar to the Sub-Saharan environments has been going on for some time in recent years [25, 26]. However, there is little literature on ongoing research projects which seek to provide an optimized design for deploying highly flexible and scalable WiMAX networks to suite the peculiar Sub-Saharan African environment. The work in this research will focus on the network design and optimization of a newly deployed 4G-WiMAX network in Ghana. This research may provide the basis for choosing system configurations for deploying highly scalable WiMAX networks in Ghana and other Sub Saharan African countries.

1.5 OUTLINE OF THESIS

The thesis is structured as follows: Chapter Two presents a brief technological overview of the 802.16 standard. A review of related literature is presented. Chapter Three presents the optimization methodology which will be used in this research. The adopted processes which will be used in analyzing the various antenna configurations are discussed.

Chapter Three also discusses the assumptions and parameters used in the network simulations. A simple step function for evaluating the effect of antenna radiations in a typical multicarrier network is presented. The various selected models used in the coverage and capacity estimations are also discussed.

Chapter Four discusses the various MIMO configuration simulation results. This chapter also proposes solutions to problems that limit the network performance of the deployed MIMO systems. An optimal radio network plan, which reduces the cost of deployment from short to medium term, and appropriate network striping techniques which improves the BER performance of the deployed adaptive 2x2 MIMO configurations are presented.

Chapter Five describes the methodology used in the outdoor measurements. The results of interference, received signal strength and throughput measurement campaigns conducted that provided the basis for proposing the interference mitigation technique are presented. The field measured results of the network performance of the deployed network is compared with other documented performance of WiMAX and long term evolution (LTE) in similar environments.

Chapter Six examines potential sectors of the economy that can benefit from the

successes of the deployed WiMAX network. Secure communication models and network architectures are also presented.
Chapter Seven summarizes the major contribution of the thesis. Recommendations for future work that would enhance and complement the thesis contributions are also presented.

REFERENCES

[1] David Turahi. WSIS The Way Forward. Online:www.kus.uu.se/pdf/ publications/ICT/ Post- WSISDrTurahi, Accessed on 27/02/2013, 02 2013.

[2] D. Kim, H. Cai, M. Na, and S. Choi. Performance measurement over Mobile WiMAX IEEE 802.16e network. In *in Proc. of WoWMoM*, pages 1–8, June 2008.

[3] IEEE Standard 802.16. Part 16. Air interface for fixed broadband wireless access systems, 2004.

[4] Kamran Etemad. Overview of mobile wimax technology and evolution. *IEEE Communications Magazine*, 46:31–41, 2008.

[5] Fang Wang. Mobile WiMAX systems: Performance and evolution. *IEEE Communications Magazine*, 46:45–48, 2008.

[6] WiMAX Forum White paper. WiMAX and IMT-2000. online:www.wimaxforumn.org, 2007.

[7] NCA White paper. broadband wireless access in ghana-selection and award procedure. online:www.nca.org, 02 2014.

[8] J. Camp, J. Robinson, C. Steger, and E. Knightly. Measurement driven deployment of a two-tier urban mesh access network. In *In Proceedings of the 4th International Conference on Mobile Systems, Applications and Services (MobiSys, 06)*, pages 96–109, 2006.

[9] W. Fan, A. Ghosh, C. Sankaran, and S. Benes. WiMAX system performance with multiple transmit and multiple receive antennas. In *Proceedings of IEEE VTC07, Ireland*, pages 2807–2811, 2007.

[10] S. Liu and J. Virtamo. Performance analysis of wireless data systems with a finite population of mobile users. In *19th International Teletraffic Congress*, pages 76–82, 2005.

[11] A. Ahmadzadeh. Capacity and Cell-Range Estimation for Multitraffic Users in Mobile WiMAX. Master's thesis, University of Boras : Hogskolan, 2008.

[12] O. Grondalen, P Gronsund, T Breivik, and P Engelstad. Fixed wimax field trial measurements and analyses. In *Mobile Summit 2007, Budapest (Hungary*, pages 41–46, July 2007.

[13] Mauro F. Guillen and Sandra L. Suarez. Explaining the global digital divide: Economic, political and sociological drivers of cross-national internet use. In *84 SOC. FORCES*, page 681, 2005.

[14] U.N. Econ. Communication for Africa. Meeting the challenges of unemployment and poverty in africa. In *Economic Report On Africa*, page 252, 2005.

[15] U.N. Econ. Communication for Africa. Capital flows and development financing in africa. In *Economic Report On Africa*, page 139, 2006.

[16] Sandra C. Lee. WiMAX in africa: the new frontier. Master's thesis, the Catholic University of America, Columbus School of Law, 2008.

[17] Internet/broadband penetration statistics in Ghana. Broadband wireless access license in the 2.50GHz- 2.69GHz band selection and award procedure documentation. Online: www. Nca.org.gh, 10 2011.

[18] ECC. The analysis of the coexistence of FWA cells in the 3.4 - 3.8GHz bands.

In *European Conference of Postal and Telecommunications Administrations*, number 33, 2003.

[19] ITU-R. Prediction procedure for the evaluation of microwave interference between stations on the surface of the earth at frequencies above about 0.7 GHz. In *Tech. Rep*, page 452, 2007.

[20] WiMAX Forum White paper. TDD-TDD Interference Analysis involving Synchronized WiMAX systems. online:www.wimaxforumn.org, 09 2009.

[21] White paper. Alpha wireless antennas helps operator increase sector capacity-case study of mezon mobilusis 4G internetas. online http/:www.alphaantennas.com accessed on 18/09/2014, 09 2014.

[22] NITA Official document. WiMAX networks deployment roadmap. accessed online:www.nita.org, on 11/12/2013, 12 2013.

[23] Jyrki Penttinen. The LTE / SAE Deployment Handbook. Accessed online: http://my.safaribooksonline.com. Accessed 11/01/2012, 01 2012.

[24] Bharathi Upase and Mythri Hunukumbure. Dimensioning and Cost Analysis of Multihop Relay-Enabled WiMAX Networks. *FUJITSU Sci. Tech. J*, 44: 303–317, 2008.

[25] WiMAX forum. monthly newsletter. http:// www.wimaxforum.org. accessed on 20/02/2014, 08 2011.

[26] Special topics in computing and ICT research. Strengthening the role of ICT in development. *Fountain publishers Kampala*, 3:27–39, 2011.

CHAPTER 2

LITERATURE REVIEW

2.1 INTRODUCTION

This chapter presents a brief overview of what already exist and helps put the existing theories and knowledge into the context of the thesis. Section 2.2 presents a brief review of research works done on antenna sidelobe suppression and its relationship with optimal network planning. A review of performance evaluation of WiMAX networks in other environments is also presented. Background information on the developments leading to a successful deployment of WiMAX network in Ghana is presented in Section 2.3, and Section 2.4 concludes the chapter with a brief overview of WiMAX MIMO configuration profiles.

2.2 REVIEW OF RELATED LITERATURE

The Telecommunication Industry Association (TIA) recorded an explosion in the number of WiMAX subscribers from 1.2 million in 2009 to 37 million in 2011. The number of subscribers is further expected to increase to 80 million by the end of 2015 [1]. Industry experts are now predicting a 1000X of data increase by 2020 [2]. Encouraged by this optimism, radio planning engineers are expected to design and optimize the use of available network infrastructure and radio resources to help WiMAX and other Fourth Generation (4G) technologies achieve the objective of providing enough capacity to serve the ever increasing user demand.

Before the first WiMAX networks were deployed, sidelobe emissions from antennas of many certified vendors were considered acceptable within the overall cost benefit analysis. However, many deployed WiMAX networks have recorded degradation in network throughput [3] and capacity [4, 5] due to the presence of optimally unsuppressed emissions from antenna sidelobes. Authors in [6] recommended that since the cost in addressing the degradation caused by emissions from the upper sidelobes are high, network and radio planning engineers must model additional suppression factors to help improve the overall network performance of WiMAX antenna. Authors in [7] and [8] recorded 20% - 30% increase in network throughput and 8% - 12% increase in sector capacity after additional suppression factors were modeled for the WiMAX BS antennas. The authors in [7] developed some genetic algorithms in trying to minimize the sidelobe emission problem. They went further to simulate the network performance of the MIMO antenna with the algorithms, implemented the algorithms in a practical deployment scenario and tested the performance of network after the algorithms were implemented, and recorded 20-30% increase in network throughput. The authors in [8] also analytically modeled the coupling effects of the MIMO antenna in a mobile multihop relay WiMAX network. They went further to implement a particle swarm algorithm and measured the performance of the network in a field trial measurement, and recorded 8-12% in sector capacity. The results presented in [8] showed that network deployment of either an old WiMAX profile, thus 802.16e, or a current profile, thus 802.16j are both affected by antenna sidelobe emissions. Modeling of these emissions in [7] and [8] helped the deployed networks achieve the objective of providing greater coverage and improved network connectivity to subscribers.

Performance evaluations for WiMAX networks have also been done with the aim of improving spectral efficiency of WiMAX networks. In [9], the authors developed a coverage model for WiMAX, to estimate the downlink performances in a fixed radio channel based on the assumption of uniform traffic spread over the entire cell area. A field trial of WiMAX was carried out in the urban city of Milan, Italy with European standards operating frequency at 3.5 GHz. The advantageous feature of WiMAX, Adaptive Modulation and Coding (AMC), was tested in the field trial to evaluate spectral efficiency and coverage. The WiMAX layout used for the field trial in [9] included a BS antenna at a height of 47 meters above ground level, channel bandwidth of 3.5 MHz, 18 dBi antenna gain and two 120^0 sectored antenna. The duplexing mode for trial was FDD (Frequency Division Duplex). The Erceg model was used to evaluate the propagation path loss. Separate configuration measurements were made on antenna sectors. The major findings concluded that, coverage radius fluctuates and is firmly based on terrain and propagation environments.

Testbed measurements and field trials have also been carried out on WiMAX networks in [10–16]. The results of the field trials carried out in [10–15] were usually throughput values given at a specific receive signal strength. It is worth mentioning that all the measurements done in [10–16] were carried out in US, Europe and Asia. The authors in [16] used the results obtained in the field trials as a basis to model and optimize the network parameters to suit their environment.

Moreover, the promising performance of MIMO systems used in deploying WiMAX networks has been evaluated by simulations presented in a large number of works in [17–24]. In contrast to [17–23], in [24] Single Input Single Output (SISO) simulation results are presented in terms of physical layer data throughput including link adaptation. The impressive performance of these link techniques make MIMO systems configuration of choice for many network planners. However, there is little or no information on the performance of MIMO systems used in deploying 4G technologies under the Sub-Saharan African environment.

This research seeks to analyze the additional suppression needed to minimize the sidelobe emissions from the BS antennas which were used to deploy the network under evaluation. This work will also measure the outdoor performance of MIMO configurations used in deploying a 4G-WiMAX network in Ghana. Since the environment in many Sub-Saharan African countries are similar, the results of the field measurements in this thesis will form the basis for proposing optimized parameters for efficient network deployments under the Sub-Saharan African terrain conditions. The results in [9] imply that deploying WiMAX in an arid region, for example, will perform differently from its network performance in a tropical region and hence even though there is a lot of literature on measurements of the performance of MIMO configurations used in deploying WiMAX network out there, since the Ghanaian propagation environment is different, it is important to carry out configuration tests to come out with the correct parameters to help network operators dimension their networks to meet the basis objective of serving many users with minimum resource. As validated by results in [11], environmental conditions play an important role in network performance, and since the Sub Saharan African environmental condition is different from the conditions in [17, 18, 18, 20–24], it is also imperative for us to do an independent performance evaluation to come out with the correct performance parameters pertinent to Sub-Saharan environment to enable network operators effectively deploy WiMAX networks to afford subscribers the chance to benefit from this open standard. Even though the methodologies used in [7–9] may seem unrelated to the methodology used in this thesis, they all agree that MIMO configuration effect analysis helps to achieve the basic network dimensioning objective.

2.3 BACKGROUND STUDY OF WIMAX NETWORKS DEPLOYMENT IN GHANA

Broadband internet is quite expensive in Ghana and in most Sub- Saharan African countries. Subscribers in most African countries with high consumer demand have no option than to rely on network operators who offer poor Digital Subscriber Lines (DSL) access and long customer connection times [25]. Most broadband subscribers in Ghana are therefore eagerly waiting to enjoy the numerous advantages and service support WiMAX promises.

The first proposal for a nationwide network WiMAX deployment in Ghana was brought forward by Internet Ghana, a leading Internet and data service provider, using Navini?s Ripwave MX solution with Smart WiMAX. That would have been the first 802.16e software upgradeable network deployed in Africa but the deployment failed due to interferences and other coexistence issues with their existing WiFi networks [26].

Vodafone Ghana also followed with a pilot deployment in the 1800MHz but the interferences the WiMAX network suffered from their 3G systems led them to abandon wide scale deployment. The National Information Technology Agency (NITA) was the first institution to have successfully deployed 4G WiMAX networks on a large scale to provide connectivity for Government Ministries, Departments and Agencies in 2012 [27]. Currently DiscoveryTel Ghana (DTG) Limited is the first private operator to offer 4G-WiMAX broadband internet service in Ghana providing both mobile and fixed WiMAX services to the general public. Licenses for two more Operators have been granted and expected to begin operations by the end of 2014.

An early deployment of WiMAX networks in Ghana was greatly hindered by Radio Frequency Interferences (RFI) from other cellular networks but now steady deployments have begun. It is necessary to undertake studies to find solutions to the interference issues to enable subscribers in Ghana benefit from this promising technology.

2.4 WiMAX MIMO OVERVIEW

WiMAX uses multiple transmit and receive antennas to achieve superior performance. By using Multiple Input Multiple Output (MIMO) channels, N transmitters and M receiver antennas can be used for transmission as shown in Figure 2.1. The complex channel gain from i^{th} transmit antenna to j^{th} receive antenna is denoted by α_{ij}. The complex channel matrix which characterizes the various gains is called the channel matrix.

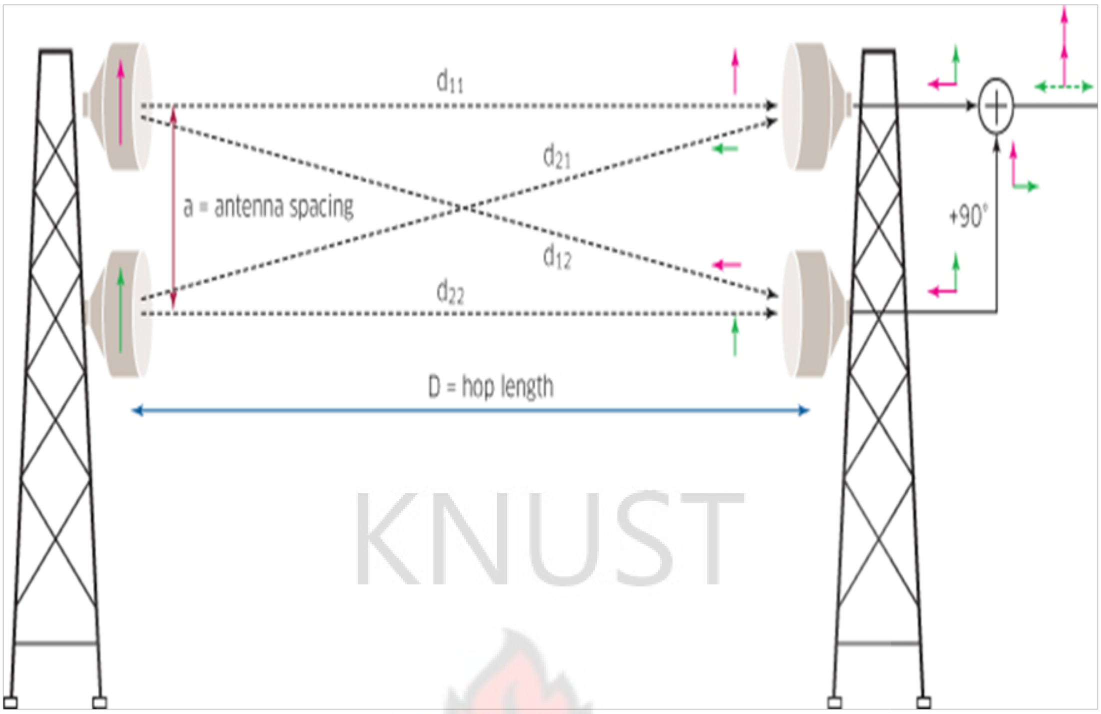

Figure 2.1: Multiple Input Multiple output Antenna

WiMAX supports three MIMO techniques for transmission, namely; MIMO A, MIMO B and MIMO C techniques. These techniques are typically segregated into two types: Closed loop and Open loop MIMO techniques.

2.4.1 Closed loop MIMO

Closed loop MIMO technique uses a feedback mechanism to transmit data in accordance with the channel quality between a transmitter and receiver [28]. WiMAX standard imposes each MS to measure channel quality for each downlink transmission from the BS, and feedback the measured channel quality to the BS in the uplink duration (along with rate requests). Based on the received channel quality, BS determines the modulation and coding scheme and MIMO technique that MS has to encode/decode for transmissions. MIMO C uses a closed loop technique [29]. By using MIMO C technique, WiMAX supports beamforming vectors to be used for transmission.

2.4.2 Open loop MIMO

Open loop MIMO techniques that do not need specific feedback from the receiver are highly supported in WiMAX networks, due to their lower complexity. The supported MIMO techniques are MIMO A and MIMO B [30]. MIMO A technique is supported to improve reliability of data transmitted in each transmission. This improvement is possible by transmitting one stream of data across multiple antennas. The receiver performs a set of combining techniques (such as Maximum Ratio Combining, Selection Combining and Equal Gain Combining techniques) to retrieve the transmitted stream (with qualities better than stream received at each antenna separately). MIMO B technique improves effective capacity of the channel between a transmitter and receiver. Each antenna at the transmitter transmits different streams of data for transmission. The receiver can decode each stream correctly if channel quality is very high. Hence, MIMO B techniques are applied only when measured channel quality is above the considered threshold (specific to the BS).

Adaptively applying these MIMO techniques is a widely studied topic. The capacity analysis which will be presented in subsequent chapters will be done using MIMO B techniques.

2.5 SUMMARY

In this chapter, the evolution and the requirements for 4G networks have been presented. A brief introduction to the MIMO techniques used by WiMAX is also presented.

The background study of the processes leading to the successful deployment of a WiMAX network in Ghana is done, and a review of related works on performance evaluation has been done. Results from the reviewed literature show that the Antenna sidelobe emissions, the MIMO configuration, and the propagation environments play an important part in the network performance of

WiMAX systems.

The next chapter presents an overview of the propagation environment and discusses the various performance evaluation methodologies. The technique which will be used for the network configuration optimization is also discussed

REFERENCES

[1] Rysavy research Whitepaper. Mobile broadband explosion. online; http:/www.rysavy.com, 01 2013.

[2] Gee Rittenhouse. A 1000x of data-technology directions in the wireless market. In *Conference proceedings, IEEE Wireless Telecommunications symposium, Phoenix, Arizona*, 2013.

[3] MTI Wireless Edge White paper. David shani-smart antenna for WiMAX base station. onlineon August 2012, 08 2012.

[4] A. Suban, Jeswill Prathima, and G. C. Suganyasree. Sidelobe Suppression and PAPR Reduction for Cognitive Radio MIMO-OFDM Systems using Convex Optimization Technique. *International Journal of Information Sciences and Techniques (IJIS)*, 4:70–75, 2014.

[5] I Georgas, I. Petropoulos, and K. Voudouris. Relay vs. repeater architectures in WiMAX. In *In Proc. of the 6th International ICST Conference on Mobile Multimedia Communications, MOBEMEDIA*, 2010.

[6] WiMAX Forum White paper. WiMAX's technology for LOS and NLOS environments. online: www.wimaxforum.org; accessed on 12/8/2014, 8 2014.

[7] White paper Alpha Wireless. Optimized antenna patterns to reduce interference in high capacity wireless networks. online http/:www.alphaantennas.com; accessed on 21/11/2014, 11 2014.

[8] I. Petropoulos, K. Voudouris, Raed A. Abd-Alhameed, and S. M. R. Jones.

Coupling Measurements of an Antenna System Suitable for Relay-Aided WiMAX Network. *Progress In Electromagnetics Research C*, 51:20–28, 2014.

[9] F Alshaalan, S Alshebeili, and A Adinoyi. On the performance of mobile wimax system: Measurement and propagation studies. *International Journal of Communication, Network and System Sciences*, 3:63–69, 2010.

[10] Y. H. Lee, H. W. Tseng, W. C. Lee, J. Y. Lin, Y. G. Jan, and H.W. Tsao. The measurement and analysis of WiMAX base station signal coverage. *Progress In Electromagnetics Research C*, 25:223–232, 2012.

[11] Jeffrey De Bruyne, Wout Joseph, LeenVerloock, and Luc Martens. Measurement and evaluation of a network performance of a fixed wimax system in suburban environments. In *conference proceeding; Wireless Communication Systems. 2008. ISWCS '08. IEEE International Symposium*, 2008.

[12] R Mardeni and T Siva Priya. Performance of path loss model in 4G WiMAX wireless communication system in 2390 mhz. In *In Proc. of International Conference on Computer Communication and Management*, pages 55–61, 2011.

[13] K.Majewski, U. Tuerke, X.Huang, and B.Bonk. Analytical cell load assessment in OFDM radio networks. In *in Proceedings of the 18th Annual IEEE International Symposium on Personal, Indoor and Mobile Radio Communications (PIMRC 07)*, pages 120–124, 2007.

[14] M. Tanno, Y. Kishiyama, N. Miki, K. Higuchi, and M. Sawahashi. Evolved UTRA - physical layer overview. In *in Proc. IEEE 8th Workshop on Signal Processing Advances in Wireless Communications 2007 (SPAWC 2007)*, 2007.

[15] J. J. Sanchez, D. Morales-Jimenez, G. Gomez, and J. T. Enbrambasaguas.

Physical layer performance of long term evolution cellular technology. In *in Proc. 16th IST Mobile and Wireless Communications Summit 2007*, 2007.

[16] T. Tang and R. Heath. Opportunistic feedback for downlink multiuser diversity. *IEEE Communications Letters*, 9:948–950, 2005.

[17] C. Hoymann. Analysis and performance evaluation of the OFDM-based metropolitan area network IEEE 802.16. *Computer Networks*, 49:341–363, 2005.

[18] M. A. Hasan. Performance evaluation of WiMax/IEEE 802.16 ofdm physical layer. Master's thesis, Helsinki University of Technology, Department of Electrical and Communications Engineering, Communications Laboratory, 2007.

[19] P. Gronsund, P. Engelstad, T. Johnsen, and T. Skeie. The physical performance and path loss in a fixed wimax deployment. In *in Proc. International Conference on Wireless Communications and Mobile Computing 2007 (IWCMC 2007)*, pages 439–444, 2007.

[20] C. Eklund, R. Marks, K. Stanwood, and S. Wang. IEEE standard 802.16: a technical overview of the wirelessman air interface for broadband wireless access. *IEEE Communications Magazine*, 40:98–107, 2002.

[21] D. H. Cho, J. H. Song, M. S. Kim, and K. J. Han. Performance analysis of the IEEE 802.16 wireless metropolitan area network. In *in Proc. 1st International Conference on Distributed Frameworks for Multimedia Applications (DFMA 2005)*, pages 130–136, 2005.

[22] S. Ramachandran, C. Bostian, and S. Midkiff. A link adaptation algorithm for IEEE 802.16. *IEEE Wireless Communications and Networking Conference (WCNC 2005)*, 3:1466–1471, 2005.

[23] F. Wang, A. Ghosh, R. Love, K. Stewart, R. Ratasukt, R. Bachu, Y. Sun, and Q. Zhao. IEEE 802.16e system performance: analysis and simulations.

In *in Proc. 16th IEEE International Symposium on Personal, Indoor and Mobile Radio Communications (PIMRC 2005)*, 2005.

[24] M. Malkowski. -level comparison of ip-ofdma (mobile wimax) and UMTS HSDPA. In *in Proc. IEEE 18th International Symposium on Personal, Indoor and Mobile Radio Communications 2007 (PIMRC 2007)*, 2007.

[25] E.T. Tchao, W.K. Ofosu, and K. Diawuo. Radio planning and field trial measurement for a 4G WiMAX network in a sub- saharan africa environment. In *Conference proceedings, IEEE Wireless Telecommunications symposium, Phoenix, Arizona*, 2013.

[26] E.T. Tchao, W.K. Ofosu, K. Diawuo, E. Affum, and K. Agyekum. Interference simulation and measurements for a deployed 4G-WiMAX network in an urban sub-saharan african environment. *International Journal of Computer Applications*, 71:36–43, 2013.

[27] E.T. Tchao, W.K. Ofosu, and K. Diawuo. A Performance Case Study of Electronic Governance Implementation in Ghana with WiMAX Technology. *International Journal of Computer Applications*, 71:20–26, 2013.

[28] F. Rubio, D. Guo, M. L. Honig, and X. Mestre. On optimal training and beamforming in uncorrelated MIMO systems with feedback. In *Proceedings of Conference on Information Sciences and Systems*, pages 54–60, 2008.

[29] W. Santipach and M. L. Honig. Optimization of training and feedback overhead for beamforming over block fading channels. *IEEE Transactions on Information Theory*, 56:103–115, 2010.

[30] D. J. Love, J. Choi, and P. Bidigare. A closed-loop training approach for massive MIMO beamforming systems. In *Proceedings of Conference on Information Sciences and Systems*, pages 80–87, 2012.

CHAPTER 3

NETWORK PARAMETERS MODELING

3.1 PERFORMANCE EVALUATION

Wireless systems can be categorized by the coverage area they provide; these coverage areas range from the largest, macro-cells, to the smallest, femto-cells. Today, macro-cells are used to provide cellular coverage for large areas (typical radius 1 to 8 km) with low user density since they operate with relatively high transmit powers [1]. As user densities increase, smaller coverage cells are required to provide adequate system capacity through the application of frequency re-use [2]. Increasing user densities is motivating research into communication systems which can provide better reliability and performance. The work in this research aims to use scientific methods to optimize the use of radio resources in a newly deployed WiMAX network in Ghana to meet this ever increasing user demand.

For the performance evaluation of communication systems, different approaches with their individual strengths and weaknesses have been developed. Figure 3.1 compares five approaches in terms of flexibility and the degree of realism that can be achieved. The degree of realism is always closely related to the time needed for implementation.

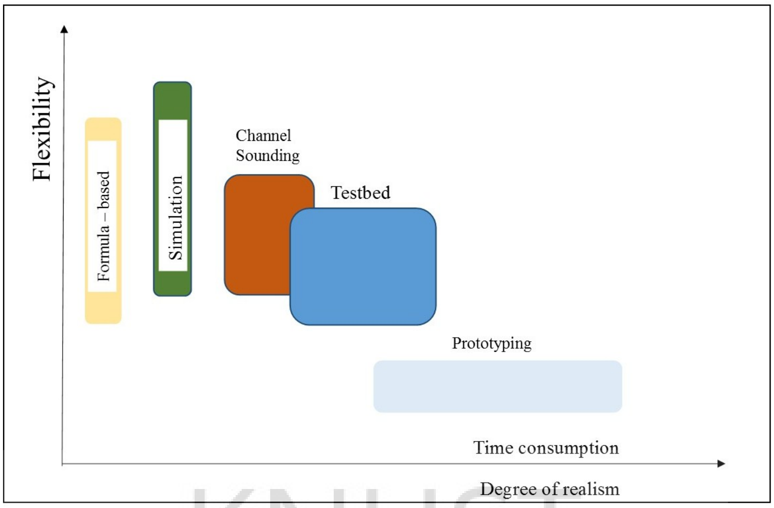

Figure 3.1: Performance Evaluation Approaches [redrawn from [3]]

For example, a prototype that requires a tedious real-time implementation offers a much higher degree of realism than a double-precision Matlab simulation. The four performance evaluation approaches shown in Figure 3.1 are:

- **Formula-based:** In the formula-based evaluation approach, the communication system is described by analytic expressions [4]. The analytic expressions give a very good insight into the dependency of the system performance on different parameters. However, modern communication systems are usually too complex to allow for closed form expressions, except for some idealized and oversimplified cases.

- **Simulation:** The simulation approach is preferred by the majority of researchers [5]. It allows the highest degree of flexibility because simulation code can be written and changed very quickly and almost without any restriction. However, simulations always rely on existing channel models that are only available for specific scenarios. If no appropriate channel model is available for the communication system under investigation, only assumptions can be made to model the channel. Also, since simulations are usually carried out in double-precision on a computer, hardly any conclusions about the feasibility of a real-time implementation are drawn.

- **Channel Sounding:** In the channel sounding approach, typical impulse responses of the wireless channel are recorded using a channel sounder [5, 6]. The channel sounder transmits specific training sequences over the wireless channel and records the corresponding receive samples. Using channel estimation techniques, the received samples are mapped in a subsequent step to impulse responses. By doing so, several effects such as time variation, jitter, or phase noise are neglected. These effects are only considered by the testbed or the prototyping approach. The impulse responses measured with the channel sounder can be directly used in simulations for the derivation of channel models which emulate the wireless channel in a deterministic way [7]. The channel sounding approach has the advantage that the results of one measurement campaign can be used in as many simulations as desired. Also, other workgroups can directly repeat a simulation by using the same measured impulse responses and/or the derived channel models. However, it turns out that carrying out channel sounding experiments requires very specialized and expensive equipment. Therefore, this equipment is usually rented for a short period of time to minimize the equipment costs of the evaluation process.

- **Testbed:** In the testbed approach, signals of the system to be investigated are directly transmitted over a wireless channel by using a testbed [8]. Compared to the channel sounding approach, the testbed approach is relatively cheaper [9], especially over longer periods of time. Also, once a testbed has been built, it allows carrying out a multitude of different measurements. For example, the impact of different base station antennas (and also their spacing) on the throughput of a transmission system can be directly investigated [10, 11].

- **Prototyping:** The prototyping approach is the most tedious of the four approaches. Although during recent years a lot of effort was put into the development of rapid prototyping methods [12, 13], the prototyping approach still requires much more time than all the other approaches.

However, since a prototype can already operate quite close to a final product, it allows drawing the most accurate conclusions about the feasibility, the complexity, and also the expected cost of an implementation.

In Ghana adherence to frequency blocks allocated to the various network service providers is a major challenge. Moreover, system deployments by the service operators are uncoordinated and as such radio frequency (RF) interference mitigation is a major deployment issue. Hence, for a meaningful physical layer performance evaluation of the deployed WiMAX network, the performance of the MIMO systems used in the presence of noise must be considered. Out of the above described evaluation approaches, the simulation and the use of commercial testbed approach, which offers a tradeoff between flexibility and a high degree of realism is used. In order to do a realistic evaluation of the impact of the different MIMO systems, this work will concentrate on the coverage, BER and throughput performance of the configuration considered in the system deployment.

3.2 RADIO NETWORK PLANNING

In order to analysis how MIMO antenna configurations affect the performance of the deployed network, the network dimensioning processes which will be used in this thesis has to be discussed. As presented by authors in [14], the main aim of the network topological design process is to come out with an efficient connectivity matrix using an aspect of mathematics called graph theory. The connectivity matrix helps to optimally locate network infrastructure and resources using a theoretical approach. The main objective of the network dimensioning process in this thesis is to evaluate the various MIMO antenna configurations and determine the number of BS required in providing coverage and capacity to deliver the needed quality of service when the MIMO antenna configurations are deployed. Certain aspects of the dimensioning process will also analyze the economic information concerning costs in using two MIMO configurations in deploying a 4G-WiMAX network under the Ghanaian radio environment. This in turn will provide a basis for network configuration optimization.

The network dimension process which determines the sizes and the type of system configurations needed to achieve the network objective is usually done after network survey and all the technical requirements and specifications of the network have been identified. This information is then used as input in the preliminary network design, which includes the preliminary distribution of base station (BS) sites in service areas and preliminary BS configuration. The output of the dimensioning phase which is part of the network synthesis stage has an effect on the long term and short term business planning phase in any deployment environment. It essentially assists in the business planning and budget planning process and allows an investor to identify the best proposed strategy and understand the likely return on investment. The benefit of a good network dimensioning design is its ability to provide a diversity of strategies that address the crucial issues such as the reduction of capital and operational expenditures [15]. These issues are crucial as earlier attempts to deploy WiMAX networks in Ghana failed due to high startup costs. This chapter discusses the network dimensioning process and the analytical models which will be used to effectively analyze the effect of the MIMO configurations.

3.2.1 Network Dimensioning Process and Design

The network evaluation and optimization methodology which will be used in this research uses an iterative process. This process uses Key Performance Indicators (KPI) and system configuration parameters such as antenna radiation pattern, network coverage, and capacity as input in the network synthesis stage to derive a radio network plan. The network realization stage will use input information such as the economic information concerning the cost the various network components. This economic information and the acquisition of external data will be the basis for deriving the business plan. The technical details of WiMAX network which will help the deployed network achieve acceptable KPI values will be obtained analogously from experienced field engineers. As part of the network realization analysis, theoretical and technological expertise will be obtained during the initial feasibility studies in the deployed network under evaluation.The dimensioning process is shown in Figure 3.2.

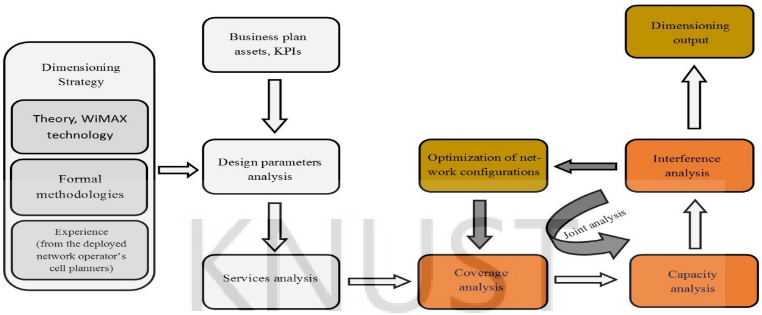

Figure 3.2: Network Dimensioning Methodology

The first step which will be taken will be to obtain all the necessary information on the configurations which will be used in the process to perform the coverage analysis.

The coverage analysis will be performed in order to make sure that the variation between theoretical and simulation results is minimized. This will ensure that the final deployed network will provide the required coverage during the actual network deployment. The feasibility studies which involve surveying the sites locating potential sites will ensure that after the coverage analysis, the potential users in the network area understudy will be identified. A particle swarm optimization algorithm which is incorporated into the planning tool will help to optimally estimate the number of BS number required to give ubiquitous coverage. The locations of BS will be done with the aim of providing the required network capacity derived using the subscriber densities and user profiles in the network synthesis stage. The output of this stage is an efficient connectivity matrix which is able to provide the required number of BS to achieve the simulated network capacity. The simulated number of WiMAX sites will form the basis for selecting the MIMO antenna configuration of the BS in initial network analysis. After the topological design, network synthesis and network realization stage, the results of the selected configurations would be evaluated followed by network configuration optimization is the acceptable KPI values are not achieved. The network coverage and system capacity analysis will be done iteratively to produce the final optimized MIMO configuration for the Ghanaian environment.

The MIMO configurations effects on the network deployment will be analyzed using various parameters such as BER estimates, coverage, and capacity. This analysis will use analytical methods to model the effect of selected antenna parameters on interference, coverage and capacity. Simulation and field trial measurements will be used to test the various models to derive the optimized MIMO configuration for the Ghanaian environment. The main aim of determining the effects of MIMO configurations used in planning the WiMAX network under study is to provide the knowledge to pave a way towards rapid nationwide deployment of cost effective and high capacity 4G-WiMAX networks. In the context of this thesis, since the network has already been deployed on a pilot basis, the dimensioning process seeks to retrace the steps using data and information provided by the radio planning engineers in the initial planning process and propose the best MIMO antenna configuration which could help in deploying a nationwide high capacity 4G-WiMAX network.

The aim in the initial planning process of the pilot network was to provide ubiquitous coverage to offer broadband access for users in the urban centers of Accra and Tema. In order to achieve this aim, knowledge about wireless communication theory, technology standard, equipment together with topology and demographics are important prerequisites. Furthermore, knowledge and experience with the radio planning tool is also important. The service area of the pilot network with its user distribution is shown in Figure. The users in the network are mainly in ministries, departments and agencies (MDAs). The locations were derived by plotting the coordinates of the MDAs on a map and as such Figure 3.3 represents a realistic distribution of the target users.

From the deployed network operator's point of view, ubiquitous coverage provided by minimum number of base stations is desirable. This will make the system more cost efficient. In urban areas, that is the area under survey, wireless communication systems are often capacity limited rather than range limited. Increasing the number of Base Stations in an area where it is expected to be coverage limited is thus a countermeasure.

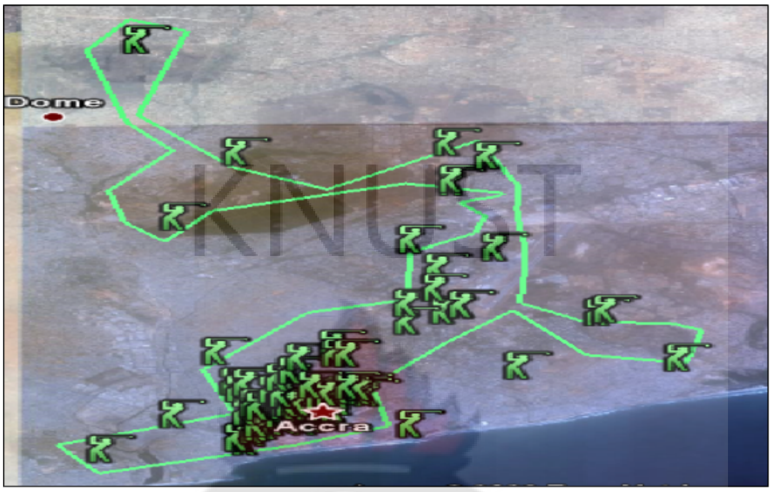

Figure 3.3: Distribution of users to be covered by the deployed network

Building the WiMAX network under study demanded some level of radio planning in order to deliver acceptable services while keeping the business aspect intact. An important feature in the way of planning the network was to create a good business case, and a reliable budget. Furthermore, a reliable and robust access solution and backhaul were required to provide high quality services to the users. The network planning alone served one purpose; to satisfy the coverage and capacity requirements in order to deliver the promised services of high speed media streaming on the internet and live video conferencing. During the preliminary planning, a thorough analysis setting up the user requirements to match expectations in the business case was done.

The next phase of the thesis deals with the major task of analyzing the deployed MIMO antenna configurations to make sure that the system will deliver as keenly anticipated by users of the network. The previous chapter has already discussed the various technological requirements of WiMAX. The theories, assumptions and various models which will be used in the dimensioning process will therefore be discussed in this chapter. In order to effectively model the network, the next section reviews the role antennas play in a basic communication system and discusses the effect of antenna radiations in a multicarrier network. A simple step function will be developed to effectively model the effect of antenna emissions on network coverage. The developed step function will hopefully help to model sidelobe suppression factors to minimize the effect of interference to help plan the network to achieve greater coverage with minimum number of BS. The rest of the sections will discuss already existing coverage and capacity models which were selected for the coverage and capacity planning phase. The reasons for selecting the models are thoroughly discussed.

3.3 ANTENNA RADIATION

The basic blocks of a communication system consists of a transmitter, the channel and the receiver. The transmitter produces a signal that is modulated onto the carrier frequency. On its way to the receiver, the signal reacts with a number of obstacles and is then induced on the receiver's antenna and demodulated [16]. Obstacles in the environment cause the signal to be reflected, refracted, and/or diffracted, which attenuate the power of the signal and cause scattering and secondary waves [17]. Obstacles that are near the line of sight (LOS) path are said to obstruct the Fresnel zone and are most problematic [4].

In reality it is slightly more complicated than this. Because an antenna radiates its signal simultaneously in different directions, the signal can take many paths to the receiver. Each path may interact with the environment in a chaotically different way and arrive at the receiver delayed by some amount.

The geometry of antennas that the transmitter and receiver use emphasizes signals arriving from some directions over others. An omnidirectional antenna emphasizes signals in the azimuthal plane and de-emphasizes signals arriving from above or below [18]. A directional antenna, such as a patch panel, parabolic dish, or sector, typically emphasizes signals arriving from a single direction (lobe) within some beamwidth.

An Adaptive Antenna Systems (AAS) was used in deploying the WiMAX network under discussion. The advantage in using adaptive antennas is that, it utilizes beam forming techniques for focusing and directing the wireless signal between the base station and the receiver station. This reduces interference from other external sources and noises, as the beam is focused directly between two points. The use of these techniques provides advantages on the basis of coverage, self-installation, power consumption, frequency re-use and bandwidth efficiency. Use of beam forming techniques and MIMO under WiMAX reduces interference while increasing throughput and efficiency [19].

Even with AAS, perfect isolation is impossible and geometries that emphasize a single direction also have substantial gain in other directions as a result. Antennas used in wireless communications have unwanted upper sidelobes. Sidelobes are known sources of interference in wireless networks. When the antenna has no downtilt, the upper sidelobes travel upwards and there is little chance of interference. When downtilt is applied to the antenna as in the case of the deployed network, these unwanted upper sidelobes are now directed towards neighbouring cells as shown in Figure 3.4. This has the potential of causing interference in the network since frequency is being reused.

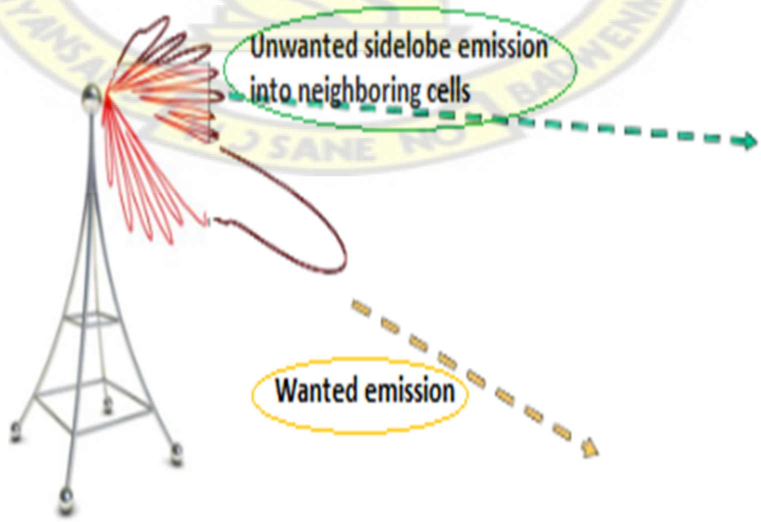

Figure 3.4: Antenna radiating pattern

The gain of an antenna is typically measured in dBi, which is decibels relative to an isotropic transmitter.

3.3.1 Radiation Pattern Modeling

The advent of technology has made the application of analytical and numerical optimization techniques to antenna design possible. Numerous works on the field of antenna array analysis and design have been presented in [20] and [21], where the relative position of the antenna elements has been optimized by particle swarm optimization (PSO) and other genetic algorithms to obtain the minimum Side-Lobe Levels (SLL) suppression factors. This part of the thesis seeks to investigate the effect of antenna sidelobe emissions on multicarrier MIMO systems when the antenna beamwidth and side lobe level are considered with respect to other system parameters using the concept of the effective radiation pattern. There are several techniques discussed in the open literature that avoid both the mutual coupling effects and the different implementation mismatches introduced by antenna sidelobe emission [22–26]. This is because it is more difficult to take into account the effects of the radio channel on the real radiation pattern due to its volatility. This work focuses on these issues and proposes a solution using a simple concept of the effective radiation pattern (ERP). The results of this solution will be used to determine appropriate sidelobe emission suppression factors. This suppression value will be used in the antenna simulation parameters to simplify the coverage analysis and yet produce realistic performance estimations during the radio planning phase later in this work.

3.3.2 Definition of Terms

The analytical solution which will be presented in the next section is developed with an assumption that the radiation pattern ($G_{real}(\varphi)$) is produced after the effect of the radio channel. Effective Beamwidth (BW_{effect}) and effective Sidelobe suppression level (SLL_{effect}) are used in the thesis to reflect the modified beamwidth and average sidelobe level of an ideal radiation pattern, if multipath is taken into consideration, both calculated via a cost function minimization that best fits the ERP with the real radiation pattern. The ERP concept also assumes beamforming capability in a real environment, that is, appropriate array geometry, the necessary number of antenna array elements, and adaptive algorithms that produce radiation patterns with the desired characteristics in terms of beamwidth and average sidelobe level.

3.3.3 Analysis of The Sidelobe Emission

In this analysis, an N element MIMO antenna system in a one tier multicarrier system assuming a frequency reuse of one is considered. The multicarrier system is shown in Figure 3.5. In the system, each BS antenna receives unsuppressed sidelobe emission from the antenna of adjacent cell BS.

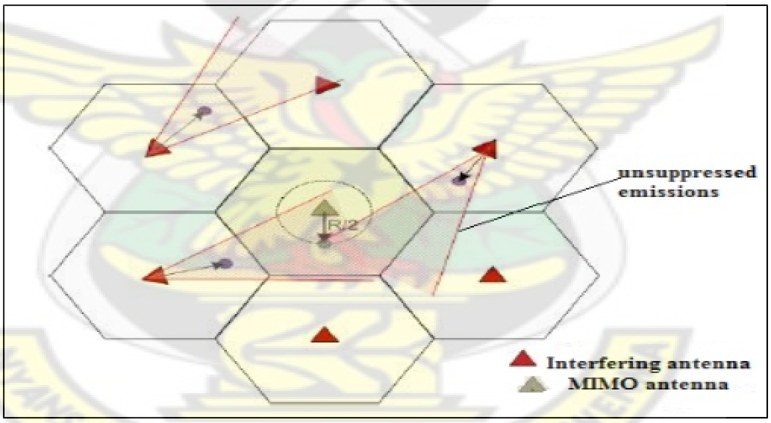

Figure 3.5: Multicarrier communication system

The BS antenna employs appropriate adaptive antenna arrays which produce effective radiation as shown in Figure 3.6.

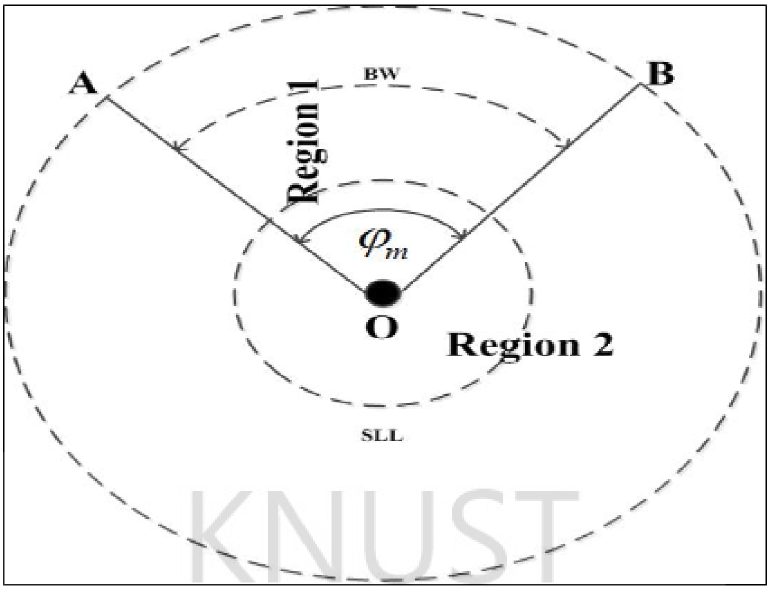

Figure 3.6: Antenna's effective Radiated Power

In measuring the gain of an antenna, authors in [27] started by modeling the azimuth (φ) radiation pattern ($G_{real}(\varphi)$) in Regions 1 and 2 by spreading the ideal antenna pattern ($G_{ideal}(\varphi)$) over the environment power azimuth pattern ($A(\varphi)$). The real radiation pattern on the antenna in Figure 3.6 can also be modeled this way by determining the convolution of the ideal radiation pattern with the environment power azimuth pattern. Using this approach, the radiation pattern can be expressed as:

$$G_{real}(\varphi) = \oint_{\varphi} G_{ideal}(\varphi).A(\varphi - \varphi_0)d\varphi \tag{3.1}$$

Following the approach in [28], the best way to model the power azimuth spectrum (PAS) around the base station for urban environments is to find the Laplacian distribution (LD). The LD of the environment power azimuth $A(\varphi)$ can be solved as:

Let $f(\varphi) = A(\varphi - \varphi_0)$

Then LD of $f(\varphi)$ denoted as $F(s) = \oint_0^{\infty} f(\varphi)e^{-(\varphi-\varphi_0)\sigma}d\varphi$ which implies $F(s) = \oint_0^{\infty} A(\varphi - \varphi_0).e^{(-\varphi-\varphi_0)\sigma}d\varphi$

$$F(s) = \frac{1}{\sqrt{2}\sigma} e^{((-\sqrt{2}|\varphi-\varphi_0|)/\sigma)} \tag{3.2}$$

Substituting $A(\varphi)$ in Eq. (3.1) with its LD in Eq. (3.2), the antenna radiation pattern can be rewritten as:

$$G_{real}(\varphi) = \frac{1}{\sqrt{2}\sigma} \oint_{\varphi} G_{ideal}(\varphi).e^{((-\sqrt{2}|\varphi-\varphi_0|)/\sigma)} d\varphi \tag{3.3}$$

Where, σ is the angular spread (AS). Let us assume an ideal N element linear antenna array with an element distance of $\lambda/2$ and bore-sight radiation. From Figure 3.6, the ideal antenna radiation pattern ($G_{ideal}(\varphi)$) for the N array antenna can be found by solving for the area of Region 1 in Sector AOB. The ideal radiation pattern is calculated as:

$$G_i deal(\varphi) = \left| \frac{\sin(N/2)\pi\cos(\varphi)}{(N/2)\pi\cos(\varphi)} \right| \tag{3.4}$$

The impact of the environment azimuth power profile on $G_{ideal}(\varphi)$ can be calculated using Eq. (3.1)–(3.4) as follows:

$$G_i deal(\varphi) = \frac{1}{\sqrt{2}\sigma} \int_0^{\pi} \left| \frac{\sin(N/2)\pi\cos(\varphi)}{(N/2)\pi\cos(\varphi)} \right| .e^{((-\sqrt{2}|\varphi-\varphi_0|)/\sigma)} d\varphi \tag{3.5}$$

where $\varphi \in (-\pi, \pi)$.

The antenna analysis in this research consider only the upper part of the antenna array pattern; that is, $\varphi \in (0, \pi)$. The aim is to model the antenna radiation pattern diagram with an effective radiated power (ERP) given by a simple step function with the effective beamwidth (BW) and sidelobe level (SLL). From Figure 3.6, the ERP can only have two values, that is:

- The ERP=1, if the emission from the sidelobe of the antenna of the adjacent cell falls within the main lobe of the MIMO antenna (Region 1).
- The $ERP = 10^{-SLL/10}$, if the emission from the sidelobe of the BS of the adjacent cell falls outside the main lobe (Region 2).

The total amount of interference on the MIMO antenna from the sidelobe emissions depends on the number of interfering Base Station antennas having the N element MIMO antenna in their side lobe emission path. Since the antennas is uniformly distributed in the multicarrier system in Figure 3.5, the probability of ERP=1 depends only on the antenna array's main lobe beamwidth, $b = \frac{BW}{2}$. Hence, the ERP values are given as:

$$G_E RP(\varphi) = f(x)$$

$$f(x)(\varphi) = \begin{cases} 1 & \varphi \in \left[\varphi_m - \dfrac{BW}{2}, \varphi_m + \dfrac{BW}{2}\right] \\ 10^{\frac{-SLL}{10}} & \varphi \left[0, \left(\varphi_m - \dfrac{BW}{2}\right) \cup \left(\varphi_m + \dfrac{BW}{2}\right), \pi\right] \end{cases} \tag{3.6}$$

where φ_m is the pointing angle of the main lobe. In order to provide the best fit between G_{real} and G_{ERP} the BW and SLL parameters must be defined in a way that the *cosine* function given in Eq. (3.5) is minimized. As such:

$$\{BW_{effect}, SLL_{effect}\} = \underset{BW \in (0,\pi), SLL \in (a,0)}{argmin} \int_0^\pi |G_{ERP}(\varphi) - G_{real}(\varphi)| d\varphi \tag{3.7}$$

Where a is the minimum value of the side lobe level that is used to define the search area for the effective SLL. The antenna radiation patterns would be simulated with Matlab and Numerical Electromagnetic Code (4-NEC 2) and discussed in the Chapter four.

3.4 PROPAGATION ENVIRONMENT MODELING

In order to estimate the signal parameters accurately in wireless communication systems, it is necessary to estimate signal propagation characteristics in different terrain environments, such as free space, urban, suburban, country and indoor. To some extent, the communication quality is influenced mainly by the applied terrain environment [29]. Propagation analysis provides a good initial estimate of the signal characteristics.

There are two general types of propagation modeling: site-specific and site general [30]. Site specific modeling requires detailed information on building layout, furniture, and transceiver locations. It is performed using ray-tracing methods. For large-scale static environments, this approach may be viable. For most Sub- Saharan environments however, the knowledge of the building layout and materials is limited and the environment itself can change. Thus the site-specific technique is not commonly employed. Site general models provide gross statistical predictions of path loss for link design and are useful tools for performing initial design and layout of wireless systems especially under Sub-Saharan African conditions.

The Hata-Okumura model which is best suited for large cell coverage can be used to model the propagation environment for this WiMAX network. Because of its simplicity, it is a widely used model for most of the signal strength predictions in macro-cellular environment [31, 32] even though its frequency band is outside the band of WiMAX.

In order to estimate the coverage range, two existing coverage models, that is simple slope and dual slope models will be discussed to determine the best model to effective model the network understudy. The objective of the coverage range modeling which will be done in this section is not to reinvent the wheel but to use existing and well known methods to achieve the objective of dimensioning the network to provide coverage to the users with minimal number of BS. Two existing models, that is single and the dual slope pathloss models will be analyzed. Based on the terrain profile of the pilot network, one of models will be selected to do the coverage modeling. The implication of the coverage analysis will then be extended to find the range for the other sites in the network area.

3.4.1 Coverage Modeling

For the purposes of the coverage analysis, two sites in the network will be used to determine the best fit model for the coverage analysis. The coordinates of the CPEs which would be served by the two selected sites have been mapped and the distribution is shown in Figure 3.7. The selection of these two sites is based on the fact that the distribution of users in these selected sites is similar to the user distribution at the other sites in the deployed pilot network

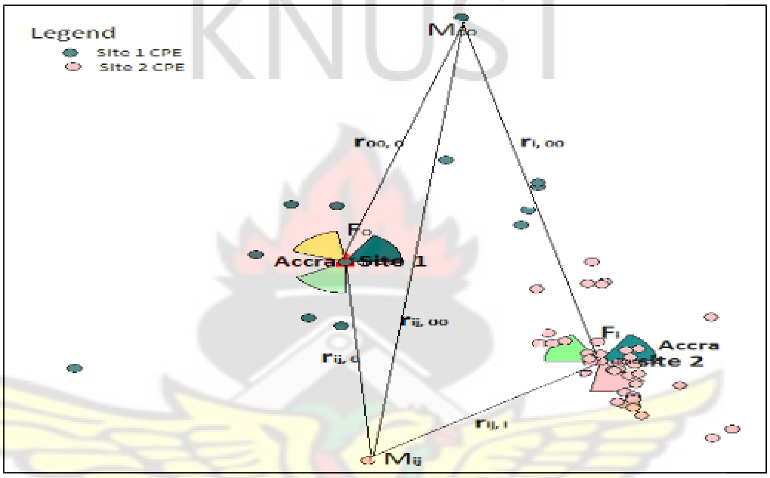

Figure 3.7: Distribution of CPEs in the pilot network

Based on the distribution of users and BS in the selected cell sites, the propagation environment will be modeled using the distribution of CPEs as shown in Figure 3.7. It consists of a fixed station F_o (site 1) and a mobile Station M_{00} attempting to establish a radio link in the presence of n additional fixed stations $F_1\{1 \leq i \leq n\}$. Each fixed station communicates with additional mobile stations. M_i is the total number of mobile stations communicating with the CPE M_{ij} at a power F_{ij} on the downlink channel.

Different propagation models are required for different environments. The simplest coverage which can be used to model the network in Figure 3.7 is the single slope pathloss model. This model is well used in literature and is expressed as [33]:

$$P_r = G_t G_r \left(\frac{d}{d_0}\right)^{\gamma} \quad d \geq d_0 \tag{3.8}$$

where P_r is the power received at a distance d (relative to the reference distance) from a transmitter radiating at a power P_t. The parameter γ is the path loss exponent (in free space) and κ is the free space path loss between the transmission antenna and the reference distance d_o:

$$\kappa = G_t G_r \left(\frac{\lambda}{4\pi d_0}\right)^2 \tag{3.9}$$

Where G_t and G_r are the antenna gains of the transmitter and receiver respectively and λ is the wavelength of the transmission. The single slope path loss model is used to describe the mean path loss in large area environments [34, 35]. Figure 3.7 shows propagation at close ranges in an urban environment. Propagation at close ranges behaves more like the plane earth model and a dual slope path loss model can also be used. The dual slope model is also widely used in planning GSM and 3G networks. This model is expressed as [36, 37]:

$$P_r = \begin{cases} kP_t \left(\frac{d}{d_0}\right)^{-\gamma_1} & d_0 \leq d \leq b \\ kP_t \left(\frac{d}{d_0}\right)^{-\gamma_1} \left(\frac{d}{b}\right)^{-\gamma_2} & b \leq d \leq \infty \end{cases} \tag{3.10}$$

where b is the breakpoint distance, γ_1 is the path loss exponent before the breakpoint and γ_2 is the path loss exponent after the breakpoint. The breakpoint is related to the height above plane earth of the transmitter antenna h_t and receiver antenna h_r and is approximately given by [37]:

$$b = 4h_t h_r / \lambda \tag{3.11}$$

Equation 3.11 gives one theoretical expression for the breakpoint in the plane earth model, however the breakpoint is not well defined due to the oscillatory nature of the signal envelope in the plane earth model, and different definitions of where the breakpoint occurs gives slightly different expressions [38, 39]. Over a region of tens of wavelengths, a received signal will exhibit variation about the mean power predicted by the path loss models of Eq. (3.8) and (3.10). Measurements have consistently indicated these power variations exhibit lognormal statistics [33, 39]. This phenomenon is called lognormal shadowing and can be incorporated into either path loss model as a multiplicative factor to the path loss P_L:

$$P_r = P_L 10^{\frac{\zeta}{10}} \tag{3.12}$$

where ζ is a normally distributed dB variable with zero mean, and a standard deviation σ typically between 6 and 12 dB in macrocell systems [33]. Equation (3.12) shows that, shadowing affects both signal attenuation due to obstructions and signal amplification due to waveguide effects. At a receiver, a link will be considered successful if the signal to noise plus interference ratio $\frac{S}{N+1}$ is greater than or equal to the system protection ratio Z, otherwise an outage is deemed to occur. The region in which this threshold is maintained is the region in which radio communication is considered successful and is called the “cell”. The extent of the cell is thus a function of the radio signal and interference statistics [40]. Examining Figure 3.6, M_{00} is communicating with F_o in the presence of a single interferer F_i which spills a power P_u into the wanted uplink and P_d into the wanted downlink. A spatial analysis of link outage in the presence of an interferer but in the absence of receiver noise was presented by Cook [41] using the single slope path loss model. When the effect of receiver noise is incorporated (assuming that the same protection ratio applies to noise and interference), $M'_{oo}s$ uplink outage contour is a family of circles centered on the fixed station F_o, but the downlink outage contour is a higher plane curve [42]. Because Figure 3.6 show propagation at close range and it is not certain $r_{(ij,i)}$ is greater than the break distance (b), the best way to accurately estimate the coverage range is to introduce a parameter called the Interference to Noise Ratio (n) into the equations for both outages of the single slope pathloss model. Interference to Noise Ratio is the total interference power at a receiver divided by the receiver noise power. For a single interferer under the single slope path loss model, n at the uplink of the fixed station F_o is given by

$$n_u = \frac{\kappa P_u r^{\gamma}_{(i,o)}}{N} \tag{3.13}$$

whiles the downlink (DL) interference power n_d at the CPE M_{oo} is given by:

$$n_d = \frac{\kappa P_d r^{\gamma}_{(i,o)}}{N} \tag{3.14}$$

Using this parameter and the approach in [42], it can be shown that the equation for the uplink outage contour can be written as:

$$r^{\gamma}_{oo,o(u)} = K_u r^{\gamma}_{i,oo}\left[\frac{n_u}{n_u+1}\right] = \varphi\left[\frac{1}{n_u+1}\right] \tag{3.15}$$

and the DL outage contour equation can be written:

$$r^{\gamma}_{oo,o(d)} = K_d r^{\gamma}_{i,oo}\left[\frac{n_d}{n_d+1}\right] = \varphi\left[\frac{1}{n_d+1}\right] \tag{3.16}$$

where φ and the parameter K is given by [38]:

$$K = \frac{P_t G_t G_r W_i L_s}{Z P_i W_t}$$

where L_s is a system loss factor, P_i is the interference power, and W_i and W_t are the bandwidths of the interfering and wanted signals respectively. Since the receiver threshold of $S = [N + I]$ must be exceeded on the uplink and downlink directions in order for the duplex link to be successful, the range of the mobile terminal from any direction is the minimum of r_u and r_d. Thus the range described by Eq. (3.15) represents the cell radius regardless of the downlink conditions. Eq. (3.15) simply indicates that a CPE in the pilot network in Figure 3.7 will be covered by signals from a BS as long as $s > n$. The cell range for the pilot network would be evaluated with U-Net and presented in Chapter Four.

3.5 CAPACITY MODELING

The increasing demand for high capacity 4G networks has turned spectrum into a precious resource. For this reason, there is always a need for methods to pack more information into a small bandwidth. A particular solution is to use multiple antennas at both transmitter and receiver side. Such a system is called multiple-input multiple-output (MIMO) system. Another proposition is to reuse the frequencies. However, in real propagation environment of broadband communication systems, channel reuse causes co-channel interference which degrades MIMO channel performance.

In multi-cell deployments, such as the network under study, in order to avoid inter cell interference, directional antennas, frequency-reuse schemes and careful radio frequency (RF) planning have been employed.

As stated earlier in Section 2.4, MIMO configurations of OFDM-Based WiMAX networks can split available spectrum into a number of parallel orthogonal narrowband subcarriers. These splited subcarriers can be assigned independently to different users in a cell. Resources of an OFDMA system occupy place both in time and frequency domains thus introducing both the time and frequency multiple access [43]. OFDMA with its various subcarrier allocation schemes improves performance in multi-cell deployments by averaging the interference across multiple cells. The interference becomes a function of cell loading and can be significantly reduced by efficient scheduling. OFDMA systems are very flexible in terms of RF planning and support a variety of frequency reuse schemes. In this thesis two reuse schemes namely; fractional frequency reuse (FFR) and Partial Usage Sub-Channelization (PUSc), will be discussed. These schemes will be denoted by $N_c \times N_s \times N_f$, where:

- N_c is number of independent frequency channels in the WiMAX network
- N_s is the the number of sectors per cell
- N_f is the number of segments in exploited frequency channel.

The reuse scheme PUSC $1 \times 3 \times 3$ is shown in Figure 3.8a. The scheme uses three sector antennas and requires only one RF channel for all sectors. The scheme uses three different sets of tones for each sector of a BS thereby reducing inter-cell interference and minimizing the outage area of the cell.

This scheme also simplifies RF planning because one need only assign segments to sectors while using the same RF channel among all Base Stations. This could result in co-channel interference. Co-channel interference typically affects system configuration performance in the cell border. Authors in [44] evaluated the capacity of MIMO systems in the cell borders and realized that, the degradation in network performance at cell borders were due o the presence of recorded high CCI values.

PUSc simplifies RF planning because one need only assign segments to sectors while using the same RF channel among other base stations. Co-channel interference (CCI) becomes more critical for the users in the border areas of a cell. Authors in [44] indicated that (CCI) limits the capacity of PUSc reuse schemes in OFDMA-based networks since CCI becomes more critical for the users present in the border areas of a cell. To combat this problem, fractional frequency reuse (FFR) was proposed in [45].

Authors in [46] proposed the use of Fractional Frequency Reuse (FFR) where the network area is divided into outer and inner regions as shown in Figure 3.7b. The allocated network bandwidth is assigned to users in the two regions in such a way that the inner region uses the same sets of frequency whiles the outer region uses a reuse K scheme. Authors in [46] indicated that an optimal adjustment of the inner and outer regions results in 18-25 % improvement in network connectivity.

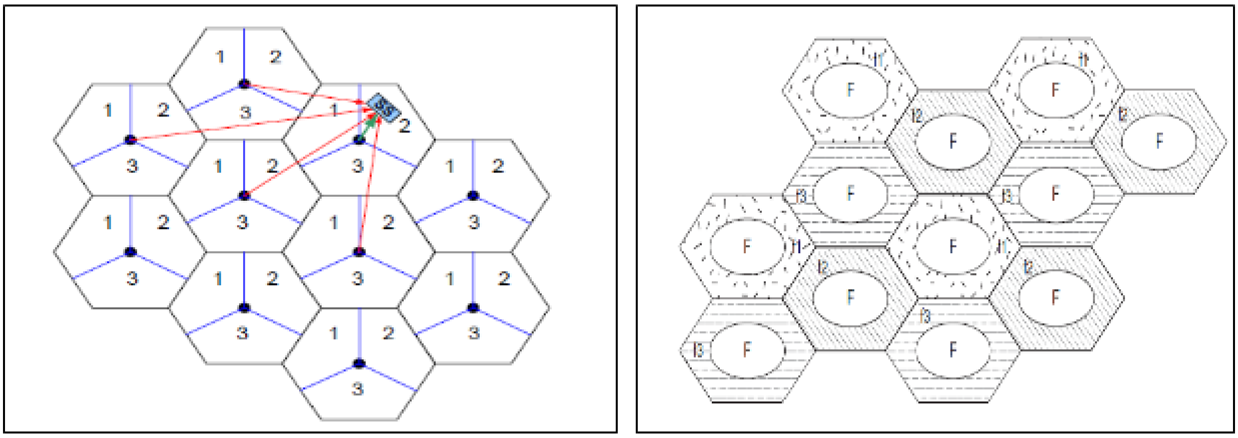

(a) PUSC (b) FFR

Figure 3.8: Frequency Reuse Schemes

Authors of [47] used system level simulation (SLS) to study the network configuration performance of an OFDMA based system and found FFR to be very useful in interference prone areas. In [48] and [49], authors used an efficient inter-cell interference mitigation algorithm to study the configuration performance of MIMO antenna systems used in deploying a city-wide data centric WiMAX application. Authors in [50] extended the works in [48]] and [49] to propose two new algorithms. The proposed algorithms helped to improve the network connectivity in the outer regions. In [51] and [52] an impressive performance of FFR was recorded in simulated and practical deployment scenarios.

From brief literature review above, it can be seen that the different frequency allocation techniques which have been analyzed by simulations and analytical models for mitigating interference were devised to mathematically evaluate these schemes. However, there remains the evaluation of these schemes under various parameters, such as, an exact dimensioning of the frequency allocation schemes and their best use in a typical WiMAX network deployment scenario. In the next subsection, the fluid model proposed in [53] which will be used to analyze the two frequency schemes, FFR $1 \times 3 \times 3$ and PUSc $1 \times 3 \times 3$, which will be considered for the WiMAX network, is discussed. The results will be implemented in the simulator to compare the two frequency allocation schemes.

3.5.1 System Modeling

This research considers a single OFDM sub-carrier in the downlink direction. In the rest of the analysis, we will consider a subscriber M_i which is connected to a Base Station F_i. The relationship between the subscriber and the BS is defined as $F_i = \Phi(Mi)$. The path gain which is equal to the inverse of the propagation pathloss between the BS and the subscriber is modeled as $g_{(F,M)} = Ar^{(-n)}_{(g(F,M))}$, where:

- A denotes the propagation constant.
- The distance between the BS and the subscriber is denoted by $r_{(F,M)}$.
- The propagation pathloss exponent is denoted by n.

The other parameters which will be used in this capacity modeling are defined below:

- The transmitted power per OFDM sub-carrier which is assumed to be constant is denoted as $P_{(Tx)}$.
- The useful received power at the subscriber station which is denoted by P_r is modeled as $P_r = P_{Tx}g_{(F,M)}$.
- The bandwidth allocated to the service area is denoted by B and the dedicated bandwidth to each subscriber station is denoted by B_{Fi}.
- The estimated cell radius, half distance between BS and coverage range are respectively denoted by R, R_c and R_u.
- The subscriber and network BS densities are denoted by P_M and P_{Fi} respectively
- The total cell capacity and the assigned data rate to each subscriber within the cell are denoted by D_T and D_u respectively.

- The total number of cell sites within the network and the number of subscribers per cell are denoted by N_{BS} and N_M respectively. The spectral efficiency is measured in bps/Hz.

The total received power at a subscriber station within the network can be split up into the useful received signal, radio interference and other external noise. Authors in [54] stated that, in the modeling of the network capacity of cellular systems, the received power could be expressed:

$$I_u = I_{int} + I_{ext} \tag{3.17}$$

where $I_{(int)}$ and I_{ext} denote the internal and external received interference respectively. The useful signal P_r is considered to be part of the internal received interference. In a typical code division multiple access network, because there is lack of complete orthogonality between the individual codes, the presence of the internal and external received noises induce inter-cell interference. OFDMA systems are able to achieve perfect orthogonality between the users and this makes OFDMA systems superior over CDMA networks. The interference factor for users in an OFDMA network is defined by authors in [55] as the ratio of total received power from other Base Stations to the total received useful power from the BS which serves the subscriber. This is modeled by the authors as:

$$f_u = \frac{I_{ext}}{I_{int}} \tag{3.18}$$

The authors in [55] stated that the interference factors, received external noise, and the received internal noise are location dependent. These parameters can be modeled at any distance from a Base Station once the interfering Base Station is known. In an OFDMA system however, I_{ext} is defined as the total received interference, and f_u is defined as the inverse of the signal to interference plus noise ratio (SINR) per sub-carrier. The capacity modeling in this section neglects the effects of noise in order to simply the analysis done in this thesis. This method of neglecting the effect of noise is employed in macro-cells network capacity modeling in dense urban areas. The SINR for a subscriber u can then be referred to as signal to interference ratio (SIR). The SIR in an OFDMA network was modeled by authors in [56] as:

$$\Upsilon_u \approx \frac{P_r}{I_{ext}} = \frac{1}{f_u} \tag{3.19}$$

Comparing Eq. (3.18) and Eq. (3.19), as soon as the orthogonality factor in a CDMA network is zero, the SIR model used in the CDMA model can be used in OFDMA networks to analyze the effect of interference on the system. The authors in [56] further modeled the SIR per sub-carrier in an OFDMA network as simply the inverse of the CDMA interference factor considered when the orthogonality is zero. This is modeled as:

$$\Upsilon_u = \frac{(r_u^{(-\eta)}(\eta - 2))}{(2\pi\rho_{BS}(2R_c - r_u)^{(2-\eta)})} \tag{3.20}$$

Eq. (3.20) estimates the SIR per subscriber with respect to the user distance r_M, away from its serving Base Station. The SIR, network capacity, and subscriber distance are user specific. As a result, the rest of the capacity modeling will omit the subscript M. The network BS density is defined as $P_{Fi} = \frac{1}{\sqrt{3}R_c^2}$. The distance parameter, r, in the rest of the analysis is normalised such that $r = r/R_c$. The SIR parameter in Eq (3.20) can be rewritten as:

$$\gamma IFR1(r) = \frac{\sqrt{3}}{\pi}(\eta - 2)(2 - r)^{(-2)}\left(\frac{2}{r} - 1\right)^{\eta} \tag{3.21}$$

The spectral efficiency (in bps/Hz) as a function of the normalized distance parameter r in a frequency reuse K scheme is given as:

$$C_{IFR1}(r) = \log_2[1 + \gamma IFRK(r)] \tag{3.22}$$

The scheduler assumed in this modeling efficiently allocates resources and guarantees fairness of throughput among subscribers within the system. The network resource is scheduled in such a way that the effective data rate per subscribers, D_u, within the network is equal. In cellular systems, the farther the distance from the BS, the lower the available capacity, and as such higher numbers of sub-carriers are allocated to users farthest from the Base Station. From Eq. (3.21) and Eq. (3.22), it can be seen that the SIR and the spectral efficiency depend on the normalized distance parameter. With the allocated bandwidth per subscriber denoted by B_u, the user data rate, D_u, can be modeled as:

$$D_u = B_u(r)C(r) \tag{3.23}$$

Under the assumption that total cell bandwidth B cannot be exceeded, that is:

$$B = \iint\limits_{(cell\ area)} B(r)\rho_u ds \tag{3.24}$$

By performing Integration operation on Eq (3.24), the network bandwidth can be modeled as:

$$B = 12\int_0^{(\pi/6)}\int_0^{(R_c/\cos\theta)} B_u(r)\rho_u r dr d\theta \tag{3.25}$$

If N_u denotes the number of subscribers in a cell, the network subscriber density can be modeled as $P_{Fi} = \frac{N_u}{\sqrt[2]{3}R_c^2}$. Using Eq. (3.23) and Eq. (3.25), the achievable subscriber data rate is modeled as:

$$B_u = \frac{\frac{\sqrt{3}B}{6}}{(N_u\int_0^{(\pi/6)}\int_0^{(1/\cos\theta)} \frac{r}{(C_{IFR1}(r))} dr d\theta)} \tag{3.26}$$

where $C_{IFR1}(r)$ is given by Eq. (3.19). Because the allocation of resources has been assumed to be fair, if there are N_u subscribers in the cell, the total cell data rate can be modeled as:

$$D_{T,IFR1} = \frac{\frac{\sqrt{3}W}{6}}{(\int_0^{(\pi/6)}\int_0^{(1/\cos\theta)} \frac{r}{(C_{IFR1}(r))} dr d\theta)} \tag{3.27}$$

It can be seen from Eq. (3.27) that $D_{T,IFR1}$ neither depends upon the number of users in the cell nor upon the distance away from the Base Station. The total cell data rate can be rewritten as:

$$D_{T,IFR1} = \frac{\frac{\sqrt{3}W}{6}}{(\int_0^{(\pi/6)} \int_0^1 (y/\cos\theta))/\cos z C_{IFR1} \frac{y}{\cos z} dy d\theta} \tag{3.28}$$

To avoid the complexity of calculating double integral, it is also possible to integrate B_u over a disk, whose area equals the hexagon area. Such a disk has a radius, $R_e = \sqrt{\frac{\sqrt{3}}{\pi R_c}}$. $D_{T,IFR1}$ can then be integrated over a disk whose area equals a hexagon area. The integrated area of the hexagonal disk has a radius R_e . The total cell data rate can subsequently be evaluated as:

$$D_{(T,IFR1)} = \frac{(\sqrt{3}W/\pi)}{\int_0^a \left(\frac{r}{C_r}\right) dr} \tag{3.29}$$

For a reuse K PUSc scheme, where the value of K is greater than one, the network capacity modeling is very similar to the reuse 1 case above. The difference lies in the fact that co-channel BS are considered in the interference calculation and thus the half-distance between BS and BS density have to be modified. As a consequence, previous analysis results are still valid provided that R_c is replaced by $\sqrt{K}R_c$ and BS density is divided by K, that is, P_{Fi} is replaced by P_{Fi}/K. Hence using Eq. (3.21), the SIR can be evaluated as:

$$\Upsilon(r) = \frac{(r^{(-\eta)}(\eta-2))}{(2\pi.\frac{\rho BS}{\kappa}(2\sqrt{K}R_c - r)^{(2-\eta)})} \tag{3.30}$$

Using the same distance normalization as before and after few manipulations, SIR can be written as:

$$\gamma_{PUSc(r)} = \frac{K\sqrt{3}}{\pi}(\eta-2)(2\sqrt{K}-r)^{-2}\left(\frac{2\sqrt{K}}{r-1}-1\right)^{\eta}$$

Hence capacity (in bps/Hz) for PUSc with reuse K can be given as:

$$C_{PUSc}(r) = \log_2[1 + \gamma IFRK(r)] \tag{3.31}$$

For total cell data rate, Eq. 3.27 is still valid provided that CIFR1(r) is replaced by Eq. 3.31 and cell bandwidth is divided by 3.

The FFR deployment scenario is depicted in Figure 3.9. As can be seen in the figure, cell space is divided into two regions, inner and outer. Inner region is a circular disc with radius R0 and rest of the hexagon space forms the outer region. Bandwidth is allocated to inner and outer in a way that former incorporates frequency reuse 1 while the latter applies frequency reuse 3. As can be seen in Figure 3.8, the network bandwidth B is equal $B = B_o + B_1 + B_2 + B_3$ to. It is also considered that $B_1 = B_2 = B_3$. SINR and capacity will be analyzed as functions of the distance to the BS. The total cell data rate can be derived assuming a scheduler fair in throughput.

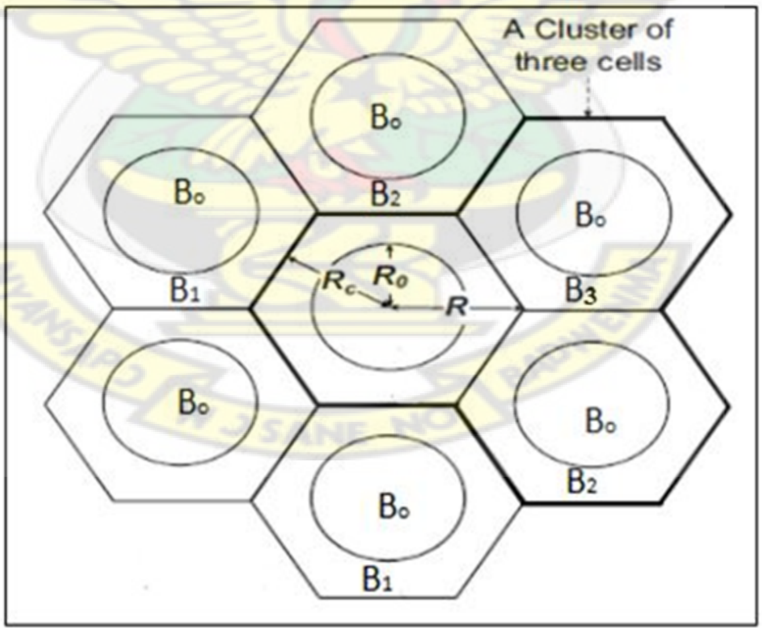

Figure 3.9: FFR Deployment Scenarios

First, considering the inner circular region since for this region, the frequency reuse is 1, the expression of SINR is given by Eq. (3.21). Once again, it is considered that users are uniformly distributed in the cell space with $P_{Fi} = \frac{N_u}{\sqrt{3}R_c^2}$.

Since it is a circular region, the elementary area can be simply taken as $2\pi r dr$ and the bandwidth of inner region is given as:

$$B_0 = \int_0^{(R_0)} B_u(r)\rho_u 2\pi r dr. \tag{3.32}$$

After replacing P_{Fi} by its value, transformation of variable r and using Eq. (3.20), we get

$$B_0 = \frac{\pi}{\sqrt{3}} D_u N_u \int_0^{R_0/R_c} \frac{r}{C_{IFR3}(r)} dr \tag{3.33}$$

where $CIFR1(r)$ is given by Eq. (3.22). Let I_0 be the integral in the previous expression, so that $B_0 = \frac{\pi}{\sqrt{3}} D_u N_u I_0$. The outer area which applies reuse 3 will be analyzed. SINR for reuse 3 is given by Eq. (3.30). In order to calculate the total bandwidth used in the outer region, double integral used in Eq. (3.25) is applied with change of limits and replacing B_u by B_1 to derive:

$$B_1 = 12 \int_0^{(\pi/6)} \int_{(R_0)}^{(R_c/\cos\theta)} B_u(r)\rho_u r dr d\theta. \tag{3.34}$$

Where B_u, assuming fairness in throughput, is given as:

$$B_u(r) = B_u C_{IFRK}(r)$$

After replacing P_{Fi} by its value and using Eq. 3.33, B_1 is derived as:

$$B_1 = \frac{6}{\sqrt{3}} D_u N_u \int_0^{(\pi/6)} \int_0^{(1/\cos\theta)} \frac{\chi}{C_{IFRK}(r)} dr d\theta. \tag{3.35}$$

Let I_1 be the double integral in the previous expression, so that $B_1 = \frac{6}{\sqrt{3}} D_u N_u I_1$. Considering the fact that total network bandwidth $B = B_o + B_1 + B_2 + B_3$ and $B_1 = B_2 = B_3$, B can be written as: $B = B_o + 3\chi B_1$ The total cell data rate DT, for the FFR case is:

$$D_{(T,FFR)} = \frac{\sqrt{3B}}{\pi I_o + 18 I_1} \tag{3.36}$$

For each target user, the throughput will be evaluated on the base of instantaneous values collected over all the Monte-Carlo trials and the results will be presented in the next chapter.

3.6 SUMMARY

Antennas with efficient sidelobe suppression techniques are very expensive. In order to reduce the initial cost of network deployment, a mathematical model for estimating the effective beamwidth and sidelobe suppression factors under a multicarrier deployment scenario has been presented in this chapter. The derived step function has been developed to be used to help minimize the effect of antenna sidelobe emission in a realistic deployment scenario. Selected analytical models which will be used in the coverage and capacity simulation stage have also been discussed. The impact of MIMO configurations on coverage and capacity, which relates to propagation conditions and frequency reuse was also discussed.

REFERENCES

[1] L. Nuaymi. WiMAX technology for broadband and wireless access. In *John Wiley, New York*, 2007.

[2] White paper. A comparative analysis of mobile WiMAX deployment alternatives in the access networks. In *WiMAX forum*, 2007.

[3] M. C. Jeruchim, P. Balaban, and K. S. Shanmugan. Simulation of communication systems: Modeling, methodology and techniques. In *2nd ed. Springer,*, 2000.

[4] L. Nissirat, M.A. Nisirat, M. Ismail, and S. Al-Khawaldeh. A terrain roughness correction factor for hata path loss model at 900 MHz. *Progress in Electromagnetics Research C*, 22:11–22, 2011.

[5] R. S. Thoma, D. Hampicke, A. Richter, G. Sommerkorn, and U. Trautwein. MIMO vector channel sounder measurement for smart antenna system

evaluation. *European Transactions on Telecommunications*, 12:427–438, 2001.

[6] L. Hentila, P. Kyosti, J. Ylitalo, X. Zhao, J. Meinila, and J. P. Nuutinen. Experimental characterization of multi-dimensional parameters at 2.45 and 5.25 GHz indoor channels. In *in Proc. International Symposium on Wireless Personal Multimedia Communication (WPMC)*, pages 254–258, 2005.

[7] J. P. Kermoal, L. Schumacher, K. I. Pedersen, P. E. Mogensen, and F. Frederiksen. A stochastic MIMO radio channel model with experimental validation. *IEEE Journal on Selected Areas in Communications*, 20:1211–1226, 2002.

[8] S. Caban, C. Mehlfuhrer, R. Langwieser, A. L. Scholtz, and M. Rupp. Vienna MIMO testbed. *EURASIP Journal on Applied Signal Processing, Special Issue on Implementation Aspects and Testbeds for MIMO Systems*, 23:20–28, 2006.

[9] R. Pabst. Relay-based deployment concepts for wireless and mobile broadband radio. *IEEE Communications Magazine*, 42:80–89, 2004.

[10] M. Rupp, S. Caban, and C. Mehlfuhrer. Challenges in building MIMO testbeds. In *in Proc. 15th European Signal Processing Conference (EUSIPCO)*, 2007.

[11] A. Yarali, J. Wheatley, J. Ponder, M. Sharifi, and H. Behrooz. Wireless cellular and pcs network cell count estimator. In *ASEE Conference at E Peoria, IL,*, 2004.

[12] B. A. Jones and J. R. Cavallaro. A rapid prototyping environment for wireless communication embedded systems. *EURASIP Journal on Applied Signal Processing*, 25:603–614, 2003.

[13] C. Mehlfuhrer, F. Kaltenberger, M. Rupp, and G. Humer. A scalable rapid

prototyping system for real-time mimo ofdm transmissions. In *In Proc. 2nd IEE/EURASIP Conference on DSP enabled Radio, Southampton*, 2005.

[14] A. Toskala H. Holma. Wcdma for umts. In *Wiley Online Library*, volume 4, 2000.

[15] A.R Mishra. Fundamentals of cellular network planning and optimization. In *Wiley Online Library*, 2004.

[16] V. Havary-Nassab, S. Shahbazpanahi, A. Grami, and Z. Q. Luo. Distributed beamforming for relay networks based on second-order statistics of the channel state information. *IEEE Transactions on Signal Processing*, 56: 4306–4316, 2008.

[17] Y. Zheng and S. Blostein. distributed beamforming through relay networks. In *in Proceedings of the IEEE GlobalTelecommunications Conference (GLOBECOM 09)*, 2009.

[18] O. Norklit, P. C. F. Eggers, and J. B. Andersen. Jitter diversity in multipath environments. *in Proceedings of the IEEE 45th Vehicular Technology Conference*, 2:853–857, 1995.

[19] K. I. Pedersen, P. E. Mogensen, and B. H. Fleury. Spatial channel characteristics in outdoor environments and their impact on bs antenna system performance. *in Proceedings of the 48th IEEE Vehicular Technology Conference (VTC 98)*, 2:719–723, 1998.

[20] C. Khodier and Christodoulou. Linear array geometry synthesis with minimum sidelobe level and null control using particle swarm optimization. *IEEE Transactions on Antennas and Propagation*, 8:2674–2679, 2005.

[21] J. Kennedy and W. M. Spears. Matching algorithms to problems: an experimental test of the particle swarm and some genetic algorithms on multi modal problem generator. In *in Proc. IEEE Int. Conf. Evolutionary Computation*, 1998.

[22] J. Zimmermann, R. Hons, and H. Muhlenbein. an evolutionary algorithm for the antenna placement problem. *Computers and industrial engineering*, 44:209–226, 2003.

[23] C. H. Hsu, W. J. Shyr, and C. H. Chen. Adaptive pattern nulling design of linear array antenna by phase-only perturbations using memetic algorithms. *Innovative Computing, Information and Control, 2006. ICICIC*, 3:308–311, 2006.

[24] V. Gunasekaran and F. C Harmantzis. Affordable infrastructure for deploying wimax systems: Mesh v. non mesh. *In IEEE Vehicular Technology Conference, 2005*, 5:2979–2983, 2005.

[25] J.K. Han, B.S. Park, Y.S. Choi, and H.K. Park. Genetic approach with a new representation for base station placement in mobile communications. *In Vehicular Technology Conference*, 4:2703–2707, 2001.

[26] S. M. Qaseem and A. A. Ali. Effect of antenna correlation and rician fading on capacity and diversity gains of wireless MIMO systems. In *International Symposium on Wireless Systems and Networks ISWSN*, volume 2, pages 25–29, 2005.

[27] P. C. F. Eggers. Angular dispersive mobile radio environments sensed by highly directive base station antennas. *In Proceedings of the 6th IEEE International Symposium on Personal, Indoor and Mobile Radio Communications (PIMRC 95)*, 2:522–526, 1995.

[28] C. M. Simmonds and M. A. Beach. Downlink calibration requirements for the TSUNAMI II adaptive antenna testbed. In *in Proceedings of the 9th IEEE International Symposium on Personal, Indoor and Mobile Radio Communications (PIMRC 98)*, pages 1260–1264, 1998.

[29] X.M. Huang and J.J. Luo. Automatic configuration and optimization of

WiMAX networks. In *In WiMAX Network Planning and Optimization*, pages 22–51, 2009.

[30] Y. Okumura. Field strength and its variability in VHF and UHF land-mobile radio-services. *Review of the Electrical Communications Laboratory*, 16:34–50, 1968.

[31] M. Hata. Empirical formula for propagation loss in land mobile radio services. *IEEE Transactions on Vehicular Technology*, 29:317–325, 1981.

[32] G.J. Foschini and M. J. Gans. On limits of wireless communications in a fading environment when using multiple antennas. In *Wireless Personal Communication*, pages 311–335, 1998.

[33] G.C. Hess. Land-mobile radio system engineering. In *Artech House, Boston*, 1993.

[34] T.S. Rappaport, S.Y. Seidel, M.J. Feuerstein, K.L. Blackard, and H.H. Xia. Path loss, delay spread and outage models as functions of antenna height for microcellular system design. *IEEE Transactions on Vehicular Technology*, 43:487, 1994.

[35] L.R. Maciel, and H.H. Xia A. Lindsay-Stewart, H.L. Bertoni, and R. Rowe. Microcellular propagation characteristics for personal communications in urban and suburban environments. *IEEE Transactions on Vehicular Technology*, 43:743, 1994.

[36] I.E.Telator. Capacity of multi-antenna gaussian channels. *European Transaction on Telecommunications*, 10:585–595, 1999.

[37] L.R. Maciel, and H.H. Xia A. Lindsay Stewart, and R. Rowe H.L. Bertoni. Radio propagation characteristics for line-of sight and personal communications. *IEEE Transactions on Antennas and Propagation*, 41:14–39, 1993.

[38] V. Erceg S. Ghassemzadeh D.L. Schilling M. Taylor, D. Li. Urban/suburban out-of-sight propagation modeling. *IEEE Communications Magazine*, 30:56, 1992.

[39] E. Green. Radio link design for microcellular systems. *British Telecom Technology Journal*, 8:85, 1990.

[40] B.C. Jones and D. J. Skellern. An integrated propagation-mobility interference model for microcell network coverage prediction. *Wireless Personal Communications*, 5:223–258, 1997.

[41] C.E. Cook. Modeling interference effects for land mobile and air mobile communications. *IEEE Transactions on Communications*, 35:151–165, 1987.

[42] B.C. Jones and D.J. Skellern. Interference modeling and outage contours in cellular and microcellular networks. In *2nd MCRC International Conference on Mobile and Personal Communications Systems, Adelaide, Australia*, 1995.

[43] G. Kulkarni, S. Adlakha, and M. Srivastava. Subcarrier allocation and bit loading algorithms for OFDMA based wireless networks. *IEEE Trans. On Mobile Computing*, 4:450–457, 2005.

[44] H. Jia, Z. Zhang, G. Yu, P. Cheng, and S. Li. On the performance of IEEE 802.16 OFDMA system under different frequency reuse and subcarrier permutation patterns. In *In Proc. of IEEE ICC*, 2007.

[45] V. Havary-Nassab, and A. Grami S. Shahbazpanahi, and Z. Q. Luo. Distributed beamforming for relay networks based on second order statistics of the channel state information. *IEEE Transactions on Signal Processing*, 56:4306–4316, 2008.

[46] IEEE document 802.11-04-172r1. The Black Box PHY Abstraction Methodology. published by Atheros, Mitsubishi, 08 2013.

[47] G. Liu, F. Jiang J. Zhu, B. Zhou, Y. Wang, and P. Zhang. Initial performance evaluation on TD SCDMA Long Term Evolution System. In *In Proceedings Of IEEE VTC*, 2006.

[48] M. C. Necker. Coordinated fractional frequency reuse. In *In Proc. of ACM MSWiM*, 2007.

[49] M. C. Necker. Local interference coordination in cellular 802.16e networks. In *In Proc of IEEE VTC*, 2007.

[50] C. He, H. Yang F. Liu, C. Chen, W. May H. Sun, and J. Zhang. Co-channel interference mitigation in MIMO OFDM system. In *In Proc. of IEEE WiCom*, 2007.

[51] C. Tarhini and T. Chahed. On capacity of ofdma-based IEEE802.16 WiMAX including adaptive modulation and coding and inter-cell interference. In *In Proc. of IEEE Workshop on LANMAN*, 2007.

[52] Mobile WiMAX-Part II. A comparative analysis. technical report. In *WiMAX Forum*, 2006.

[53] Philippe Godlewski, Masood Maqbool, Marceau Coupechoux, and Jean Marc Kelif. Analytical evaluation of various frequency reuse schemes in cellular OFDMA networks. *Telecom ParisTech*, 5:5–11, 2011.

[54] J. M. Kelif and E. Altman. Downlink fluid model of CDMA networks. In *In Proc. of IEEE VTC*, 2005.

[55] S-E. Elayoubi, O. B. Haddada, and B. Fouresti. Performance evaluation of frequency planning schemes in OFDMA based networks. *IEEE Wireless Comm. Trans*, 7:1623–1633, 2008.

[56] Y. Xiang, J.Luo, and C. Hartmann. Inter cell interference mitigation through flexible resource reuse in OFDMA based communication networks. In *in Proc. 13th European Wireless Conference EW 07*, 2007.

CHAPTER 4

MIMO CONFIGURATIONS SIMULATION

4.1 INTRODUCTION

Unsuppressed sidelobe emissions distort the performance of MIMO antenna systems used in deploying multicarrier networks. In order to accurately evaluate the performance of any MIMO antenna configurations used in a realistic network deployment scenario, these effects must be modeled and simulated. The effect of two MIMO configurations used in a practical network deployment scenarios are simulated in this chapter using the derived step function, and the selected coverage and capacity estimation models. This chapter presents simulation results and discusses the benefits in using a proposed striping technique in improving the BER performance of the chosen adaptive 2×2 MIMO antenna configurations in the presence of multiple interfering BS. This is done by exploring the proposed network striping technique and investigating the effect of varying the density fractions on the BER performance of the deployed 2×2 MIMO configuration. This chapter also seeks to determine if the alternate configuration, that is adaptive 4×4 MIMO, provides any advantage to the network optimization strategy. Finally the final radio network plans and system capacity for the two MIMO configurations are simulated employing the coverage and capacity models discussed in Chapter four in order to compare the effect of the two MIMO configurations on realistic network deployment scenarios.

4.2 ANTENNA RADIATION PATTERN SIMULATION

In this section, the derived expressions for the estimating the effective beamwidth and the sidelobe suppression factors, presented in Chapter Four, will be evaluated using simulation approach. The simulation packages are MATLAB and NEC. Following the conclusions derived in [1], the Angular Spread (AS) for a bad urban microcell radio node was chosen as 33 °. Therefore, we employed in the Laplacian distribution different AS values of the MIMO antenna and perform the analysis of Eq. (3.1)-(3.7) to model the real radiation patterns shown in Figures 4.1-4.3. The simulation parameters are summarized in Table 4.1.

Table 4.1: Antenna radiation Pattern Simulation

Frequency Range	2300 MHz $\sim$ 2700MHz
Angular Spread	0, 0.1, 10, 20 and 30
Number of elements	320 and 720
VSWR	$\leq$1.5
Input Impedance	50 Ω
Gain	18 dBi$\pm$0.5dBi
Polarization	$\pm$45°
Horizontal Beamwidth (3dB)	60$\pm$5°
Vertical Beamwidth (3dB)	7°$\pm$ 0.5 °
Electrical Downtilt	2°
Isolation Between Ports	$\geq$30dB
Front to Back Ratio	$\geq$30dB$\pm$2 dB
Cross Polarization Ratio	$\geq$18dB
Upper Sidelobe Suppression	$\geq$30dB
Null-Fill	$\leq$18dB
Max, power	250W

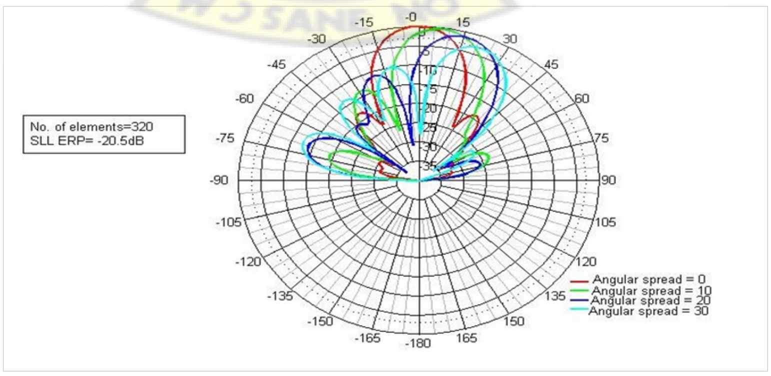

Figure 4.1: Vertical radiation Pattern, n= 320

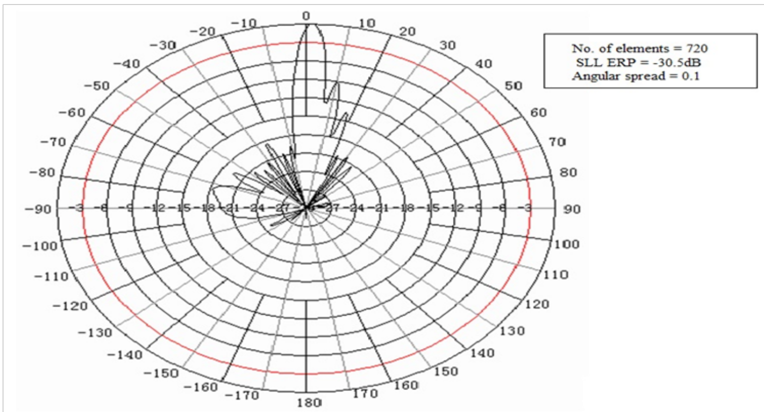

Figure 4.2: Vertical radiation Pattern; n=720

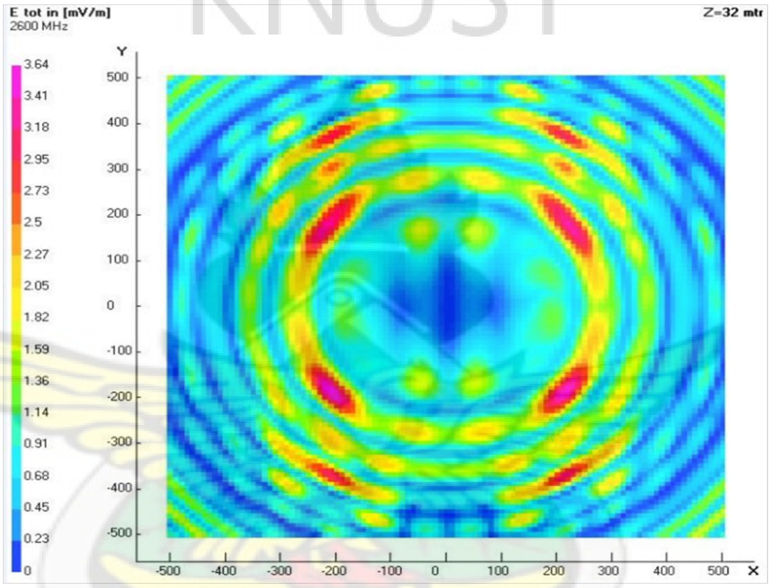

Figure 4.3: Antenna Radiation Pattern; n =720, a= - 30dB

Results of the vertical radiation patterns shown in Figures 4.1-4.3 indicates that the limiting case for the minimum value of side lobe level is when the angular spread is very low (almost zero) and the number of array elements is very large, that is n=720. From results in Figures 4.1-4.3, when the angular spread is almost 0.1 and the number of linear array elements is 720, the corresponding effective radiated sidelobe power level (a) is -30.5 dB. From these results, a value of optimal sidelobe level suppression of $\alpha \geq -30dB$ is recommended for an antenna with $n \geq 720$ for network deployment under bad urban conditions. As a result, a value of $\alpha = -30dB$ and $n = 720$ will be used to model practical deployment scenarios in this research.

4.3 COVERAGE SIMULATION

The objective of the capacity and coverage planning done by the network operator was to provide WiMAX access to both indoor and outdoor CPEs in the network with optimum number of sites to reduce initial startup cost. There are about 367 indoor and 167 outdoor CPEs which are currently on the deployed network. A distribution of these CPEs in the network enables adequate planning to find optimum locations to place antenna sites to give acceptable performance. As stated earlier, the network has been deployed using adaptive 2×2 MIMO antenna configurations. The coverage of the network will be evaluated under the deployed adaptive 2×2 MIMO scenario and other MIMO configurations. The network simulation will be done using Genex-U-Net and MATLAB in an iterative fashion. The simulation is based on a realistic distribution of CPEs in the network and the network parameters in Table 4.2. The received signal strength indicator (RSSI) results for the network have been summarized by Tables 4.3.

Table 4.2: Network Simulation

Resource frequency	2.5-2.53GHz
Channel Bandwidth	10MHz
Fast Fourier Transform (FFT) Size	1024
Average number of users per cell	10
Subcarrier spacing	10.93 kHz
Useful symbol time	91.4μs
Guard time	11.4μs
OFDMA symbol time	102.8μs
Modulation	QPSK, 16-QAM, 64-QAM
BS Antenna frequency Range	2.3-2.7GHz
Angular Spread	33 °
SLL ERP	-30dB
VSWR	$\geq$1.5
Input Impedance	50 Ω
Gain of BS antenna	18dBi
Horizontal Beamwidth (3dB)	60 °
Vertical Beamwidth (3dB)	7 °
Electrical downtilt	2 °
Maximum power	250W
Antenna height	38m
CPE antenna config.	1T2R
CPE antenna height	1.5m

Table 4.3: 3 RSSI values for CPE

Antenna config.	**SS type**	**DL traffic CINR (dB)**	**DL traffic RSSI (dBm)**	**Cell Radius (Km)**	**Site-Site Distance (Km)**
Adaptive 2 $\times$2 MIMO	USB	3	-87	0.44	0.7
	Indoor	3	-91	0.75	1.1
	Outdoor CPE	3	-92	2.99	4.5
Adaptive 4 $\times$4 MIMO	USB	3	-87	0.54	0.8
	Indoor CPE	3	-91	0.91	1.4
	Outdoor CPE	3	-92	3.61	5.4

1

From Table 4.3, it can be seen that the closer the CPE is to the BS, the greater the received power and the farther the CPE, the lower the received power. Moreover, the adaptive 4x4 MIMO configuration provides greater coverage than the deployed 2×2 MIMO configuration. From the adaptive 2×2 MIMO received power simulation results in Table 4.3 and evaluation of Eq. (3.13) and (3.14), the coverage range and the radio plan for BS F_i and F_o in the pilot network are shown in Figure 4.4 and Figure 4.5 respectively. An extension of the coverage results for the pilot network has been used to derive the final radio plan for the deployed network shown in Figure 4.6. Based on the coverage prediction in Table 4.3, fifteen sites were needed to provide coverage to the entire area using adaptive 2×2 MIMO antenna configuration as shown in Figure 4.6.

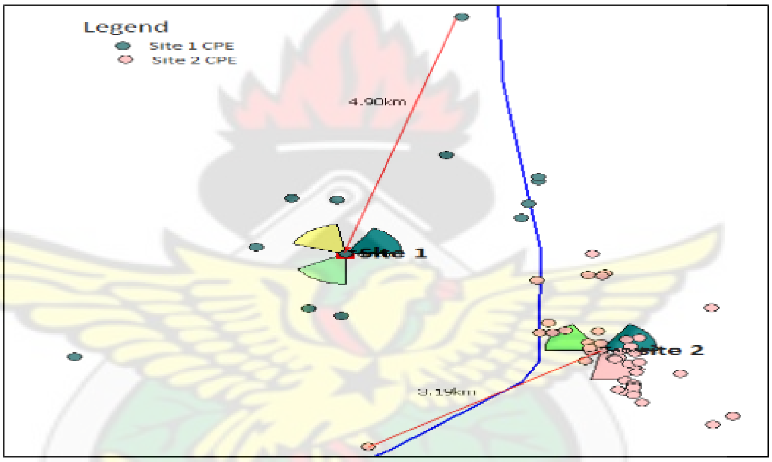

Figure 4.4: Coverage range of pilot network

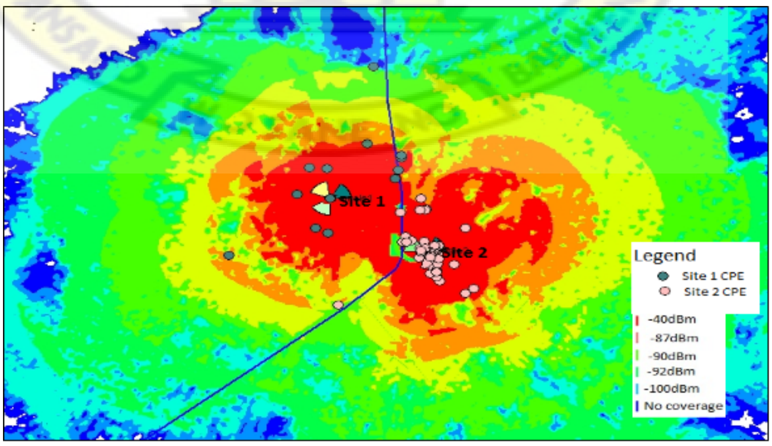

Figure 4.5: Coverage plan for the Pilot network

Figure 4.6: Coverage plan for the entire network

The main purpose of the initial planning process was to investigate and develop efficient and low cost radio access systems to provide users in an urban environment a full range of broadband services. The final radio plan in Figure 4.6 helps achieve this objective through efficient utilization of radio frequency bands and optimization of transmission capacities for the different variety of users within the pilot network. To predict the radio wave propagation in the network, the planning tool took into account the antenna radiation patterns results. Since the information used to determine the simulation parameters were obtained from the network planning engineers, the result in Figure 4.6 produces similarly structured cell plans as the one being used by the network operator. The simulated final radio plan in this thesis however achieves a coverage level above 95% as compared to the 90-92% which was derived by the network engineers during the planning stage. The increase in the coverage level could be attributed to the usage of optimally suppressed radiation pattern results in the final radio network plan. This in turn implies that the modeling of antenna sidelobe suppression factors in any multicarrier network system will maximize the overall network service level of its MIMO configuration.

4.4 CAPACITY SIMULATION

The average DL/UL throughput per sector for each user in the cell has been done using Genex-U-Net and MATLAB. The simulation is based on the network parameters in Table 4.2. The spectrum efficiency of the different MIMO configurations (in bps/Hz) under the deployed PUSc $1 \times 3 \times 3$ frequency reuse scheme is presented in Figure 4.7. This result is evaluated using the capacity models discussed in Chapter Three. The average throughput per sector under the deployment scenario for the network have been summarized in Table 4.4.

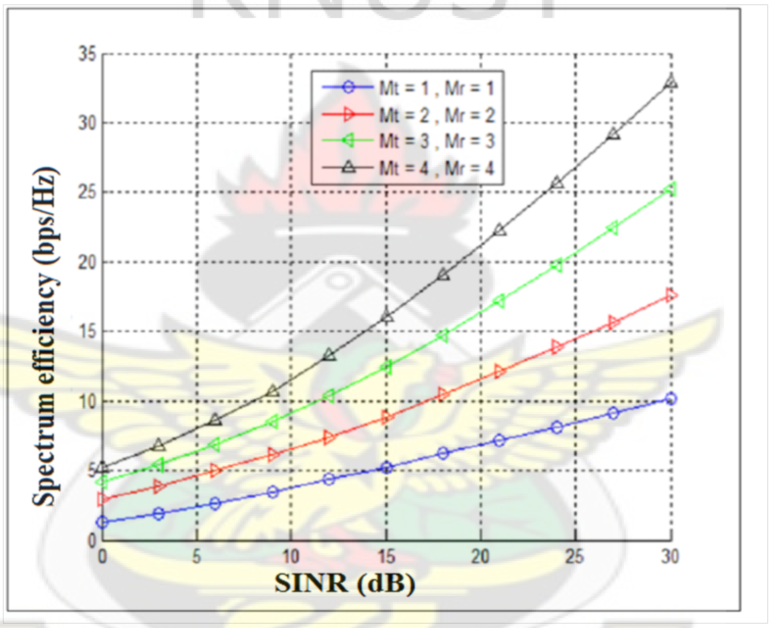

Figure 4.7: Spectrum efficiency of the different MIMO configuration

From the assumptions used to estimate the MIMO configuration capacity, the maximum error free data rate each MIMO configuration can achieve in the network under varying SNR values can be realized by multiply the spectrum efficiency (bps/Hz) value by the allocated bandwidth per sector, which is 10MHz as indicated in Table 4.2.The results in Figure 4.7 show that that the capacity of an $n \times n$ orthogonal MIMO channel is n times the capacity of the SISO channel. These results complement the work done by Zarbouti et al in comparing the theoretical and practical performance of MIMO systems in wireless communication systems [2].

Table 4.4: Capacity Simulation Results

Permutation	TDD Split Ratio	WiMAX Carrier Average Throughput per sector			
		Adaptive 2x2 MIMO (Mbps)		Adaptive 4x4 MIMO (Mbps)	
		DL	UL	DL	UL
FFR 1x3x3	26:21	5.73	2.18	5.99	2.76
FFR 1x3x3	29:18	6.64	1.81	6.93	2.3
FFR 1x3x3	31:15	7.24	1.45	7.56	1.84
FFR 1x3x3	35:12	8.45	1.09	8.82	1.38
PUSC with all SC 1x3x3	26:21	10.75	4.08	11.23	5.18
PUSC with all SC 1x3x3	29:18	12.45	3.4	13	4.32
PUSC with all SC 1x3x3	31:15	13.58	2.72	14.18	3.46
PUSC with all SC 1x3x3	35:12	15.85	2.04	16.55	2.59
PUSC 1x3x1	26:21	3.58	1.36	3.73	1.73
PUSC 1x3x1	29:18	4.15	1.13	4.33	1.44
PUSC 1x3x1	31:15	4.53	0.91	4.73	1.15
PUSC 1x3x1	35:12	5.28	0.68	5.52	0.86

From Table 4.2, the 10MHz band allocated to the network operator will have an OFDMA symbol time of 102.8microseconds. This symbol time will provide 48.6 symbols. In order to determine the symbols to be used in the TDD split (DL/UL) ratio, the symbols which would be used for the TTG (Transmit to Transmit Gap) and RTG (Receive to Transmit Gap) is catered for. 1.6 symbols out of the total are used to provide for the TTG and RTG leaving 47 symbols for the DL/UL ratio. If S of the remaining 47 symbols are used for DL as part of the TDD split ratio, then $47 - S$ symbols are available for uplink.

Based on the propagation mode, the required frequency reuse scheme and the DL/UL channel ratio are used. For a capacity limited network, a 35:12 TDD split ratio is used to serve the users in the network. When the sole purpose of the network is to cover a larger area, a DL/UL ratio of 26:21 is used. Under the adaptive 2x2 MIMO deployment scenario, the maximum average DL and UL throughput per sector are 10.75 and 4.08 Mbps respectively for a coverage limited network using a 26:21 DL/UL ratio and a PUSc 1x3x3 reuse scheme. The 35:12DL/UL split ratio is used around the Accra ministries area whiles the 26:21 split ratio is used in the Tema network. The DL/UL ratio can also be chosen based on the type of application being deployed in the network. For example, in deploying a mobile Telemedicine network which requires a higher UL throughput, a DL/UL split ratio of 26:21 is best suited for such network deployments whiles a DL/UL ratio of 36:12 can be used to deploy a network that provides online streaming services.

4.5 INTERFERENCE SIMULATION

Interference reduces the integrity of signals travelling between transmitters and receivers. In cellular networks, this can often be caused by frequency reuse; therefore, stray radiation from one cell can disrupt transmission in other nearby cells using the same frequency. As the deployed WiMAX network uses a PUSC $1 \times 3 \times 3$ frequency reuse scheme, the presence of unsuppressed sidelobes as seen from the antenna radiating pattern analysis can significantly contribute to interference in the deployed network.

In modeling the interference caused by multiple sources in a typical multicarrier system, one important practical implementation problem is that MIMO systems require knowledge of the channel conditions. Therefore, a narrowband block fading channel with η_R receiving antennas, η_T transmit antennas from an interfering source, possibly representing several different users can be characterized by [3]:

$$y = \zeta\omega + \zeta I\ \omega I + z$$

Here, $y \in \mathbb{C}^{\eta_R}$ is the received signal vector. $\omega \in C^{\eta_T}$ is the transmitted complex Gaussian distributed signal vector with zero mean and covariance $\Im = E[\omega\omega^{\zeta}], \omega_I \in C^{\eta_I}$ is the interfering complex Gaussian distributed signal vector with zero mean and covariance $\Im_I = E[\omega_I\omega_I^{\zeta}]$, and $z \in C^{\eta_R}$ is additive zero-mean white noise with entries $z_a \sim N_c(0,1)$. The channel matrices $\zeta \in C^{\eta_R \times \eta_(T)}$ and $\zeta_I \in C^{\eta_R \times \eta_I}$ have been modeled separately for correlated Rician fading. Thus, they can be written as

$$\begin{cases} \zeta = \bar{\zeta} + \rho^{1/2}\zeta_\omega \Psi^{1/2} \\ \zeta = \bar{\zeta}_I + \rho_I^{1/2}\zeta_{\omega,I}\Psi_I^{1/2} \end{cases} \tag{4.1}$$

Where $\bar{\zeta}$ and $\bar{\zeta_I}$ represent the mean values of ζ and ζ_I, respectively, and are related to the presence of LOS components, $(\zeta_\omega)_{ab}, (\zeta_{(w,I)})_{ab} \sim N_c(0,1)$, and the positive semidefinite matrices $\Psi(\Psi_I)$ and $\rho(\rho_I)$ are the transmit signal (interference) and receive signal (interference) spatial correlation matrices respectively. The covariance between the different entries of ζ and ζ_I satisfies the identities

$$\begin{cases} \mathrm{cov}((\zeta)_{ij}(\zeta)_{i'j'}) & = (\rho)_{ii'}(\Psi)^*_{jj'} \\ \mathrm{cov}((\zeta_I)_{ij}(\zeta_I)_{i'j'}) & = (\rho_I)_{ii'}(\Psi_I)^*_{jj'} \end{cases} \tag{4.2}$$

Extending these to multiple interfering transmitters, as in the case in the network under discussion, Eq. (4.1) can be applied to model multiple interfering transmitter under the assumption of a common receive correlation matrix for each interfering source. Indeed, assume that there are N_I interfering users, so that the channel of the interferer is $i(i = 1, \cdots, N_I)$ of the form $\zeta_I^i = \bar{\zeta}^i + \rho^{1/2}W^i\Psi_I^{i\ 1/2}$ and $y = \zeta\omega + \Sigma_{i=1}^{N_I}\zeta_I^i\omega_I^i + z$. Setting $\omega \triangleq [\omega_I^{1\ T}, \cdots, \omega_I^{N_I^T}]^T$,
$\Psi \triangleq \bigoplus_{i=1}^{N_I}\Psi_I^i$, $W \triangleq [W^1, \cdots, W^{N_1}]$, and $\bar{\zeta} \triangleq [\bar{\zeta}^1, \cdots, \bar{\zeta}^{N_1}]$, different receive

correlation matrices for the interfering transmitter can be modeled by introducing virtual delays in combination with a wideband channel model as proposed in [4–6]. Following the approach in [7] the covariance matrices are defined as:

$$\begin{cases} \grave{\zeta} \triangleq \bar{\zeta}\Im^{1/2}\grave{\Psi} & = \Psi^{1/2}\Im\Psi^{1/2} \\ \grave{\zeta}_I \triangleq \bar{\zeta}_I\Im_I^{1/2}\grave{\Psi}_I & = \Psi_I^{1/2}\Im_I\Psi_I^{1/2} \end{cases} \tag{4.3}$$

The transmitted signal and interference covariance matrices are implicitly accounted for in $\grave{\zeta}, \grave{\zeta}_I, \grave{\Psi}$ and $\grave{\Psi}_I$. According to these definitions, the total received power is given by [8]

$$E[\|y\|^2] = \|\grave{\zeta}\|^2 + tr(\rho)tr(\grave{\Psi}) + \|\grave{\zeta}_I\|^2 + tr(\rho_I)tr(\grave{\Psi}_I) + n_R$$

Splitting the total received power components into direct and diffused parts, the Rician factors K and K_1 are:

$$K = \frac{\|\grave{\zeta}\|^2}{(tr(\rho)tr(\grave{\Psi}))} \qquad K_I = \frac{\|\grave{\zeta}_I\|^2}{tr(\rho_I)tr(\grave{\Psi})_I} \tag{4.4}$$

Then signal-to-noise and interference-to-noise power ratios can be defined as:

$$\begin{cases} SNR = \dfrac{(K+1)tr(\rho)tr(\grave{\Psi})}{\eta_R} \\ INR = \dfrac{(K_1+1)tr(\rho)tr(\grave{\Psi}_1)}{\eta_R} \end{cases} \tag{4.5}$$

The definitions of the Rician factors and of the SNRs in Eq. (4.4) and (4.5) depend on the full transmit covariance matrices $\sqsupset$ and $\sqsupset_I$ and not only on their traces, unless they are proportional to the identity matrix. This will be an issue when the channel capacity of the MIMO channel in the presence of multiple interferers is evaluated against the SNR.

The results in Eq. (4.5) would be evaluated to compare the various MIMO configurations BER performance in the presence of multiple interferers. In order to make sure that the results are statistically significant and allow for the different

MIMO configurations to be compared in a fair manner, a Monte Carlo approach has been used to model the BER performance of a BS in the presence of 5 and 10 interfering Base Stations. The results of the simulations have been shown in Figure 4.8 and Figure 4.9.

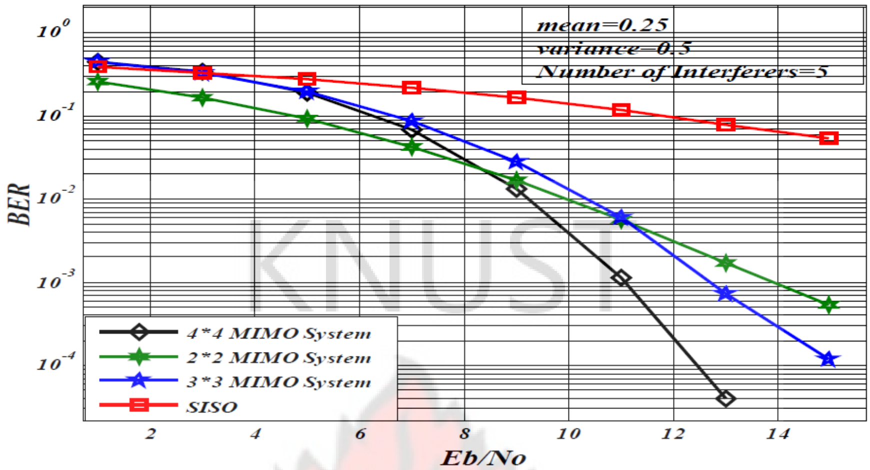

Figure 4.8: Performance of MIMO System in the presence of 5 interferers

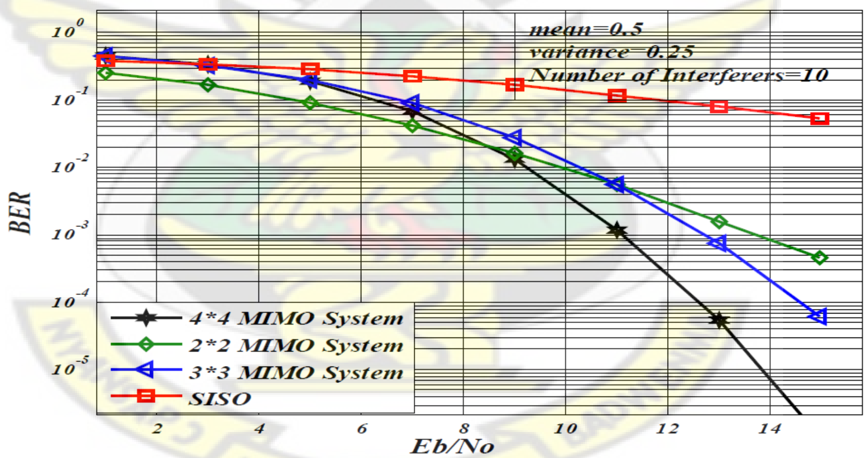

Figure 4.9: Performance of MIMO System in the presence of 10 interferers

A bounding technique for specifying the mean and variance was applied to ensure that the simulated BER estimates are fairly accurate. The BER simulation results using the Monte Carlo approach shows that the number of transmit n_T and receive n_R antennas affect the BER performance of the System. This complements the earlier results by [9] on dealing with asymptotic statistics of the mutual information for correlated Rician Fading MIMO channels with interference. The results seem to be important for a large number of antennas as the performance of the 4x4 MIMO system seemed the least affected by the variance and the number of interferers.

4.6 INTERFERENCE SIMULATION IN THE DEPLOYED NETWORK

The network in Figure 4.10 is a newly deployed network under a dense urban Sub-Saharan African environment and as such there are bound to be interference in the system.

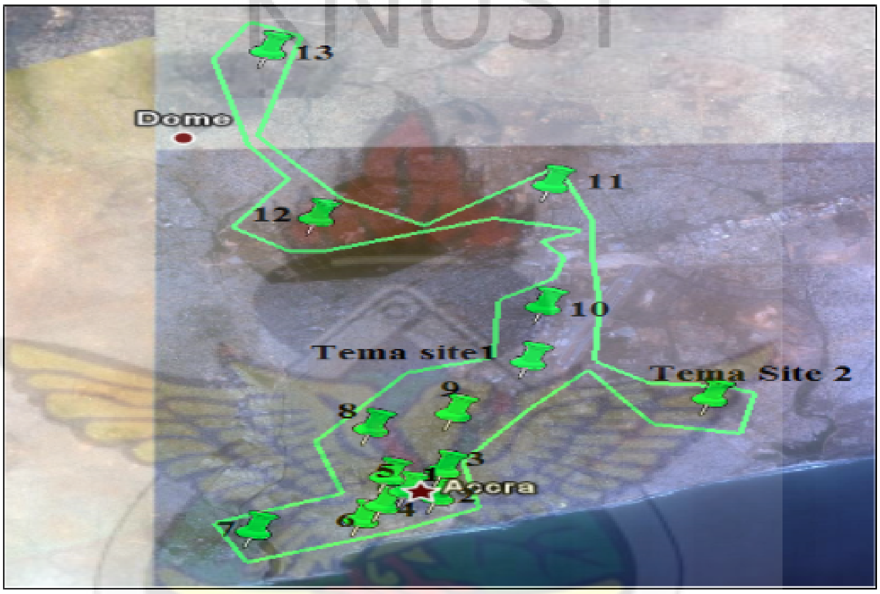

Figure 4.10: Distribution of sites in the deployed network

Possible interference scenarios that are bound to occur in the deployed network have been shown in Figure 4.11 and Table 4.5. The interference scenarios that are bound to be encountered in the network scenarios depend on the characteristics of BSs and mobile stations (MS). In scenario 1, the effect of interference between interferer system and victim system is related with their respective locations. In the second scenario, when the MS in downlink is very close to the MS of interferer system in uplink, the MS of interferer system in uplink interferes with the MS of victim system.

Table 4.5: Possible interference scenarios in the Network

Scenario	Interference Path	Direction
1	Base station to Mobile Station	Downlink to Downlink
2	Mobile Station to Mobile Station	Uplink to Downlink
3	Mobile Station to Base station	Uplink to Uplink
4	Base station to Base station	Downlink to Uplink

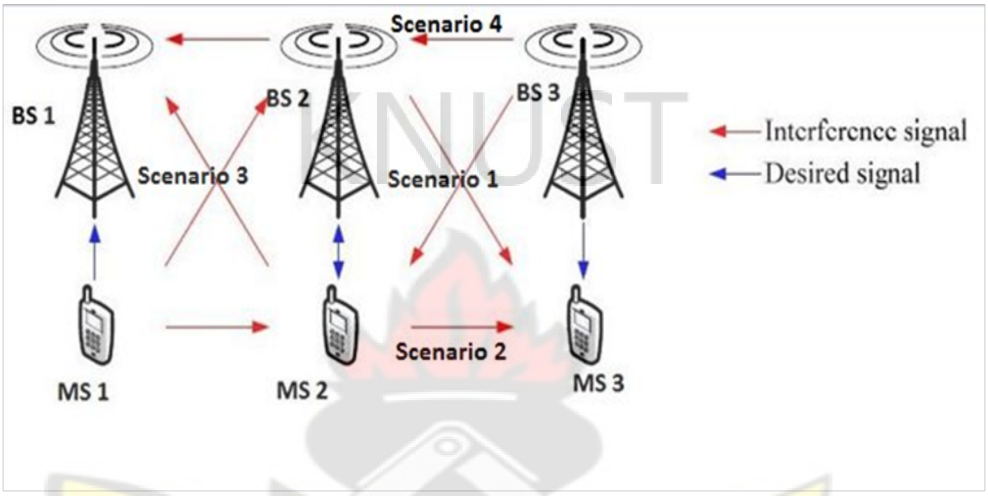

Figure 4.11: Possible interference scenarios in the Network

Because the transmitter power of the MS is smaller than that of the BS and the relative mobility of the MS can contribute to a transient nature to the interference, other studies have concluded that this interference level is negligible when considered across a network [10]. The worst case in these two scenarios occurs with a low probability [11]. The fourth scenario shown in Figure 4.12 is the most severe.

The reason is that Base Stations in the network have been located at high positions for maximum coverage, leading to a high probability that the propagation loss between BS of victim system and BS of interferer system is low [12]. In order to fully understand the impact of interference on the deployed network, this section uses a Monte Carlo simulation approach to describe the total interference scenario 4 poses to the network.

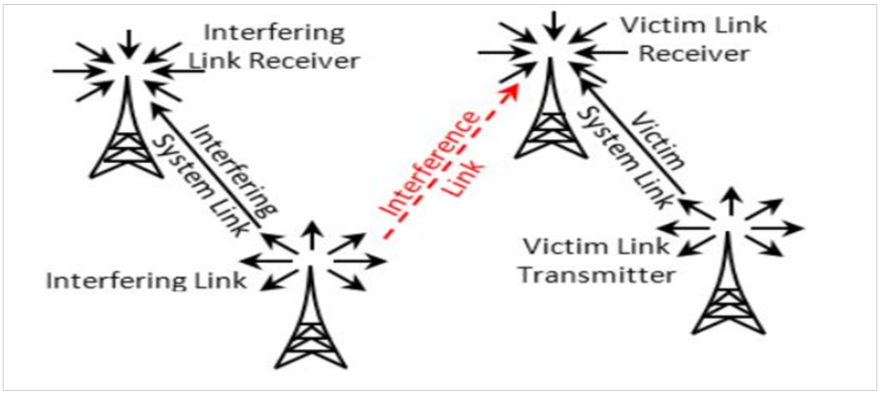

Figure 4.12: Multiple BS to BS interferers

The interference simulation will be based on a Monte Carlo simulation approach. A total of 5000 samples have been drawn for calculating the total interference. The inter-site distances from the deployed WiMAX network in the Accra and Tema municipality, shown in Figure 4.10, is summarized in Table 4.6. Two scenarios have been simulated in this research. In the first case, received power levels below the acceptable out of band emissions of -100dBm have been assigned to the interfering BS. In the second case, the out of band emissions from the interfering BS have been estimated based on the simulation results in Table 4.3 and the inter-site distances summarized in Table 4.6. The mean power from the Base Stations with their respective standard deviation in both cases which are used for the simulation is given in Table 4.6. From Figure 4.10 and Table 4.6, if there is bound to be any interference from neighboring BS, it is most likely to be high around Accra sites 1, 2, 3, 4, 5, 8,10 and Tema sites 1 and 2 because of their shorter inter- site distances.

The BS to BS interference scenario which has been simulated, models the total interference from n BS arriving at the victim's receiver as:

$$I_{tot} = 10\log(i_1 + i_2 + i_3 + \cdots + i_n) \tag{4.6}$$

where: I_{tot} =Total interference

i_1=first interfering Base Station $i_n =$ the n_{th} interfering Base station

Table 4.6: The inter-site distances of BS in the deployed WiMAX network

Site A	Site B	Inter- site distances (km)
Accra site 1	Accra site 2	1.938
Accra site 1	Accra site 3	1.472
Accra site 1	Accra site 4	2.123
Accra site 4	Accra site 5	1.563
Accra site 5	Accra site 6	2.8
Accra site 5	Accra site 8	4.542
Accra site 5	Accra site 7	7.59
Accra site 7	Accra site 9	15.342
Accra site 6	Accra site 7	5.734
Tema site1	Tema site 2	13.2
Tema site 1	Accra site 10	5.33

Table 4.7: Mean Interference and Standard Deviation

Signal	Case 1		Case 2	
	Out of band emission (dBm)	Std deviation	Estimated out of band emission (dBm)	Std deviation
Wanted signal	-90	10	-90	10
Interfering Base Station 1	-103	3	-92	8
Interfering Base Station 2	-110	10	-89	11
Interfering Base Station 3	-102	2	-88	12
Interfering Base Station 4	-105	5	-90	10
Interfering Base Station 5	-101	1	-92	8

A simple Monte Carlo simulation for interfering BS values based on Table 4.7 for wanted and interfering signals from their corresponding Gaussian distributions and total interference to the victim base station are shown in Figures 4.13-4.16.

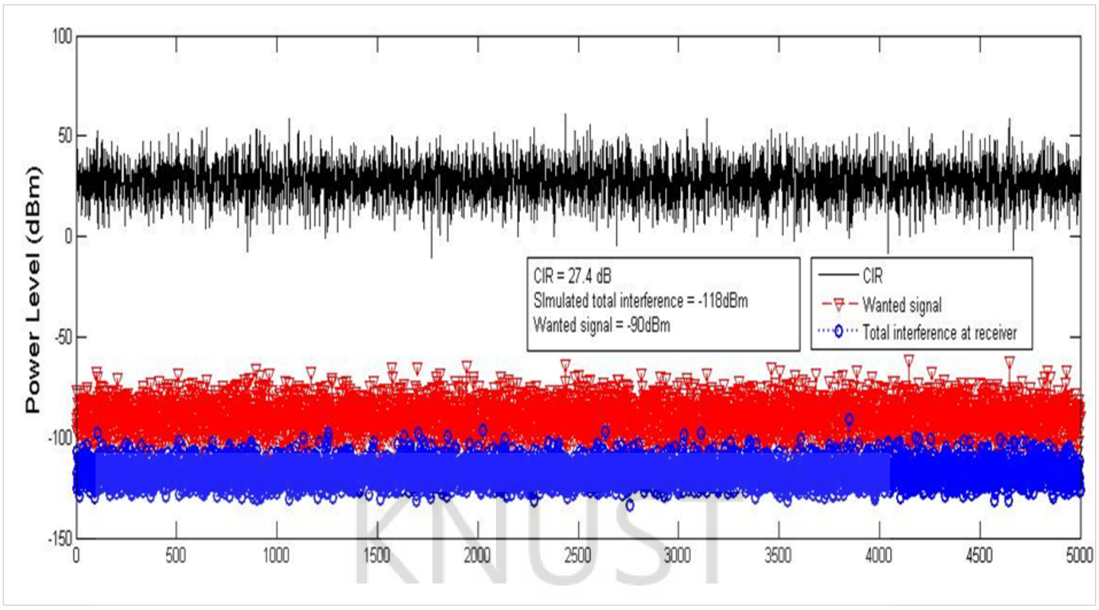

Figure 4.13: Effect of interfering signals on the wanted signal at victim's Receiver in Case 1

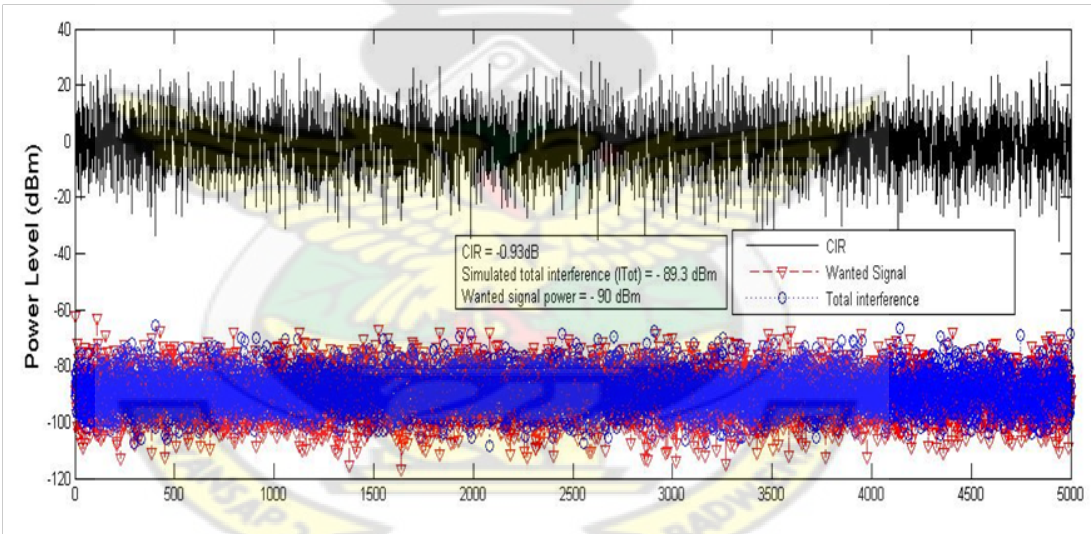

Figure 4.14: Effect of interfering signals on the wanted signal at victim's Receiver in Case 2

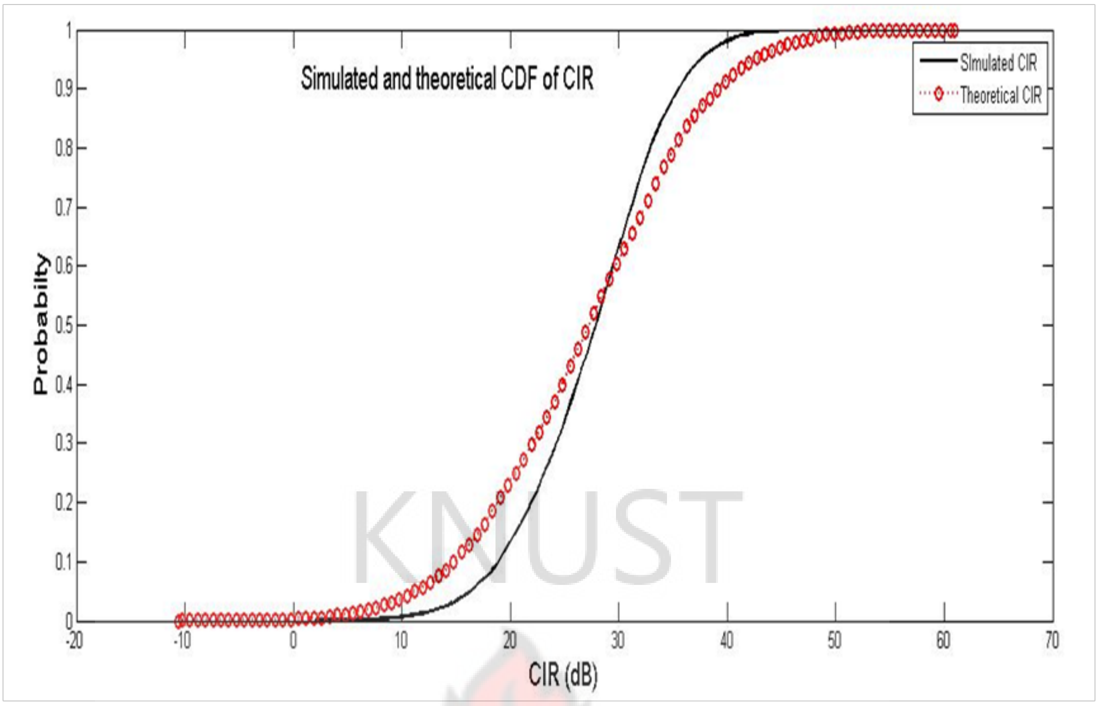

Figure 4.15: Simulated CIR at victim's Receiver in case 1

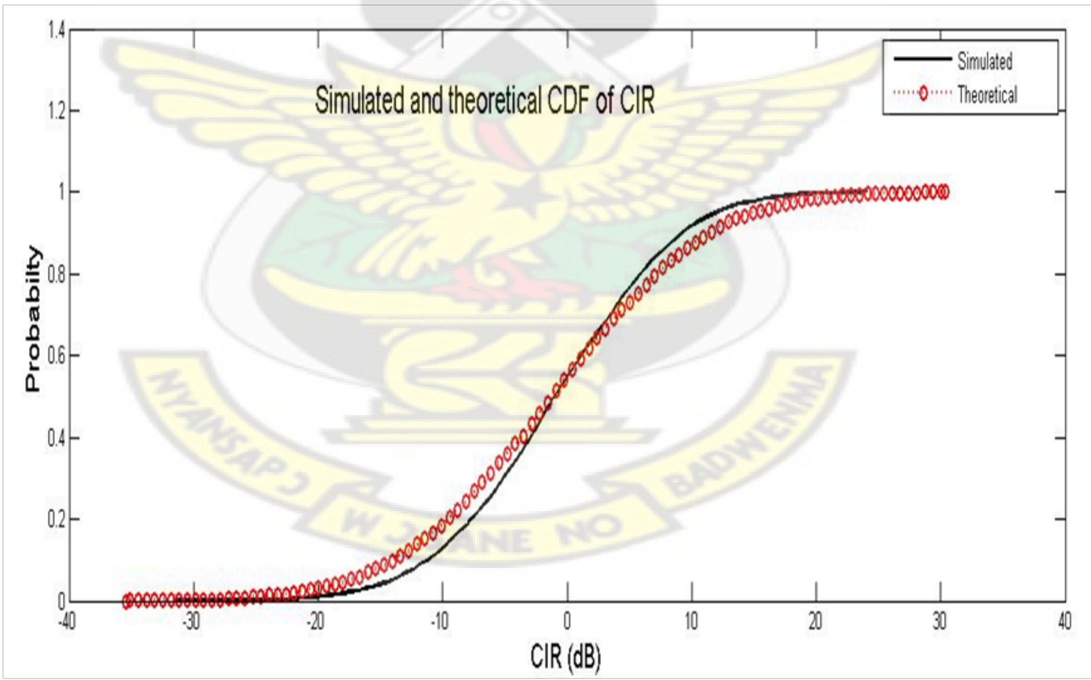

Figure 4.16: Simulated CIR at victim's Receiver in case 2

In the interference simulation results for case 1 shown in Figure 4.13 and Figure 4.15, the mean simulated total interference (I_{tot}) from the 5 Base Stations to the victim's receiver and CIR were-118dBm and 27.4dB respectively. This value is acceptable based on WiMAX system level evaluation results presented in [12].

From the simulation results for case 2 shown in Figure 4.14 and Figure 4.16, the mean simulated total interference at victim's receiver and CIR were -89.3dBm and -0.93dB respectively. The interference value of -89.3dBm is above the recommended out of bands emission of -100dBm. This significant value of interference can cause degradation to the link quality at the cell edges. This will affect the overall network performance and as such, network Optimization schemes are needed to help minimize the effect of interference.

In the subsequent sections, two proposed solutions to mitigate the high level of interference in the deployed MIMO network are presented. The first proposed solution presented in section 4.6 uses analytical methods to discuss an appropriate striping technique in improving the BER performance of the deployed 2x2 MIMO configuration in presence of multiple interfering sources. The second proposed solution presented in section 4.7 discusses the use of deploying the network with the alternative adaptive 4x4 MIMO configurations is later presented. The techno-economic benefit of using the 4x4 MIMO configurations is also discussed.

4.7 PROPOSED SOLUTION 1- NETWORK STRIPING TECHNIQUE

Vector channels, or multiple-input multiple-output (MIMO) channels, represent a very general description for a wide range of applications. They incorporate SISO (Single-Input Single- Output), MISO (Multiple-Input Single-Output) and SIMO (Single-Input Multiple-Output) channels as special cases. Often, MIMO channels are only associated with multiple antenna systems. However, they are not restricted to this case but can be used in a much broader context, for example, for any kind of multiuser communication.

Principally, single-user and multiuser communications are distinguished. In the single user case, the multiple inputs and outputs of a vector channel may correspond to different transmit and receive antennas, carrier frequencies, or time slots due to the fact that the data stems from a single user [11]. By transmitting parallel data streams over a MIMO channel, it was shown that the

Shannon capacity of MIMO channel increases linearly with the minimum number of transmits and receives antennas in [13] and [14]. Compared with single input single-output (SISO) systems, a MIMO system leads to a dramatic increase in spectral efficiency known as spatial multiplexing gain.

Many real world channels are characterized by a deterministic or line-of-sight component. In such cases, Rician fading conditions hold. The presence of a Rician component tends to reduce the multiplexing gain by reducing the rank of the MIMO channel matrix realizations. Shu-Ming et al did a comprehensive work [15] when they proposed multiple signature sequences (instead of one) per user in a multicarrier direct-sequence spread spectrum multiple access system in Rician fading channels. Every user has a distinct set of spreading sequences, with a different spreading sequence for each carrier in each user's set. They further indicated that when these sets of sequences were chosen to be mutually orthogonal complementary sets of sequences, multiple access interference (MAI) was reduced in Rician fading channels. In addition when symbols were packed more closely together, it resulted in a higher data rate. In conclusion, a distinct set of deterministic spreading sequences per user had lower MAI and higher data rate than another system with one distinct random spreading sequence per user in Rician fading channels.

The authors in [16] dealt with the training-based channel estimation scheme in Rician distributed flat fading multiple-input multiple-output (MIMO) channels. They proposed a new biased shifted scaled least squares (SSLS) technique which was a generalized form of the scaled least squares (SLS) approach. This technique was suitable for estimation of both Rayleigh and Rician fading MIMO channels and the performance of the conventional least squares (LS) and SSLS channel estimators was investigated. Moreover, the optimal choice of training sequences was probed using mean square error (MSE) criteria. Analytical and numerical results in [16] showed that the proposed SSLS estimator significantly outperformed the LS and SLS techniques. It was also demonstrated that increasing the Rice factor led to decreasing the MSE of offered technique, while the performance of LS and SLS estimators were independent of this factor. Li-Chun et al [17] in their Capacity fades analysis of MIMO Rician channels in mobile ad hoc networks used double-ring scattering model with LOS components. The authors suggested a sum-of-sinusoids MIMO mobile-to-mobile channel simulation method, which can characterize the spatial/temporal channel correlation and Rician fading effect. Their numerical results validated the ergodicity of the initial proposed channel model in section 4.4 in terms of the correctness of the analytical channel correlation, effect of spatial correlation on channel capacity, impact of the number of antennas and scatterers on capacity, capacity distribution, and level crossing. The authors in [17], based on the double-ring scattering model with LOS components suggested a sum-of-sinusoids MIMO mobile-to-mobile channel simulation method which could characterize the spatial/temporal channel correlation and Rician fading effect.

Research work done on the capacity and BER performance of multiuser scheduling over MIMO Nakagami-m fading channels in [18] presents a performance analysis for evaluating multiuser and spatial diversities in multiuser MIMO systems. This work employs orthogonal space-time block coding (OSTBC) over Nakagami-m fading channels. Two multiuser scheduling schemes were considered: Absolute SNR-based scheduling (AS) and normalized SNR-based scheduling (NS) schemes for both heterogeneous and homogeneous wireless networks. Analytical expressions were derived for the average channel capacity and average BER of these systems. The considered scheduling schemes were numerically evaluated and compared in terms of average capacity, average BER and fairness. It was shown that in the heterogeneous case, unlike the AS scheme, the NS scheme can guarantee fairness to the users. It was also shown that in the heterogeneous case, the AS scheme yielded a higher average capacity and a lower average BER compared to the NS scheme and to the homogeneous case.

The performance of transmit diversity (TD) assisted amplify-and-forward (AF) relay system with partial relay selection, which experiences mixed Rayleigh and Rician fading channels, was investigated in [19]. In this proposed solution, the application of the effects of varying the density fraction on multiple-input multiple-output (MIMO) configurations in an uncorrelated Rician interference channel using the successive decoding approach is investigated.

4.7.1 BER Estimation of MIMO Channels

MIMO systems draw much attention in 4G communication systems modeling because it offers a potentially high reliability. Modeling of the BER performance of symmetric MIMO configurations in the presence of multiple interfering sources, however have been found to be extremely complex [20]. For example Jootar applied a residual technique to model the BER performance of a second order MIMO system in [21] as:

$$P_b = \frac{1}{2\pi j}\int_{-\infty+je}^{\infty+je} \frac{1}{v\pi(1-jv\lambda_i)}dv = -Res\left[\frac{\varphi_z(s)}{s} \text{ at LHP poles }\right]$$

where λ and P_b denote the signal to noise ratio and BER respectively. Alternatively, the BER performance can be modeled using numerical methods by employing a Gauss-Chebyshev approximation. This approach has been validated by the authors in [22].Authors in [23, 24] also tried to extend the numerical simulation methods to analyze the BER performance of MIMO configurations in the presence of noise. The results of their simulation showed that BER performance of the various MIMO configurations degraded in the presence of partial band interference when a cross-correlation matrix was used.

In the next subsections, a simple closed-form expression for BER is used to analyze the deployed MIMO systems based on successive cancellation methods. This cancellation method is based on an extension of MIMO systems with n_R receive antennas and n_T transmit antennas to partial-band interfering transmitter under the assumption of a common receive correlation matrix.

4.7.2 Proposed Successive Cancellation Technique

Striping or successive cancellation is a decoding technique based on a simple and natural idea. A given user is decoded treating all the other users as noise, then the signal due to that user is remodulated with the decoded information and subtracted from the received waveform. The process is repeated until all transmitted information streams have been remodulated. A popular approach is to demodulate the user in the order of decreasing received powers. However, this fails to take into account the cross correlations among users. The best alternative is to order users according to [25]:

$$E[(\int_o^T y(t)s_k(t)dt)^2] = \sigma^2 + A_k^2 + \Sigma_(j \neq k)A_j^2\rho_{jk}^2 \tag{4.7}$$

This can be estimated easily from the receiver outputs. Given a synchronous two – user channel, demodulating user two by its matched filter $\hat{b}_2 = sgn(y_2)$ and remodulating the signal of user two results $A_2\hat{b}_2s_2(t)$, which upon subtracting from the received signals yields [25]

$$\begin{aligned} \hat{y}(t) &= y(t) - A_2\hat{b}_2s_2(t) \\ &= A_1b_1s_1(t) + A_2(b_2 - \hat{b}_2)s_2(t) + n(t) \end{aligned} \tag{4.8}$$

processing $\hat{y}$ with the matched filter for s_1 yields

$$\hat{b}_1 = sgn(\langle\hat{y}, s_1\rangle) = sgn(y_1 - A_2\hat{b}_2\rho) \tag{4.9}$$

$$= sgn(y_1 - A_2\rho sgn(y_2)) \tag{4.10}$$

$$= sgn(A_1b_1 + A_2(b_2 - \hat{b}_2)\rho + \sigma\langle n, s_1\rangle) \tag{4.11}$$

Thus, the detector output will be $\hat{b}_2 = sgn(y_1 - \rho y_2)$; where sgn denotes the signature of the two permutations y_1 and y_2

4.7.3 Partial Band Interference

This form of interference is modeled as a zero- mean Gaussian Random Process with a flat power spectral density over fraction $\beth$ of the total bandwidth W and zero elsewhere. For non zero power spectral density regions, its value $\varphi_{zz}(f) = J_o/\beth$, $0 < \beth \leq 1$. Partial-band interference from a jammer for optimization selects $\beth$ for the effect of the communication system maximizes the error probability [26]. For Optimization

$$\beth^* = \begin{cases} \dfrac{1}{\delta_b/2J_o} = 2\dfrac{J_{av}/P_{av}}{W/R} & (\delta_b/J_o < 2) \\ 1 & (\delta_b/J_o \geq 2) \end{cases} \tag{4.12}$$

and the corresponding error probability for the worst-case partial-band jammer is

$$P_2 = \frac{e^{-1}}{\delta_b/J_o} = \left[e \left(\frac{W/R}{J_{av}/P_{av}} \right) \right] \tag{4.13}$$

We have already defined the signal-to-noise and interference-to-noise power ratios in section 4.4 as:

$$\begin{cases} SNR = \dfrac{(K+1)tr(\rho)tr(\grave{\Psi})}{\eta_R} \\ INR = \dfrac{(K_1+1)tr(\rho)tr(\grave{\Psi}_1)}{\eta_R} \end{cases} \tag{4.14}$$

In what follows, it is further assumed that:

1. The spatial correlation matrices are normalized by

$$tr(\rho) = tr(\rho_I) = n_R$$
$$tr(\Psi) = n_T$$
$$tr(\Psi_I) = n_I$$

2. The matrices are normalized according to the identities

$$\begin{cases} \|\grave{\zeta}\|^2 = \dfrac{\eta_R K SNR}{K+1} tr(\grave{\Psi}) = \dfrac{SNR}{K+1} \\ \|\grave{\zeta}_1\|^2 = \dfrac{\eta_R K_1 INR}{K_1+1} tr(\grave{\Psi}_1) = \dfrac{INR}{K_1+1} \end{cases} \tag{4.15}$$

If the MIMO channel is subject to unwanted radio interference, then the $n_R \times n_R$ random matrix $\xi\xi^H$ follows a Wishart-type distribution. By defining the $m \times m$ random matrices $\mathbf{S}$ and Ω such that:

$$\mathbf{S} := \begin{cases} \xi\xi^H, \text{ if } n_T \geq n_R \\ \xi^H\xi, \text{ if } n_T < n_R \end{cases} \qquad \phi := \begin{cases} \aleph M M^H, \text{ if } n_T \geq n_R \\ \aleph M^H M, \text{ if } n_T < n_R \end{cases} \tag{4.16}$$

The distribution of the nonzero eigenvalues of $\xi\xi^H$ is determined by the eigenvalue distribution of the complex non central Wishart matrix $\mathbf{S} \sim CW(n, 1/(K+1)I_m, \phi)$. Assuming that ϕ has $t > 0$ distinct eigenvalues $\omega_{m-t+1}, \cdots, \omega_m$, denoted as the column-vector $\omega_t = [\omega_{m-t+1}, \cdots, \omega_m]^T$, then, following the approach in [27–30], the PDF of a single unordered eigenmode SNR is given by:

$$\rho_\gamma 1(\gamma) = \frac{\aleph^{\omega}_{(m,n)}}{m} \sum_{i=1}^{n} \mu_\aleph [\Theta + \tilde{\omega}] \tag{4.17}$$

$$\Theta = \sum_{j}^{1} \sigma^t_{i,j} (\mu_{\aleph\gamma})^{d+i+j-2} e^{-\mu_{\aleph\gamma}} \tag{4.18}$$

$$\tilde{\omega} = \sum_{j}^{2} \sigma^t_{i,j} (\mu_{\aleph\gamma})^{d+i-1} e_o^{-\mu_{\aleph\gamma}} \bar{F}_1 \left(d+1, \mu_{\aleph\gamma\omega_i}\right) \tag{4.19}$$

$$\tag{4.20}$$

where,

$$
\begin{aligned}
\mu_{\aleph} &:= \frac{(\aleph + 1)}{\bar{\gamma}}, (\aleph^{(\omega_t)}_{(m,n)})^{-1} := K\Lambda N \\
K &= V(\omega_t)e^{\sum_{j=m-t+1}^{m}\omega_j} \\
\Lambda &= \prod_{j=1}^{m-t}\Gamma(d+j)\Gamma(j) \\
N &= \prod_{j=m-t+1}^{m}\omega_j^{m-t}
\end{aligned}
$$

With $V(\omega t)$ denoting the Van Der Monde determinant of order t associated with ωt and $\Gamma(.)$ the standard Gamma function [29]

$$
{}_o\bar{F}_1(b;\varrho) := \sum_{k=0}^{+\infty}\frac{\varrho}{\Gamma(b+\aleph)\aleph!}
$$

is a regularized confluent hypergeometric limit function, denoting the $\sigma(t)^t_{ij} :=$ $(-1)^{i+j}\det[\sigma_{ij}(\omega_t)]_{m-1}$ with $\sigma_{ij}(\omega t)$ denoting the $(i,j)^{th}$ minor of $\sigma_{ij}(\omega t) =$ $\left(\Gamma(d+i+j-1)\underset{j\leq m-t>m-t}{\Gamma(d+i)}{}_1\bar{F}_1(d+i;d+1;\omega j)\right)_m$ obtained by removing the i^{th} row and j^{th} column thereof and ${}_1\bar{F}_1(a;b;\varrho) := \sum_{\aleph=0}^{+\infty}\frac{\Gamma(a+k)\varrho^{\aleph}}{\Gamma(a)\Gamma(b+k)\aleph!}, d := n-m$ and have introduced the shorthand notations $\sum_j^i := \sum_{j=1}^{m-t}$ and $\sum_j^2 := \sum_{j=m-t+1}^{m}$ for convenience.

$$f(x) = \frac{\gamma_0}{\aleph^{\omega_t}_{m,n}} = \sum_{i=1}^{m}\sum_{j}^{1}\sigma^t_{ij}[A-E] + \sum_{j=1}^{m}\sum_{j}^{2}\frac{\sigma^t_{ij}e^{\omega_j}}{2^{i-j}}[Z-v] \quad (4.21)$$

$$f(x) = \Gamma(d+i+j-1, \mu_\aleph\gamma_o) \quad (4.22)$$

$$E = \mu_\aleph\gamma_o\Gamma(d+i+j-2, \mu_\aleph\gamma_o) \quad (4.23)$$

$$Z = \vartheta_{d+2i-1,d}(\sqrt{2\omega_j}, \sqrt{\mu_\aleph\gamma_o}) \quad (4.24)$$

$$\nu = 2\mu_\aleph\gamma_o\vartheta_{d+2i-3,d}(\sqrt{2\omega_j}, \sqrt{\mu_\aleph\gamma_o}) \quad (4.25)$$

$$\sigma^{m,n}_{em-opra} = m\frac{E_1(\mu_\aleph\gamma_o)}{In(2)} + \frac{\aleph^{\omega_t}_{m,n}}{In(2)}\sum_{i=1}^{m}[\eta+\theta] \quad (4.26)$$

$$\eta = \sum_{j}^{1}\sigma^t_{ij}\Gamma(d+i+j-1)\sum_{l=1}^{d+i+j-2}\frac{\Gamma(l,\mu_\aleph\gamma_o)}{\Gamma(l+1)} \quad (4.27)$$

$$\theta = \sum_{j}^{2}\sigma^t_{ij}\sum_{k=0}^{+\infty}\frac{\Gamma(d+i+k)\omega^k_j}{\Gamma(k+1)\Gamma(d+1+k)}\sum_{l=1}^{d+i+k-1}\frac{\Gamma(l,\mu_\aleph\gamma_o)}{\Gamma(l+1)} \quad (4.28)$$

Substituting Eq. (4.12) into $\int_{\gamma_o}^{+\infty}\left(\frac{1}{\gamma_o}-\frac{1}{\gamma}\right)\rho_{\gamma_1}(\gamma)d\gamma = \frac{1}{m}$, it is seen that the optimal cutoff value has to satisfy Eq. (4.24) where $\Gamma(a,\varrho) := \int_{\varrho}^{+\infty} t^{a-1}e^{-t}dt$ denotes the upper incomplete Gamma function and $\vartheta_{p,q}(a,b)$ is the normalized Nuttall Q function, defined as $\vartheta_{p,q}(a,b) := Q_{p,q}(a,b)/a^q$, where $\vartheta_{p,q}(a,b)$ stands for the standard Nuttall Q-function [30]

$$Q_{p,q}(a,b) = \int_b^\infty \varrho^p \exp\left(i\frac{\varrho^2+a^2}{2}\right) I_q(a\varrho)d\varrho \quad (4.29)$$

where $0 < a, b < \infty, p, q = 0, 1, 2, \cdots$, with $I_q(.)$ being a modified Bessel function of the first kind. Existence and uniqueness of γ_o satisfying Eq. (4.13) can be easily proved following a similar approach to the one used by the authors in [31]. In order to evaluate the capacity of the em-opra transmission policy, substitute Eq. (4.12) into $\sigma^{m,n}_{em-opra} = m\int_{\gamma_0}^{+\infty}\log_2\left(\frac{\gamma}{\gamma_o}\right)\rho_{\gamma_1}(\gamma)d\gamma$, then replace ${}_o\bar{F}_1(.;.)$ with its infinite series representation, and exchange the integral and summation orders which yields $y = \zeta\omega + \zeta I\omega I + z$. Following the approach in [31], where $E1(\mu) := \int_1^{+\infty}\frac{e^{-\mu t}}{t}dt$ denotes the exponential integral function of the first order. The outage probability hinges on the cumulative distribution function (CDF) of the largest eigenvalue of $\xi\xi^H$.

Accordingly, it can be shown that the outage probability induced by the em-opra policy can be expressed as functions of γ_o as

$$P_{error}^{m,n} = Prob(\gamma_{max} \geq \gamma_o) = P(\mu_K \gamma_o) \tag{4.30}$$

Where: $P_{error}^{m,n}$ is the probability of error, and $P(\varrho) \coloneqq K_{m,n}^{\omega_t} \det[\mathbf{D}(\varrho)]_m$ and the elements of the $m \times m$ matrix $\mathbf{D}(\varrho)$ for $i, j = 1, \cdots, m$ are given by

$$\{\mathbf{D}(\varrho)\}_{ij} = \begin{cases} \gamma(d+i+j-1, x) & \text{if } j = 1, \cdots m-t \\ -\dfrac{e^{\omega j}}{2^{i-1}} \vartheta_{d+2i-1,d}\left(\sqrt{2\omega_j}\sqrt{2\varrho}\right) & \text{otherwise} \end{cases}$$

where, $\gamma(a, \varrho) \coloneqq \Gamma(a) - \Gamma(a, \varrho)$. The implication of Eq. (4.30) on a Rician fading channel is explained and validated in the next sections.

4.7.4 Implications of The Derived BER Expressions

In order to analyze the implication of the BER expression, n sets of variables which can be modeled using a density distribution function, $\Gamma(a)$, will be used. The density distribution function will also be used to describe another new set of sequence $m = 1, 2, 3, \cdots, n$. n and m denote the number of transmit and receive MIMO antennas respectively. The density distribution function for an m^{th} series is generally expressed as:

$$\Gamma_m\left(\frac{a}{n}\right) = \frac{n!\Gamma(a)}{(m-1)!(n-m)!}\Gamma_c^{m-1}(a)[1-\Gamma_c(a)]^{n-m} \tag{4.31}$$

where $\Gamma(a)$ and $\Gamma_c(a)$ denote the density distribution function and the cumulative distribution function of the signal to noise ratio respectively. The mean signal to noise ratio in the set of channels subjected to Rician fading is denoted by a. is the mean signal to noise ratio in a set of channels subject to Rician fading. Following the approach in [32] which define the density distribution function (ddf) as $(\gamma) = \gamma_o e^{-\gamma/\gamma_o}$, the ddf for the striped MIMO channel can be expressed in the form of:

$$\Gamma(\gamma) = \gamma_o e^{-\gamma/\gamma_o} \tag{4.32}$$

Where γ is the SNR, and γ_o is the mean value of SNR. The cumulative distribution function will take the form of:

$$\Gamma_c(\gamma) = 1 - \gamma_o e^{-\gamma/\gamma_o} \tag{4.33}$$

Putting (4.32) and (4.33) into (4.31)

$$\Gamma_m\left(\frac{\gamma}{n}, \gamma_o\right) = \frac{n!\Gamma(a)}{(m-1)!(n-m)!}\gamma^{-1}e^{-\gamma/\gamma_o}(1-e^{-\gamma/\gamma_o})^{m-1}(e^{-\gamma/\gamma_o})^{n-m} \tag{4.34}$$

In the BER analysis of MIMO systems, the system configuration performance of interest is the sequence of $n = m$ which models the wide virtual bandwidth under a set of signal to noise ratio values. This corresponds to performance of the striped MIMO system. The evaluation of Eq. (4.34) for the $n = m$ case takes the form:

$$\Gamma_n\left(\frac{\gamma}{\gamma_o}\right) = \frac{n}{\gamma_o}e^{-\gamma/\gamma_o}(1-e^{-\gamma/\gamma_o})^{n-1} \tag{4.35}$$

In an interference prone network, it is assumed that the rate of change of γ is slow. Hence the relations in Eq. (4.34) can be used to analyze the resultant BER performance of the MIMO configuration once the acceptable threshold of γ is exceeded. The BER performance of the striped MIMO configuration can be calculated as the error probability $P^{m,n}_{error}$ for the Rician fading channel condition averaged over the density distribution function in (4.35) as:

$$P^{m,n}_{error}(\gamma_o) = \int_{\gamma_{max}}^{\gamma_o} P(\gamma)\Gamma_n\left(\frac{\gamma}{\gamma_o}\right)d\gamma \tag{4.36}$$

Equation (4.36) is just an evaluation of Eq. (4.30). The case where only $n =$

$m = 2$ is stripped is evaluated in this research. This is because of the fact that an adaptive 2×2 MIMO configuration has been used in deploying the network under study. The result of the evaluations are validated with simulation and discussed in the next subsection

4.7.5 Validation of The Proposed Technique

The result of the proposed technique is compared with earlier results obtained for MIMO systems in the presence of multiple interferers presented in section 4.4. The results of the proposed Striping technique has been evaluated with Monte Carlo numerical methods and presented in Figures 4.17-4.18. In the simulation, a given user is decoded treating all the other users as noise, then the signal due to that user is remodulated with the decoded information and subtracted from the received waveform. The partial-band interference is modeled as a zero- mean Gaussian Random Process with a flat power spectral density fraction $\daleth$ of the total bandwidth W and zero elsewhere. For maximization of error probability, the flat spectral densities over a fraction of the total bandwidth were selected to be $\daleth$= 1.0 and 0.01.

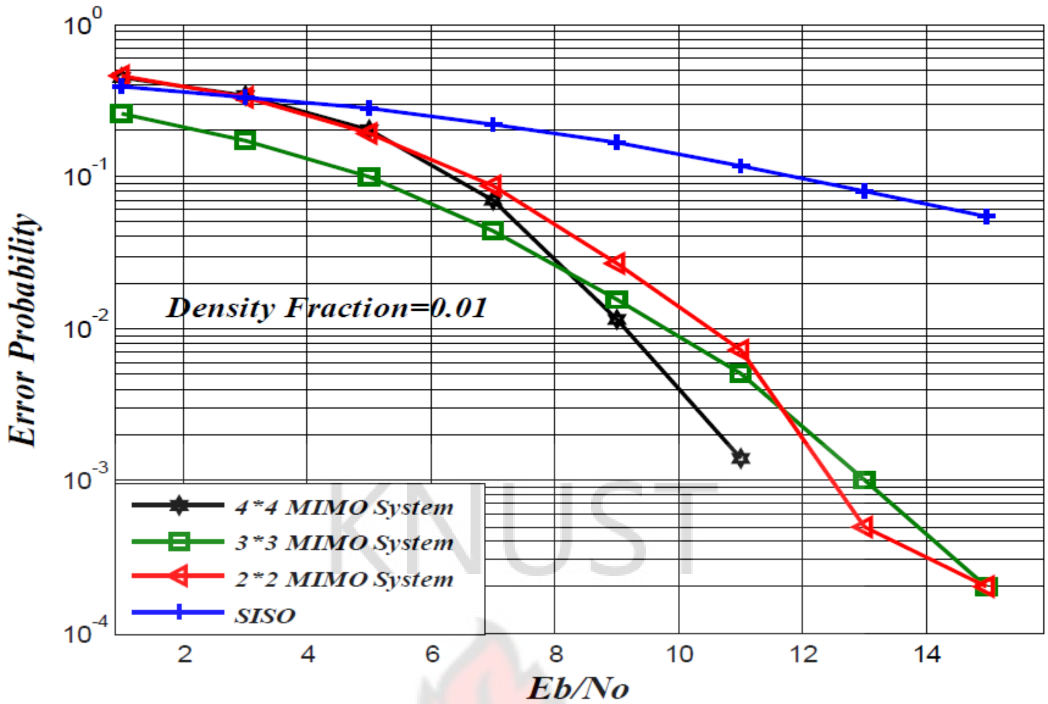

Figure 4.17: Performance of MIMO System partial-band interference with ℶ=0.01

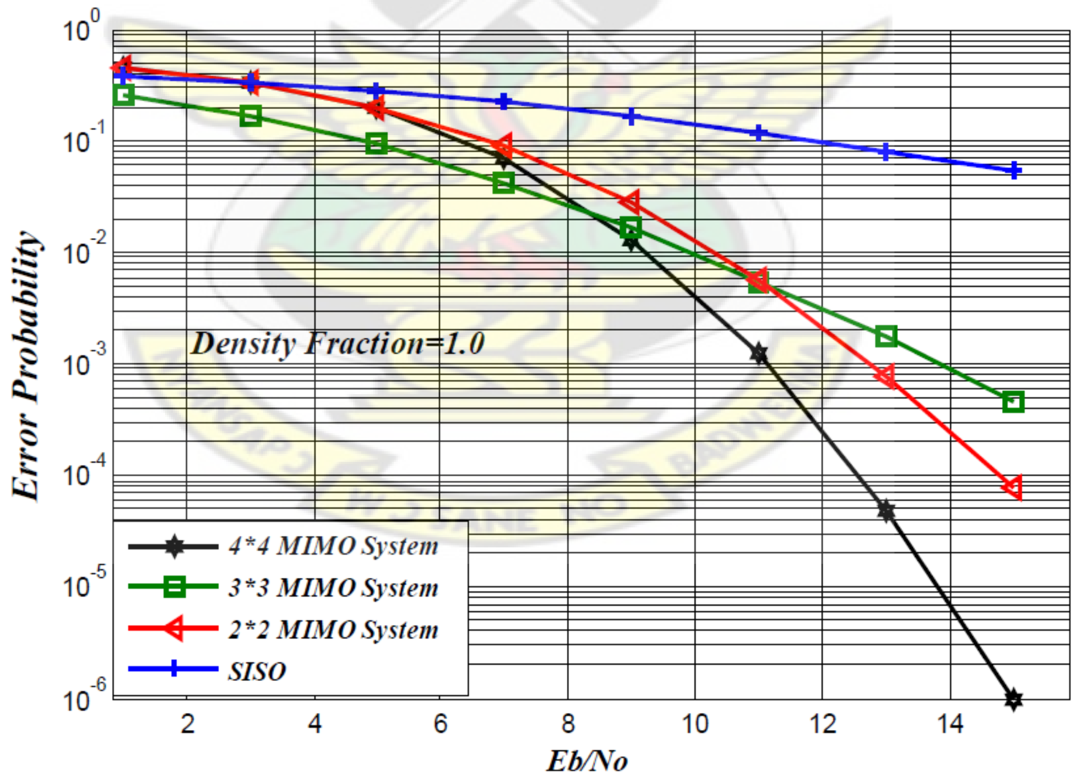

Figure 4.18: Performance of MIMO System partial-band interference with ℶ=1

The results were obtained by splitting the total received power components into direct and diffused parts before defining the SIR and SNR. The BER performance of the 4x4 MIMO configuration with $\beth$=0.01 shown in Figure 4.17 will follow earlier results presented in section 4.4 since this configuration has not been stripped. The Eb/No value of the 4x4 MIMO configurations was truncated at 11dB to increase the simulation runtime. The results of the BER estimation based on an extension of MIMO system with η_R receive antennas and η_T transmit antennas to partial-band interfering transmitter under the assumption of a common receive correlation matrix indicates that the Rician factor and SNR depend on the full transmit covariance matrix and not only their traces, unless they are proportional to identity matrix. When the results in the proposed technique is compared with the earlier results derived for the MIMO configuration in the presence of multiple interferers, it can be seen that the striped 2x2 MIMO configuration outperforms the SISO and 3x3 MIMO configurations which have not been striped.

4.8 PROPOSED SOLUTION 2 – ALTERNATE MIMO CONFIGURATION

With the comparatively low BER performance of the 2x2 MIMO configurations, data transmitted on the network could be corrupted in the presence of multiple interferers. This may result in data having to be re-transmitted, and this reduces network performance. With studies predicting a 1000X increase in data traffic from 2010-2020 [33], BER performance in the presence of interference is a critical design issue so as not to put severe strain on deployed 4G networks. With the adaptive 4X4 MIMO configurations giving high average throughput per sector, improved coverage range and better performance in the presence of interference, it is recommended that future deployment of Base Stations in the network should use 4x4 MIMO antennas with optimized sidelobes suppression techniques.

Since adaptive 4x4 MIMO configuration simulation results in Table 4.3 and Table 4.4 give an enhanced coverage capabilities and capacity, 11 base stations with a 32 sector antenna configuration will give coverage to the entire Accra and Tema network with simulated RSSI of -92dBm as shown in Figure 4.19 whiles 15 sites have been used to deploy the present network because of the limited range of the adaptive 2x2 MIMO configuration (Figure 4.19).

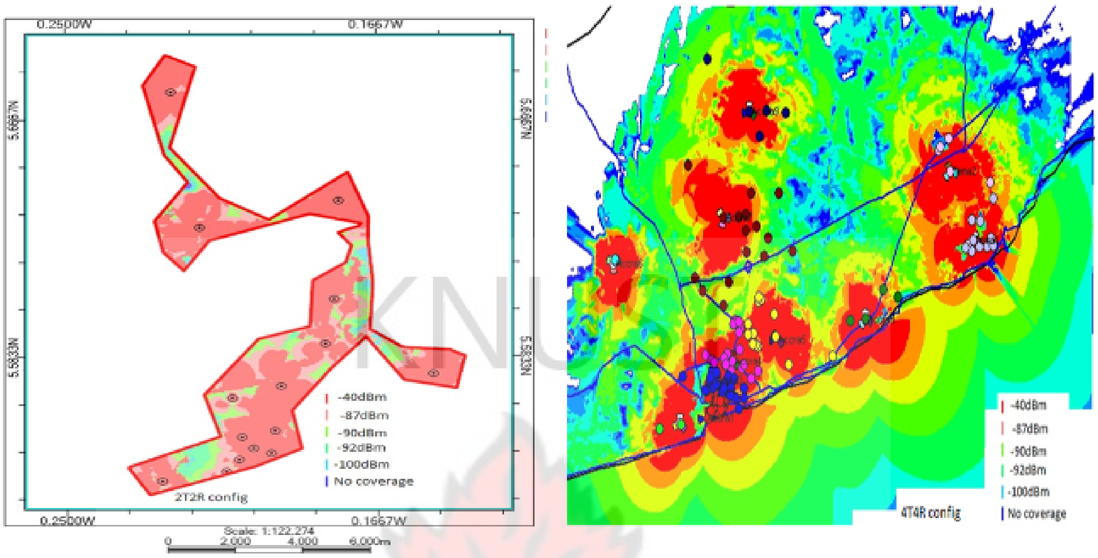

Figure 4.19: Deployed WiMAX network *vs* Proposed optimized network design

From capacity simulation results in Table 4.4, the adaptive 4x4 MIMO antenna configuration and PUSC with all SC 1x3x3 with DL/UL ratio of 35:12 which gives the highest average sector DL throughput of 16.55Mbps should be used to provide optimum use of resources and minimize initial startup expenditure in the final radio plan.

The 4x4 MIMO configuration gives a 3 dB increase in downlink/uplink coverage and higher throughput which reduces the number of base station sites in certain areas. The current cost of building a WiMAX site in Ghana is $120,000 [34]. Therefore, if the adaptive 4x4 MIMO antenna configurations had been used in deploying the network under evaluation, the operator would only need eleven BS instead of the deployed fifteen BS. This would have reduced the deployed cell sites by four (4). The initial startup cost would have been reduced by $480,000. Moreover, the cost of maintaining a WiMAX BS (maintaining the radio resources, power, air conditioning) under the current business environment in Ghana is shown in Figure 4.20.

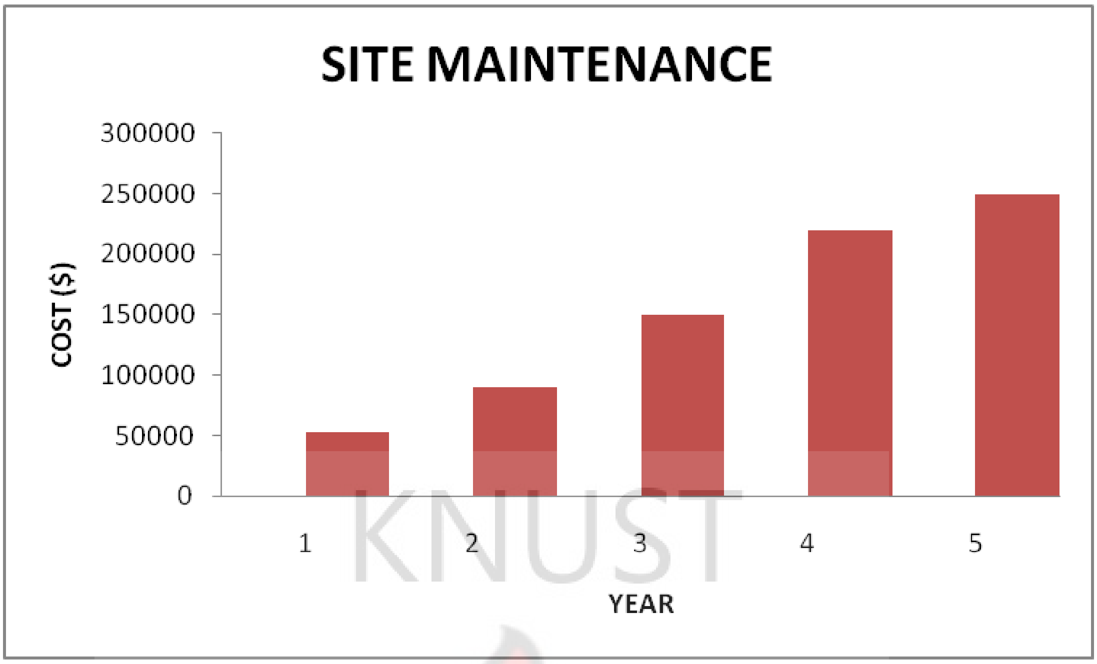

Figure 4.20: Cost of site maintenance over a 5 year period

It can be seen that using the 4x4 MIMO configuration which reduces the number of BS by four (4) will lower the total cost of ownership from the short to medium term.

4.9 SUMMARY

As stated earlier, Antennas with efficient sidelobe suppression techniques are very expensive. In order to reduce the initial cost of network deployment, this chapter presents a mathematical model to analyze the effect of antenna sidelobe emissions in a multicarrier network. An additional sidelobe suppression value of -30dB for MIMO antennas with elements greater than or equal to 720 has been proposed for network deployments in the Sub-Saharan environments.

Furthermore, the BER performance analysis of the MIMO configurations in the presence of multiple interfering BS has been done with the adaptive 4x4 MIMO configuration showing promising performance than the deployed 2x2 configuration. An appropriate network Striping technique was proposed to improve the BER performance of the deployed 2x2 MIMO configurations in the presence of multiple interfering sources. The BER optimization was obtained with flat spectral density over a fraction of the total bandwidth as $\beth$=1.0 . Also, Rician factor and SNR has been seen to depend on the full transmit covariance matrices irrespective of the type of interference. This result complements the earlier results made by Erwin et al [27] when dealing with Asymptotic Statistics of the Mutual Information for correlated Rician Fading MIMO channels with interference. Also, the striping results seem to be important for the deployed MIMO configuration as the BER performance of the stripped 2x2 MIMO is very impressive. The successive cancellation technique improves the MIMO performance with the number of interferers having less effect on the BER performance of the System. Finally, a techno-economic analysis done on the two configurations indicate that, the 4x4 MIMO configuration would reduce the cost of deployment in the short to medium term under the Ghanaian business environment.

REFERENCES

[1] Y. Zheng and S. Blostein. Downlink distributed beamforming through relay networks. In *In Proceedings of the IEEE GlobalTelecommunications Conference (GLOBECOM 09)*, 2009.

[2] George Tsoulos Dimitra Zarbouti and Dimitra Kaklamani. Theory and practice of MIMO wireless communication systems. In *Multiple-Input Multiple-Output Channel Models: Theory and Practice, first edition*, pages 29–55, 2009.

[3] R. Erwin and T. Giorgio. Asymptotic statistics of the mutual information for spatially correlated racian fading MIMO channel with interference. *IEEE Transaction on Information Theory*, 75:345–350, 2010.

[4] P. F. Driessen and G. J. Foschini. On the capacity formula for MIMO wireless channels: A geometric interpretation. *IEEE Trans. Commun*, 47(2):173–176, 1999.

[5] P. F. Driessen, G. J. Foschini, A. Lozano, and R. A. Valenzuela. Link-optimal

space-time processing with multiple transmit and receive antennas. In *IEEE Commun. Lett*, volume 5, pages 85–87, 2001.

[6] J. Ayadl, A. Hutter, and J. Farserotu. On the multiple input multiple output capacity of rician channels. *In Proc. IEEE 5th Int. Symp. On Wireless Personal Multimedia Commun*, 2:27–30, 2002.

[7] E. Riegler and G. Taricco. Asymptotic ergodic capacity region and rate optimization of a multiple access OFDM MIMO channel with separately correlated rician fading. In *In Proc. IEEE GLOBECOM*, 2008.

[8] E. Riegler and G. Taricco. Asymptotic ergodic capacity of wideband MIMO channels with separately correlated rician fading. In *in Proc. IEEE GLOBECOM*, 2008.

[9] G. Taricco. Asymptotic mutual information statistics of separately correlated rician fading MIMO channels. *IEEE Trans. Inf. Theory*, 54:3490–3504, 2009.

[10] ECC Report 119. Co-existence between mobile systems in the 2.6 GHz frequency band at the FDD/TDD boundary. In *In Kristiansand*, 2008.

[11] K. Volker. Wireless communication over MIMO channels. In *Application to CDMA and Multiple Antenna Systems, John Wiley and Sons, Ltd., South Gate, Chichester, England*, page 12, 2006.

[12] WiMAX Forum. Managing TDD-FDD interference between co-sited base stations deployed in adjacent frequency blocks. Published online;www.wimaxforumn.org, 11 2009.

[13] I. E. Telstar. Capacity of multi-antenna gaussian channels. *Europe. Trans. Telecommunication*, 10:586–595, 1999.

[14] G. J. Foschini and M. J. Gans. On limits of wireless communications in a fading environment when using multiple antennas. *Wireless PersonalCommunications*, 6:311–335, 1998.

[15] T. Shu-Ming and Chuang Chun. A multicarrier DS/SSMA system with reduced multiple access interference and higher data rate in rician fading channels. *Signal Processing*, 81:1889–1897, 2001.

[16] N. Hamid and S. M. Shahriar. A novel shifted type of SLS estimator for estimation of rician flat fading MIMO channels. *Signal Processing*, 90:1886–1893, 2010.

[17] Li-Chun W., Wei-Cheng L., and Yun-Huai C. Capacity fades analysis of MIMO rician channels in mobile ad hoc networks. *Performance Evaluation Journal*, 66:742–753, 2009.

[18] T. Mohammad, H. David, and A. Wessam. On the capacity and BER performance of multiuser scheduling over MIMO Nakagami-m fading channels. *Signal Processing*, 91:2487–2496, 2011.

[19] X. Wei, Z. Jian Hua, and Z. Ping. Performance of transmit diversity assisted amplify-and-forward relay system with partial relay selection in mixed rayleigh andrician fading channels. *The Journal of China Universities of Posts and Telecommunications*, 18:37–41, 2011.

[20] J. Proakis. Digital communications, 2nd edition. In *McGraw Hill*, 2011.

[21] J. Jootar. Performance of alamouti space-time code in time varying channels with noisy estimates. In *IEEE communication Societ, WCNC*, 2005.

[22] Jozef Pawelec. Application of positional statistic to BER formulae derivation for switching diversity MIMO systems. *Military communications and information technology Journal*, 16:435–440, 2012.

[23] J. Pawelec and K. Kosmowski. A comparison of reception strategies in MIMO systems. In *In Proceedings of Conference on theory, Reliability and Quality communication, Budapest*, 2011.

[24] S. Alamouti. Simple transmit diversity technique for wireless communications. *IEEE Journal of Selected Areas in Communication*, 8:230–237, 1998.

[25] V. Sergio. Multiuser detection. In *The Press Syndicate of the University of Cambridge, Pit Building Trumpington Street, Cambridge, CB2, 1RP, United Kingdom*, 2011.

[26] G. Proakis. Digital communication. In *Fourth Edition, Irwin/McGraw-Hill, an imprint of the Mcgraw-Hill Companies, Inc, New York, USA*, 2000.

[27] R. Erwin and T. Giorgio. Asymptotic statistics of the mutual information for spatially correlated racian fading MIMO channel with interference. *IEEE Transaction on Information Theory*, 75:235, 2010.

[28] A. Maaref and S. Aissa. On the capacity statistics of MIMO ricean and rayleigh fading channels. In *In Proc. IEEE Int. Conf. on Communications (ICC 06), Istanbul, Turkey*, 2006.

[29] G. Alfano, A. Lozano, A. M. Tulino, and S. Verd. Mutual information and eigenvalue distribution of MIMO ricean channels. *In Proc. IEEE Int. Sump.on Inform. Theory & Applications (ISITA 04), Parma, Italy*, 8:1040–1045, 2004.

[30] L. Yong Hua, L. Tie Jun, W. Xiao Fei., and Z. Lin. On the bounds of frequency-selective channel capacity with doubly correlated geometrical MIMO channel model. *The Journal of China Universities of Posts and Telecommunications*, 17:6–13, 2010.

[31] S. K. Jayaweera and H. V.Poor. Capacity of multiple-antenna systemswith both receiver and transmitter channel state information. *IEEE Trans. Inform. Theory*, 49:2697–2709, 2003.

[32] M. Fisz. Probability, calculus and statistics. In *3rd edition, State publishing Insitute, Warsaw*, 2008.

[33] Gee Rittenhouse. A 1000X of data-technology directions in the wireless market. In *Conference proceedings, IEEE Wireless Telecommunications symposium, Phoenix, Arizona*, 2013.

[34] Huawei Ghana White Paper. A proposal for a nationwide wimax implementation in ghana. In *submitted to NITA*, 2011.

CHAPTER 5

FIELD MEASUREMENTS

5.1 INTRODUCTION

The results of field experimental measurements carried out as part of the performance analysis of the deployed 2x2 MIMO configurations are presented in this chapter. Section 5.1 discusses the testbed used for the field measurements. The coverage, interference and capacity measurement results are subsequently presented.

5.2 FIELD MEASUREMENT

The testbed approach was chosen as one of the performance evaluation in this research in section 3.3. The testbed, shown in Figure 5.1, was used to test the real live performance of the WiMAX system under the Sub-Saharan African condition. The field trial measurement testbed comprised:

- Global positioning System
- Antenna (Kathrein omnidirectional with 2x2 MIMO configuration)
- RF cable
- dongle XCAL-X
- Laptop with a XCAL-X software
- WiMAX PCMCIA CARD
- Programmable field strength analyzer
- BS MIMO antenna model (SL12432A)

The measurements were divided into RSS, throughput and interference measurements [1–4]. The field trial was carried out in several parts of Accra and Tema which enabled testing of this technology under a typical Sub-Saharan terrain and clutter conditions. The experimental setup is as shown by Figure 5.2. The MIMO antenna measurements in this work deals with the network configurations of the BS antennas.

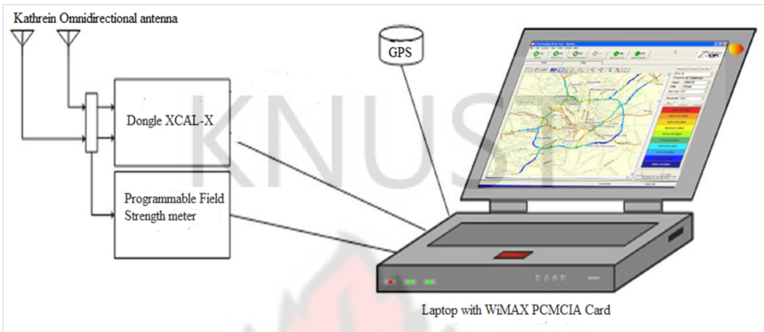

Figure 5.1: The employed performance evaluation testbed

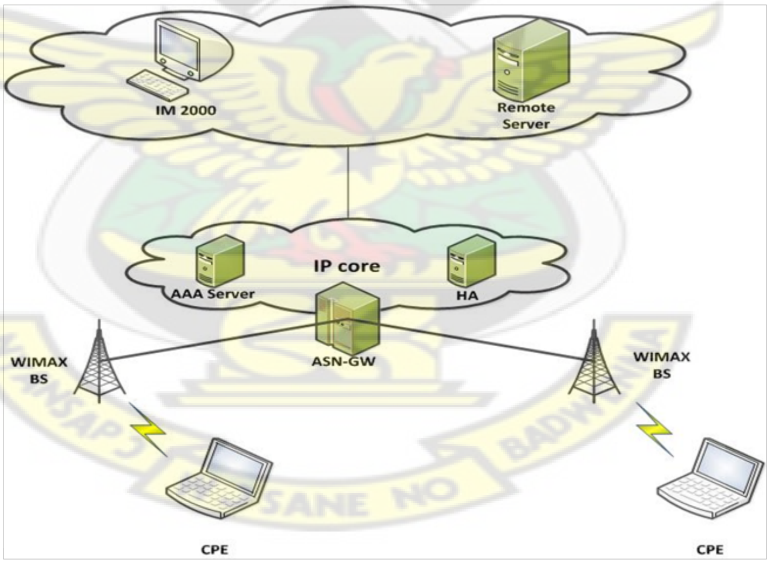

Figure 5.2: Field trial experimental setup

5.3 COVERAGE

The physical measurements collected Received Signal Strength (RSS) values in about 17,470 locations within the network. The first phase of the RSS measurement was to evaluate the simulated 4.90 km and 3.19 km coverage range for sites 1 and 2 respectively. The overview of the measurement areas for sites 1 and 2 have been shown in Figures 5.3-5.4.

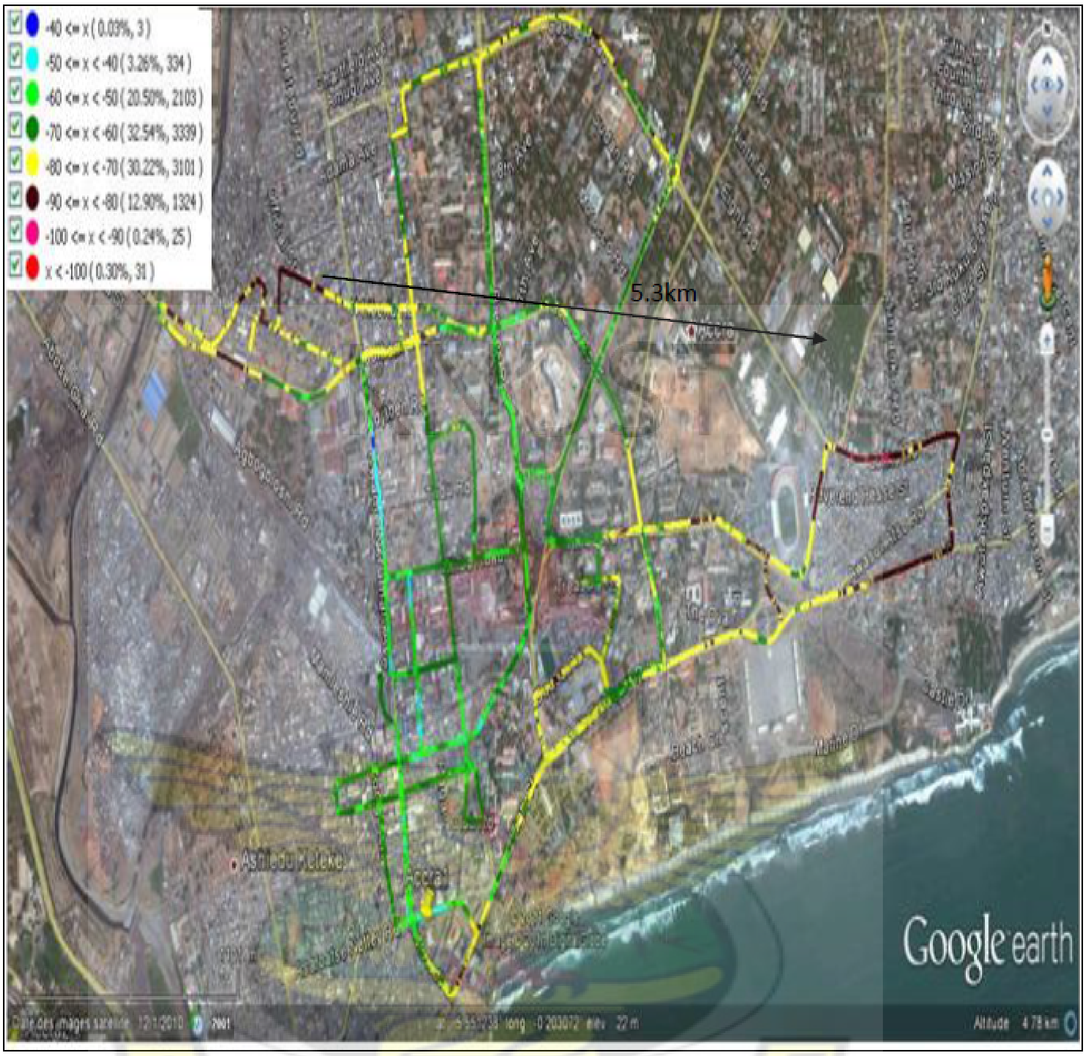

Figure 5.3: RSS Measurement Areas for Site 1

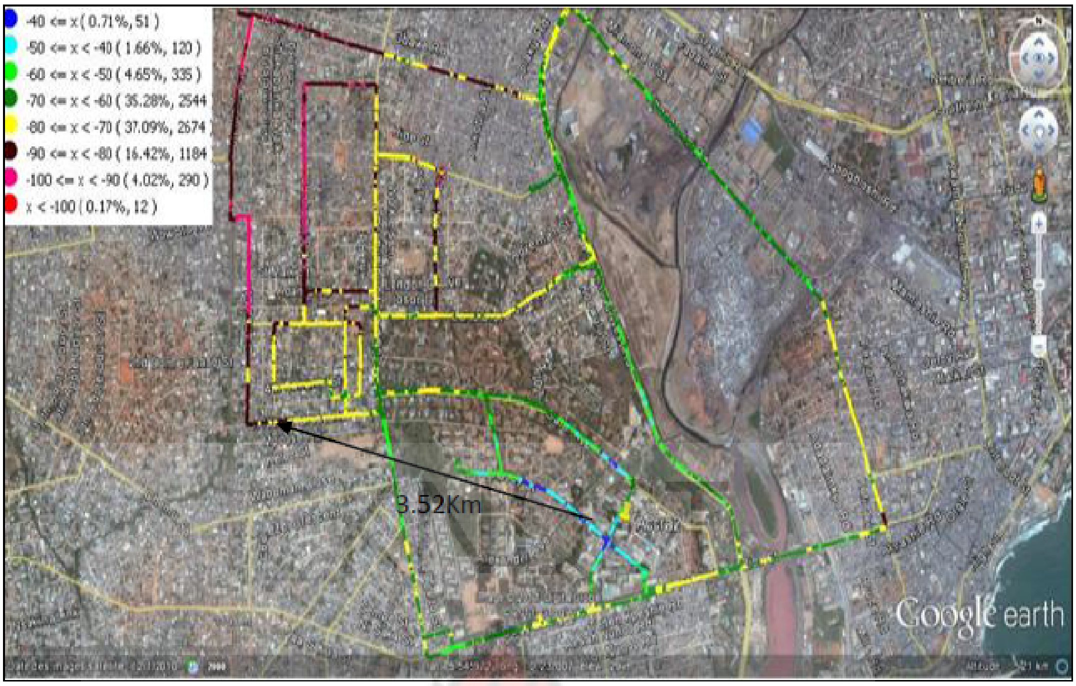

Figure 5.4: RSS Measurement Areas for Site 2

The results of the measurements have been summarized in Figures 5.5 and 5.6 below

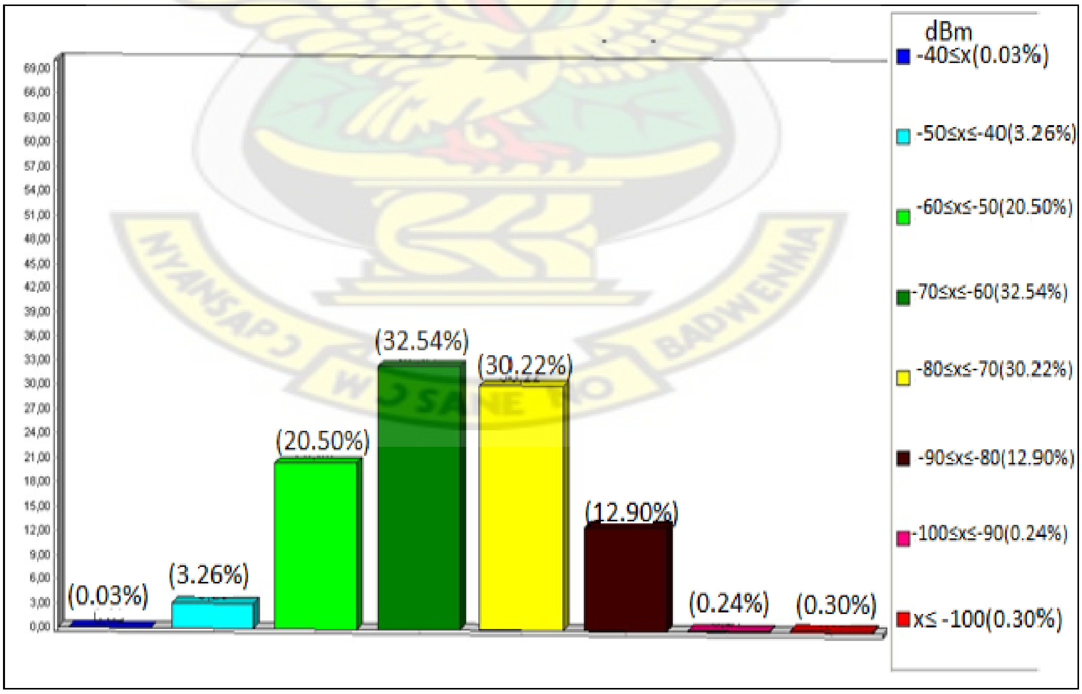

Figure 5.5: Summary of RSS Results for Site 1

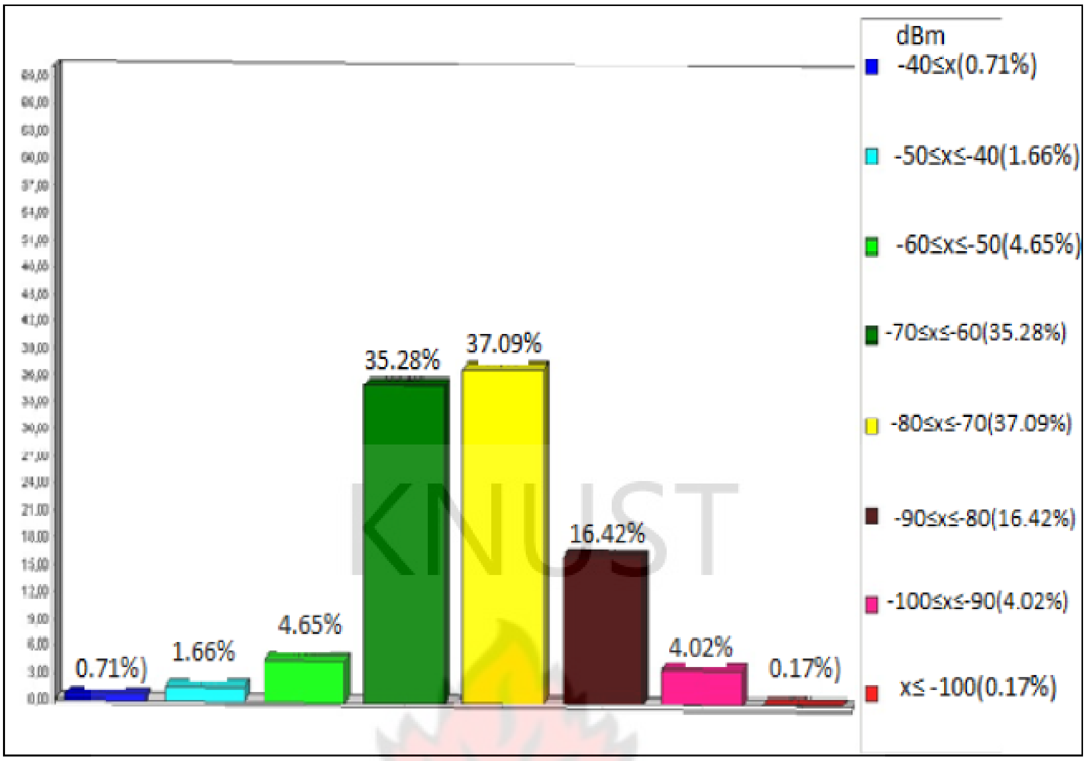

Figure 5.6: Summary of RSSI Results for Site 2

From the RSS measurements taken from about 10,206 locations in sites 1, about 86.55 % of the measured RSSI values were greater than -80dbm. From the site 2 measurements taken from 7,210 locations within the cell, 79.39 % of the measured RSSI values were greater than -80dbm. For the site 1 results shown in Figure 5.3, when the DL/UL split ratio was 26:21, 99.45 % of the measured values obtained from 500m to about 5.30 km away from the BS were greater than or equal to the simulated cell edge RSSI value of -90dBm. For site 2 results in Figure 5.4 on the other hand, with the same DL/UL split ratio of 26:21, 95.81 % of the measured RSSI values obtained from up to about 3.52km away from the BS, were greater than or equal to the simulated cell edge RSS value under NLOS condition. When the DL/UL split ratio for both sites were changed to 35:12, the measured coverage range for sites 1 and 2 were 4km and 2.67 km respectively. This confirmed the results in Eq. (4.8) that the coverage range of the cell depends on the uplink regardless of the downlink conditions.

The RSS and CINR measurements for other sites in the network are summarized in Figures 5.7-5.8 and Table 5.1

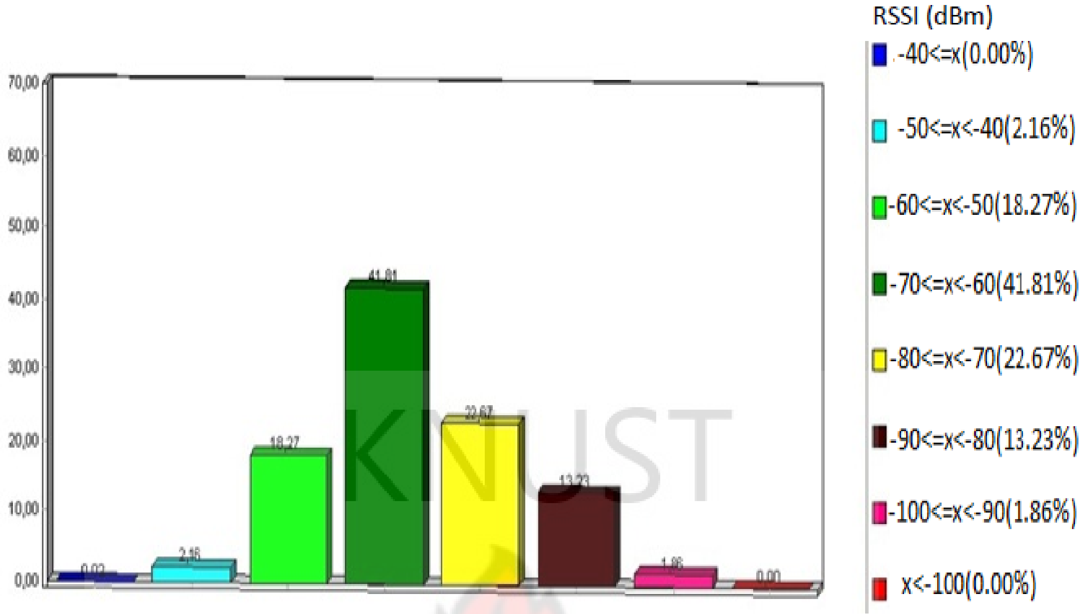

Figure 5.7: Measured RSSI during the field trial measurement

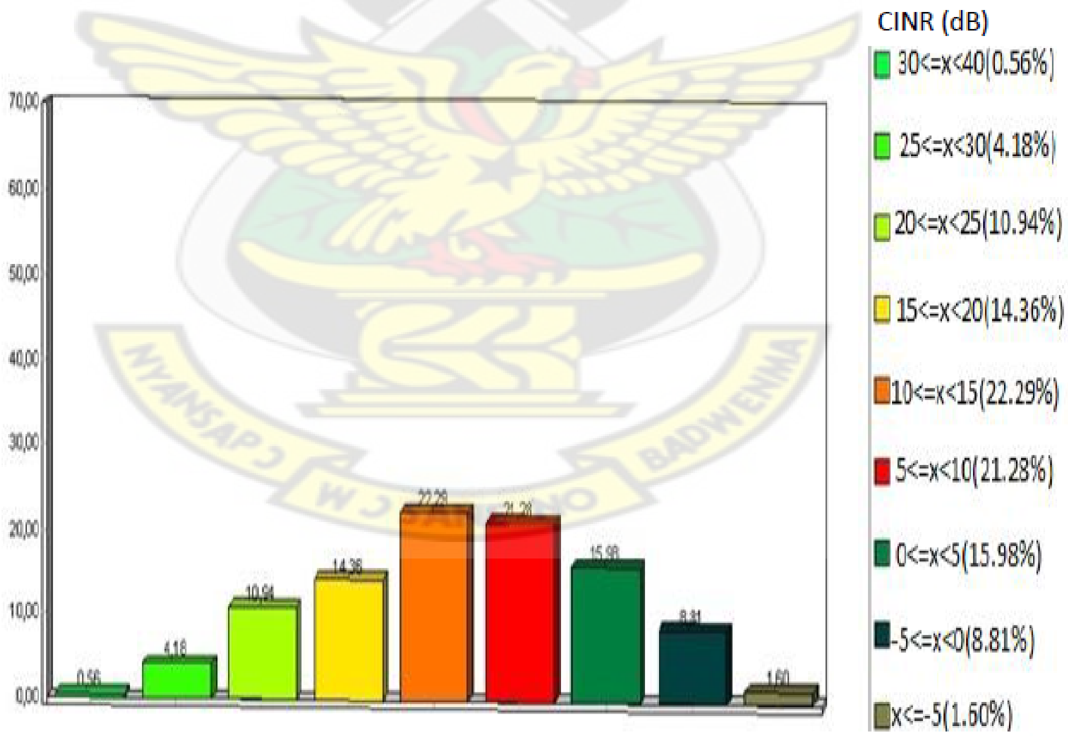

Figure 5.8: Measured CINR during the field trial measurement

Table 5.1: Comparison between field and simulated results

	RSSI (dBm)		Measured CINR (dB)	Modulation schemes	
	Simulated	Measured		DL	UL
Cell center	-40	-50	30	64-QAM	16-QAM
Cell edge	-92	-94	5	16-QAM	QPSK

From the RSSI measurements results in Table 5.1, the maximum measured RSS value of -50dBm was obtained with modulation schemes of 64-QAM and 16-QAM in downlink and uplink respectively to provide users with high connection speeds. The cell edge RSS was measured at about 3.20 km away from BS with a modulation scheme of QPSK in UL to make it possible for users to have access to the network even when the radio link was poor as evidenced by the measured value of -94dBm.

From the results in Figure 5.7, 84.91 % of the measured RSSI were greater than -80dBm which was an acceptable performance. Figure 5.8 shows that 73.6 % of the measured CINR were greater than 5dB. The simulated cell center and edge RSSI were -40dBm and -92dBm respectively but the measured cell centre and cell edge RSSI were -50dBm and -94dBm.

5.4 INTERFERENCE

In order to achieve the objectives of planning to provide coverage as required and predicted during the simulation stage and reduce channel interference levels as predicted for maintaining good quality of service in the network, it was relevant to carry out field measurement to relate the interference simulation results to practical scenarios. Real world measurements were carried out to determine the interference on the Base Stations at four selected sites; Accra sites 1, 4 and 8 and Tema site 1 based on their short inter-site distance. The Received Total Wideband Power (RTWP) for the various sector antennas were measured at the antenna front end. The measurement set up is shown in Figure 5.9. The measured

RTWP values at these four sites have been presented in Table 5.2 and Figures 5.10-5.13.

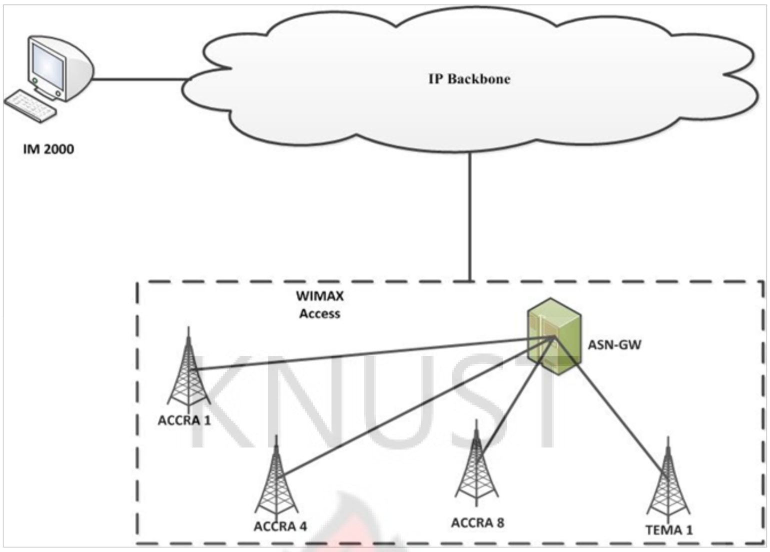

Figure 5.9: RTWP measurement setup

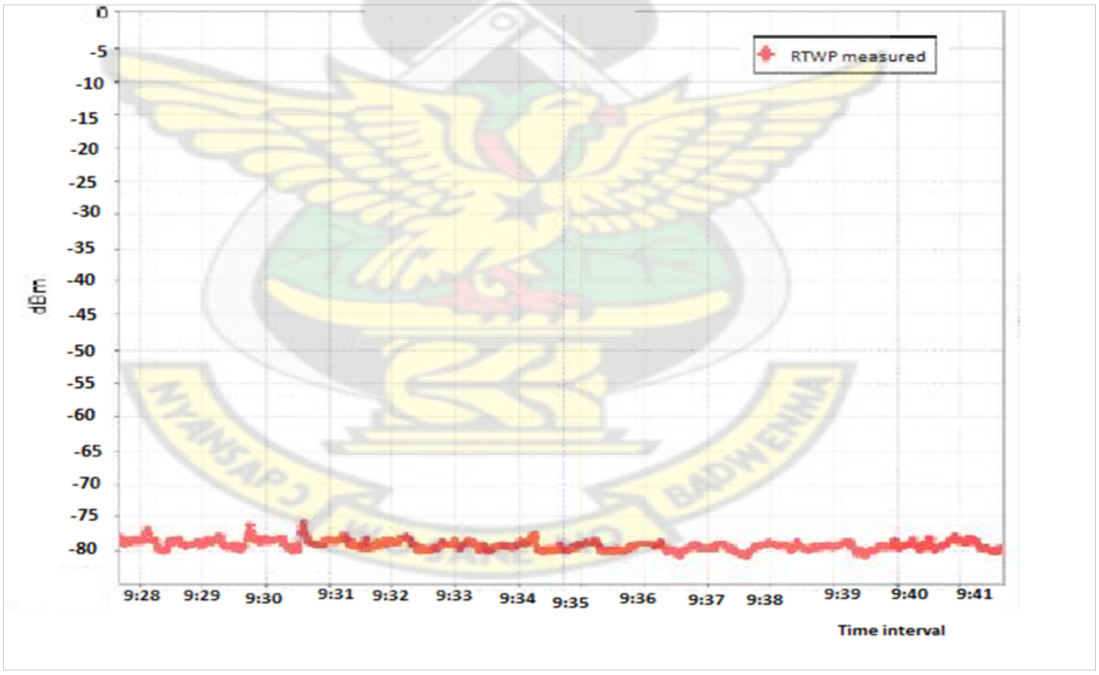

Figure 5.10: RTWP measurements for Accra site 8

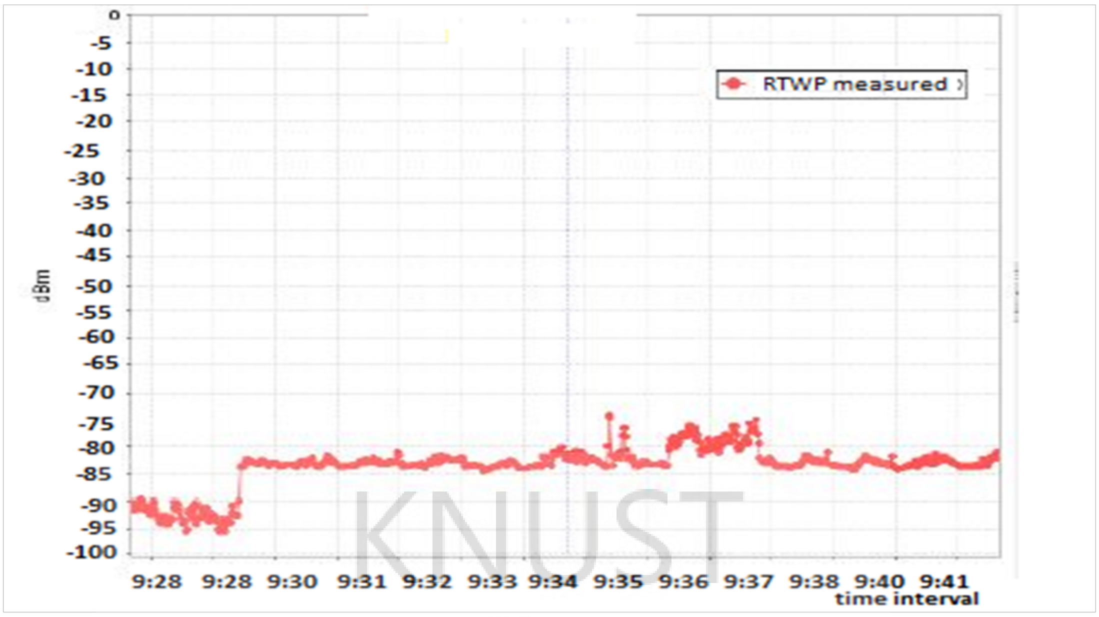

Figure 5.11: RTWP measurements for Accra site 4

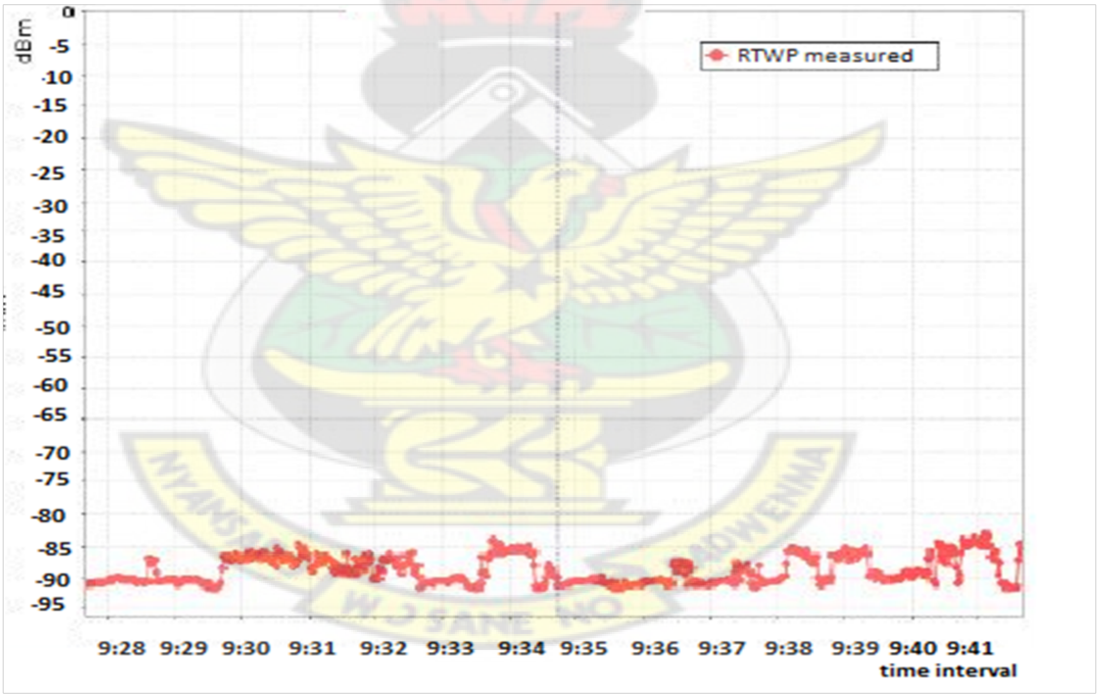

Figure 5.12: RTWP measurements for Accra site 1

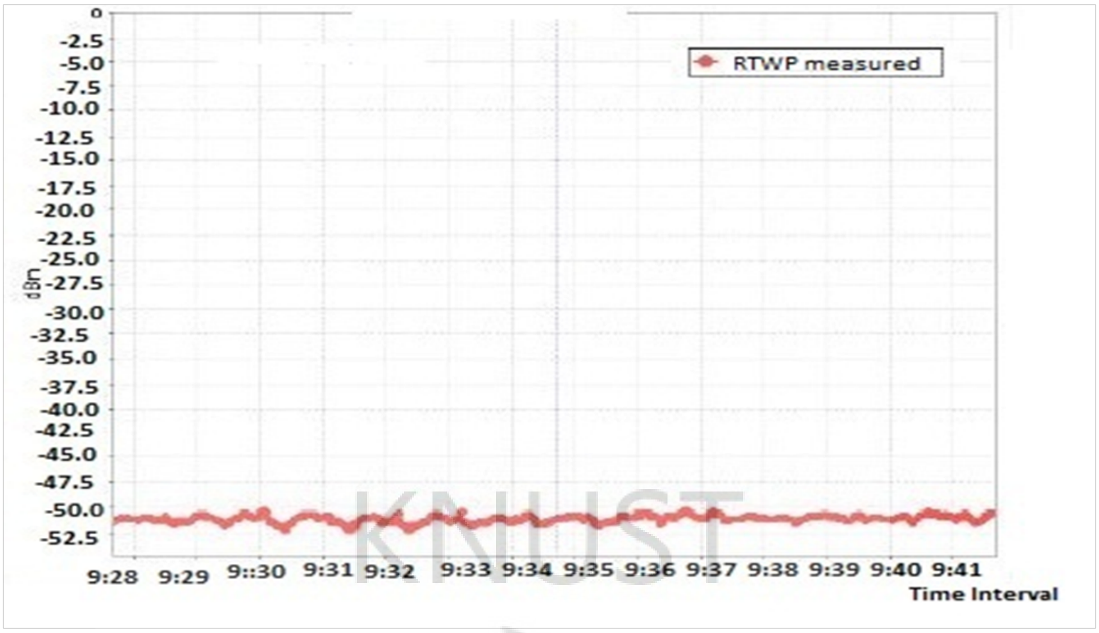

Figure 5.13: RTWP measurements for Tema site 1

From the RTWP measurements shown in Table 5.2, approximately 36% of cell sites were suffering from constant high RTWP levels and this will affect the overall network performance.

Table 5.2: RTWP measurement Results

Site	Sector	Min Measured RTWP (dBm)	Max Measured RTWP (dBm)	Average RTWP (dBm)
Accra site 1	Sector 1	-93	-83	-86
	Sector 2	-93	-82	-86
	Sector 3	-90	-85	-85
Accra site 4	Sector 1	-96	-74	-83
	Sector 2	-95	-76	-85
	Sector 3	-96	-76	-84
Accra site 8	Sector 1	-90	-75	-82
	Sector 2	-89	-76	-80
	Sector 3	-90	-76	-79
Tema Site 1	Sector 1	-55	-50	-52
	Sector 2	-53	-50	-52
	Sector 3	-52	-50	-52

The measured high average values RTWP of -86dBm, -84dBm, -80dBm and -52dBm measured in Accra sites 1, 4, 8 and Tema site 1 respectively were attributed to high sidelobe emissions from neighbouring BS. It was therefore necessary to carry out outdoor measurement to determine the source of the Radio Frequency Interference. The results of the outdoor interference measurements to trace the source of the interference in two sites are summarized in Figures 5.14-5.15.

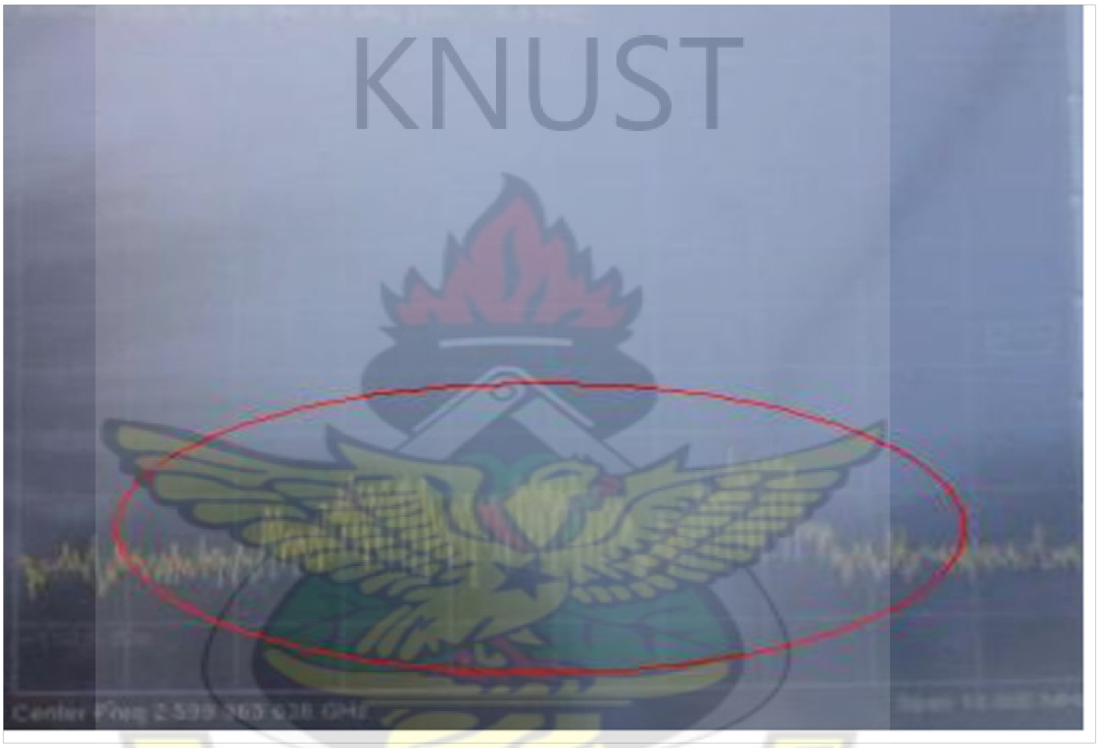

Figure 5.14: Outdoor interference measurements for Accra site 4

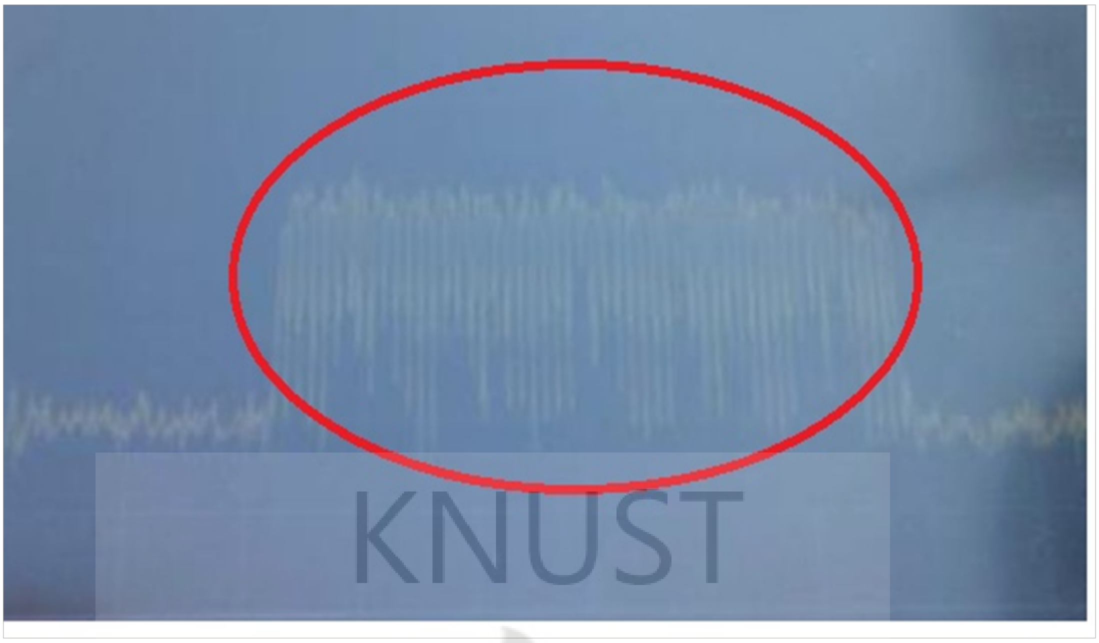

Figure 5.15: Outdoor interference measurements for Tema site 1

Interference measurements at the front end of the WiMAX antennas showed -86dBm and -60 dBm respectively. The major source of the interference in Tema site 1 was traced to a nearby BS operating on the same set of frequencies as Tema site 1. This confirmed to a large extent the presence of external RFI to the antenna systems.

The presence of high RTWP in the network validates the simulation of high interference level for the 2x2 MIMO configurations in the presence of multiple interferers. This reaffirms the need to use adaptive 4x4 MIMO configurations for future OFDM networks deployments under similar terrain profiles. The application of the proposed solutions discussed in sections 4.6 and 4.8 will enable future WiMAX network deployments to achieve a major objective of providing ubiquitous wireless broadband solution to subscribers.

5.5 CAPACITY

As part of the network capacity evaluation, FTP file size of 10MB was first downloaded from a remote server used for the experimental setup. Later, the same file size was uploaded unto the remote server. The result of the throughput measurements in sites 1 and 2, and some selected sites in the network have been summarized in Figure 5.16 and Table 5.3 respectively.

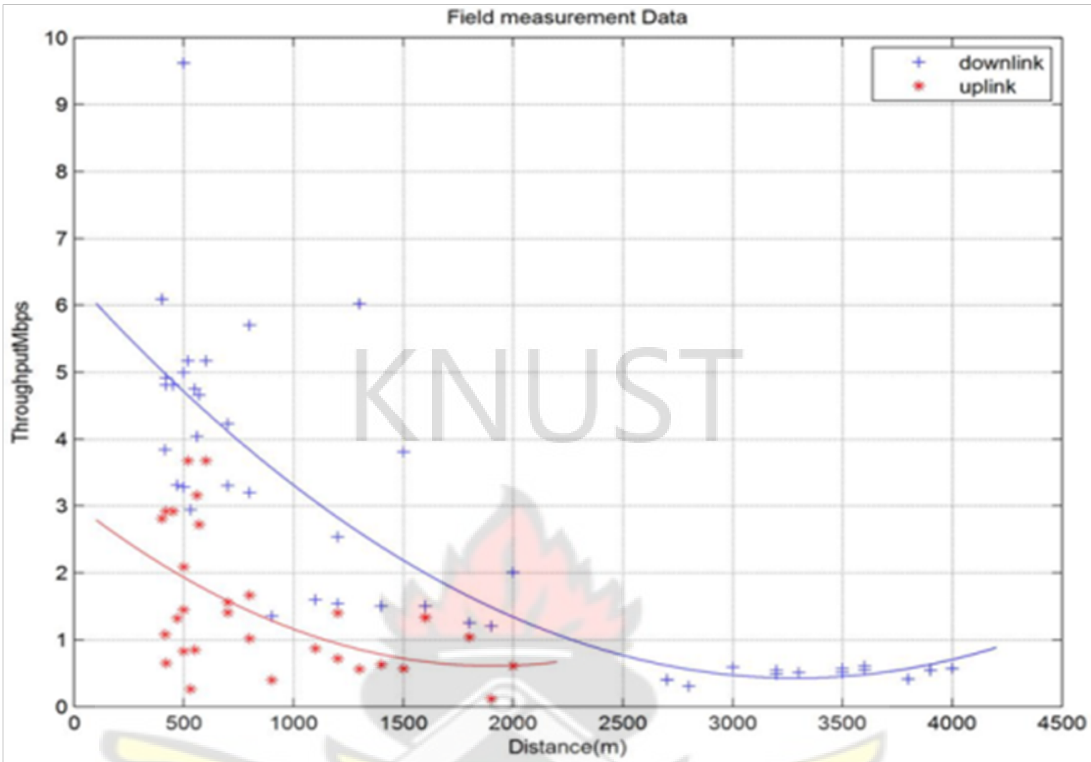

Figure 5.16: Throughput Measurements Results

Table 5.3: Measured average throughput per sector

Name	Sector	Height of Transmitter (m)	WiMAX Carrier Average Throughput per sector	
			DL Mbps	UL Mbps
Site1	Sector 1	38	6.09	2.81
	Sector 2	38	4.91	0.651
	Sector 3	38	4.99	2.09
Site 2	Sector 1	38	3.84	1.08
	Sector 2	38	9.62	0.825
	Sector 3	38	4.75	0.846
Site 3	Sector 1	38	3.31	1.32
	Sector 2	38	4.81	2.92
	Sector 3	38	5.17	3.68
Site 4	Sector 1	38	3.28	1.45
	Sector 2	38	2.94	0.26
	Sector 3	38	4.66	2.72
Site 5	Sector 1	38	4.04	3.16
	Sector 2	38	4.81	2.92
	Sector 3	38	5.17	3.68

Selected parameters results, such as throughput, latency and jitter, are shown in the Appendix. From the results, the maximum measured average throughput per sector was 9.62 Mbps as compared to simulated average throughput per sector of 15.85Mbps using the PUSC 1x3x3 configuration. The differences may be due to the use of BS antennas with optimally unsuppressed sidelobe emission. Moreover, the effect of reflection, refraction, scattering, rain fade, mineral composition and other environmental element were not modeled in the simulation and as such could not cater for such disparities.

The network performance as evidenced by the results above is quite good compared to other broadband technology field trial measurements carried out in similar environments in related evaluation works done in [5–8]. In [5], the maximum measured connection speed of 3.91Mbps was obtained at a distance of up to 500m away from the BS at a modulation scheme of 64-QAM by the authors.

Connection to the WiMAX BS dropped at about 1km away from the base station limiting the network's ability to deliver last mile broadband solution as promised by WiMAX.

In [6–8], a performance analysis of Long Term Evolution (LTE) was done. In [6] and [7], the measured outdoor throughputs of the LTE networks were 11.26 Mbps and 10.02 Mbps respectively. The maximum measured coverage of the LTE network in [8], located in the urban centre of Dresden, was 4.1 km with a cell edge throughput of 345 kbps. From throughput results in Table 5.3 and Appendix A, the measured cell edge throughput of 300 kbps at 4.0 km away from the Base Station of this newly deployed 4G-WiMAX network under evaluation is enough to support some broadband applications as indicated by Table 5.4 and as such the network will deliver as keenly anticipated by subscribers in Ghana.

Table 5.4: Broadband Speed Guide [9]

Activity	**Minimum Downlink rate (Mbps)**
Email	0.5
Job searching, navigating government websites	0.5
Interactive pages and short educational videos	1
Streaming radio Less than	0.5
Phone calls (VoIP Less than	0.5
Standard streaming videos	0.7
Streaming feature movies	1.5
HD-quality streaming movie or university lecture	4
Basic video conferencing	1
HD video conference and telelearning	4
Game console connecting to the Internet	1
Two-way online gaming in HD	4

It can also be seen that the capacity and coverage performance exhibited by the network under evaluation is good when compared to the performance of other broadband technologies in the environments studied in [5–8]. However, a network deployment using proposed adaptive 4x4 MIMO antenna configurations with optimally suppressed sidelobe emissions will further improve the network performance of the deployed WiMAX systems.

5.6 SUMMARY

A range of tests performed on the network confirmed the performance promised by WiMAX. This chapter has discussed the field trial measurements carried out in the deployed network. With WiMAX being a technology originally aimed at Line of sight (LOS) and near line of sight (NLOS) service with high modulation and the possibility of using fixed high gain directional antennas, an impressive performance of WiMAX has been demonstrated under these conditions.

REFERENCES

[1] E.T. Tchao, W.K. Ofosu, and K. Diawuo. Radio planning and field trial measurement for a 4G WiMAX network in a sub- saharan africa environment. *International Journal of Interdisciplinary Telecommunications and Networking*, 5:1–10, 2013.

[2] E. Affum, E.T. Tchao, W.K. Ofosu, and K. Diawuo. Stripping effects on partial-band uncorrelated interference rician MIMO system. In *Communications and Network, under review*, 2014.

[3] E.T. Tchao, K. Diawuo, and W.K. Ofosu. On the comparison analysis of two 4G-WiMAX base stations in an urban sub-saharan african environment. *Journal of Communication and Computer*, 71:865–872, 2013.

[4] E.T. Tchao, W.K. Ofosu, K. Diawuo, and E. Affum. Analysis of MIMO systems used in planning a 4G-WiMAX network in ghana. *(IJACSA) International Journal of Advanced Computer Science and Applications*, 4:197–201, 2013.

[5] Y.H. Lee, H. W. Tseng, W.C. Lee, Y.G. Jan J.Y. Lin, and H.W. Tsao. The

measurement and analysis of wimax base station signal coverage. *Progress In Electromagnetics Research C*, 25:223–232, 2012.

[6] Nokia Siemens Networks. LTE performance for initial deployments. In *White Paper*, 2010.

[7] K. Werner B. Hagerman, K. Wernergerman and J. Yang. MIMO performance at 700 MHz field trials of LTE with handheld UE. In *In Proceedings of the IEEE Vehicular Technology Conference*, 2011.

[8] 3GPP Release 8. Multisite field trial for LTE and advanced concepts. In *IEEE Communications Magazine*, 2009.

[9] Broadband Speed Guide. www.fcc.gov/guides/broadband-speed-guide. accessed online on 7th January,2013, 01 2013.

CHAPTER 6

BUSINESS APPLICATION AREAS

6.1 INTRODUCTION

From the initial problem statements in section 1.1, it can be reasonable understood that, the major aim of this thesis is to respond to a national need, and as such an application (WiMAX network deployments) has been chosen to help solve the problem. Chapters Four and Five have dealt with ways of optimizing the application. This chapter presents business application areas and concepts for the use of the optimized application to better the lives of the citizens of the country. This part of the research concentrates on selected key sectors of the economy namely [1–3]:

- Governance
- Health
- Power generation and distribution

Comprehensive discussions of the layout and network architecture for deploying a secured Supervisory Control and Data Acquisition system has been thoroughly discussed in [2] as part of this research.

6.2 ELECTRONIC GOVERNANCE IMPLEMENTATION

The arrival of new Information and Communication Technologies (ICTs) have significantly enhanced capabilities to collect, process and distribute information and as such many developing countries, including Ghana, are realizing the role ICT can play in the Governance sector. The National Information Technology Agency (NITA), which is the body charged in Ghana to provide technological advice and policy frameworks for Electronic Government (e-Government) service delivery, has deployed a pilot Electronic Government (e-Government) network with WiMAX technology in parts of Accra and Tema municipality in order to facilitate access to services such as e-mail, web services, data warehousing and government domain name administration. This pilot e-Governance network which is technologically simple is drastically changing the way information is distributed in Ministries, Departments and Agencies (MDAs) in Ghana.

This case study discusses the clear, comprehensive layout and network architecture of the e-Government model using WiMAX. Measurement results for traffic generation which were taken from four departments on the e-Government network before the WiMAX deployment is compared with performance evaluation results in this thesis.

6.2.1 Overview

There are several definitions of e-Government. The World Bank defines e-Government as the use of information technologies by Government agencies that have the ability to transform relations with citizens, businesses, and other arms of government (World Bank, 2005). These technologies can serve a variety of different ends:

- Better delivery of government services to citizens,
- Improved interactions with businesses and industries,
- Citizen empowerment through access of information,
- More efficient government management.

The resulting benefits can be less corruption, increased transparency, greater convenience, revenue growth, and cost reductions [4].

Ghana is a geographically challenged country with about 24 million people scattered throughout remote areas [5]. This presents a formidable barrier to sustainable growth and development. The empowerment of these remote rural areas is crucial for the overall development of the country. Bringing the people in the remote areas to the mainstream of digital technologies to access and adopt modern technologies is a major concern now in many developing countries [6].

The government of Ghana has therefore charged the National Information Technology Agency (NITA) to implement services which enables the use of ICT tools to transform the work process of government in providing more efficient, relevant and accessible, cost effective consultative and interactive services to its citizenry [7].

NITA, in order to achieve its aim, plans to use Information and Communication Technology and an affordable last mile broadband solution, WiMAX, to disseminate information to remote areas. Countries that have implemented e-Government successfully have used well-authored strategies and implementation plans. Examples of countries that have taken this approach include Singapore which has an e-Government Action Plan (eGAP) [8], Tanzania and Mozambique which have put in place e-Government implementation strategies and roadmaps [9].

This research presents the e-Government network model and bandwidth utilization measurements taken from five government departments with the highest traffic generation located within the network during a four month period and evaluates if the newly deployed WiMAX network can help deliver a reliable connection to support the proposed model.

6.2.2 Proposed E-Government Network

The National Information Technology Agency through its mandate seeks to develop and enforce ICT standards to promote interoperability and cost-effective ICT infrastructure and service solutions to promote government policies to the remotest parts of the country. They also seek to manage shared security infrastructure, networks, servers and services. In line with these objectives, NITA deployed an e-Government model as shown in Figure 6.1 using a combination of Microwave and Fiber connections to deliver broadband access to MDAs.

Due to the high cost involved and the limited coverage range for the network in the initial nationwide deployment, NITA intends to switch to WiMAX technology as shown in Figure 6.2 to provide a reliable cost effective nationwide coverage to achieve the main objective of providing last mile broadband solutions to MDAs in rural areas.

Figure 6.1: Initial e-Government Network

In order to implement the e-Governance model to build a well informed and participatory citizenry to enhance good governance, a pilot deployment with WiMAX technology has been done in Accra and Tema municipality. The objective of this network deployment is to assist the Government of Ghana to generate growth and employment by leveraging Information and Communications

Technology (ICT) and public-private partnerships to develop the IT enabled services industry. This will contribute to improved efficiency and transparency of selected government functions through e-government applications as have been achieved by e-Government projects deployed in Nepal, Bangladesh and India [10–12]. Later on, based on the success of the pilot network, the e-Governance project through WiMAX connectivity will be replicated throughout the regional and selected district capitals in the country as shown in Figure 6.2.

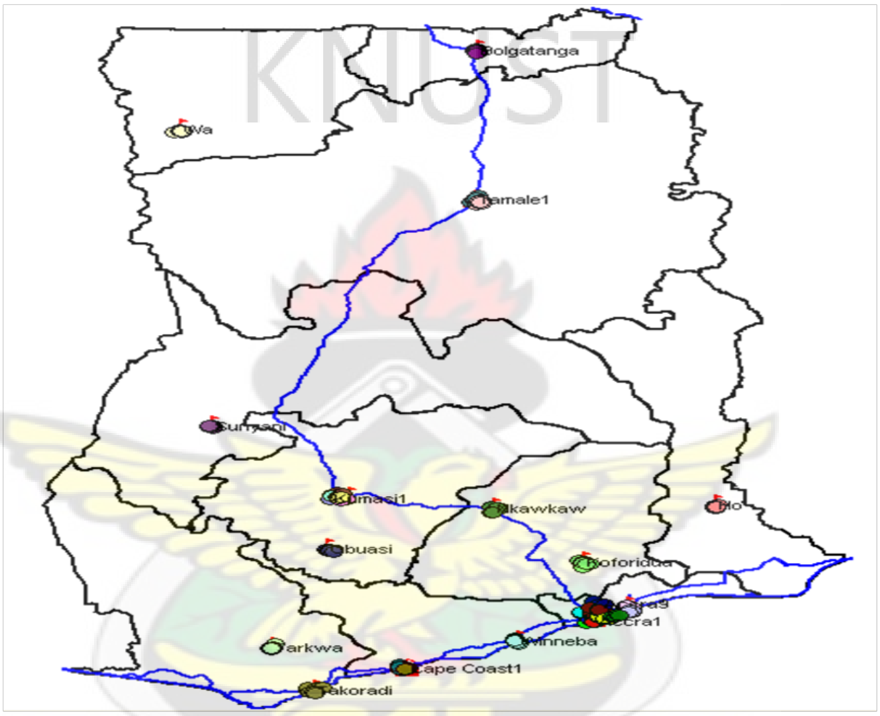

Figure 6.2: Proposed nationwide coverage using WiMAX Sites

A proposed network architecture which can be used in implementing the e-Government model is shown in Figure 6.3. The ultimate aim of the proposed e-Government network will be to ensure that even the remote MDAs can access affordable and stable broadband Internet services. This proposed solution includes macro cell and indoor access solutions, and provides adaptive network planning for different scenes. Flat network architecture and distributed base stations will have to be deployed to ensure fast network establishment to reduce capital expenditure (CAPEX) and operational expenditure (OPEX).

An end-to-end WiMAX solution with product lineup including terminals, access, transmission, and application layer equipments will be used with the Vodafone's backbone transmission being the nerve center for this proposed network architecture. This backbone transmission will help link the various sub networks which will be located all over the country for efficient network deployment as shown in Figure 6.3. The network will comprise the Accra and Kumasi sub networks which will be connected to Vodafone's backbone transmission by National Communication Backbone Company (NCBC) liaison Gigabit Ethernet (GE) whiles Tamale, Nkawkaw, Obuasi, Koforidua, Takoradi, Ho, Sunyani and Cape Coast networks will be linked to Vodafone's backbone transmission by the NCBC liason fast Ethernet. Wa and Bolga will be linked by Satellite. The design will incorporate a distinctive distributed Base Station which consists of Base Band Unit (BBU) for indoor installation and Remote Radio Unit (RRU) for mounting on walls or poles. An Advanced Power Module (APM) will be used to accommodate BBU for outdoor installation. The use of optical fiber cable to connect BBU and RRU will ensure low cable loss and high tolerance to noise.

There will also be an Access Service Network Gateway (ASN-GW), which will be based on a telecom-grade platform with high reliability and full redundancy provision. It will serve as a gateway to the Connectivity Service Network (CSN). The proposed connectivity service network shown in Figure 6.4 will provide:

- Data connectivity through Gigabit Ethernet (GE) or fiber to the regional capitals, and a point to multi-point WiMAX connection from the regional capitals to all the governmental agencies within the region.
- Voice connection through an IP based Private Automated Branch Exchange (PABX)
- Video-conferencing connectivity to connect concurrent video-conferencing sessions even from the remote districts in real time.

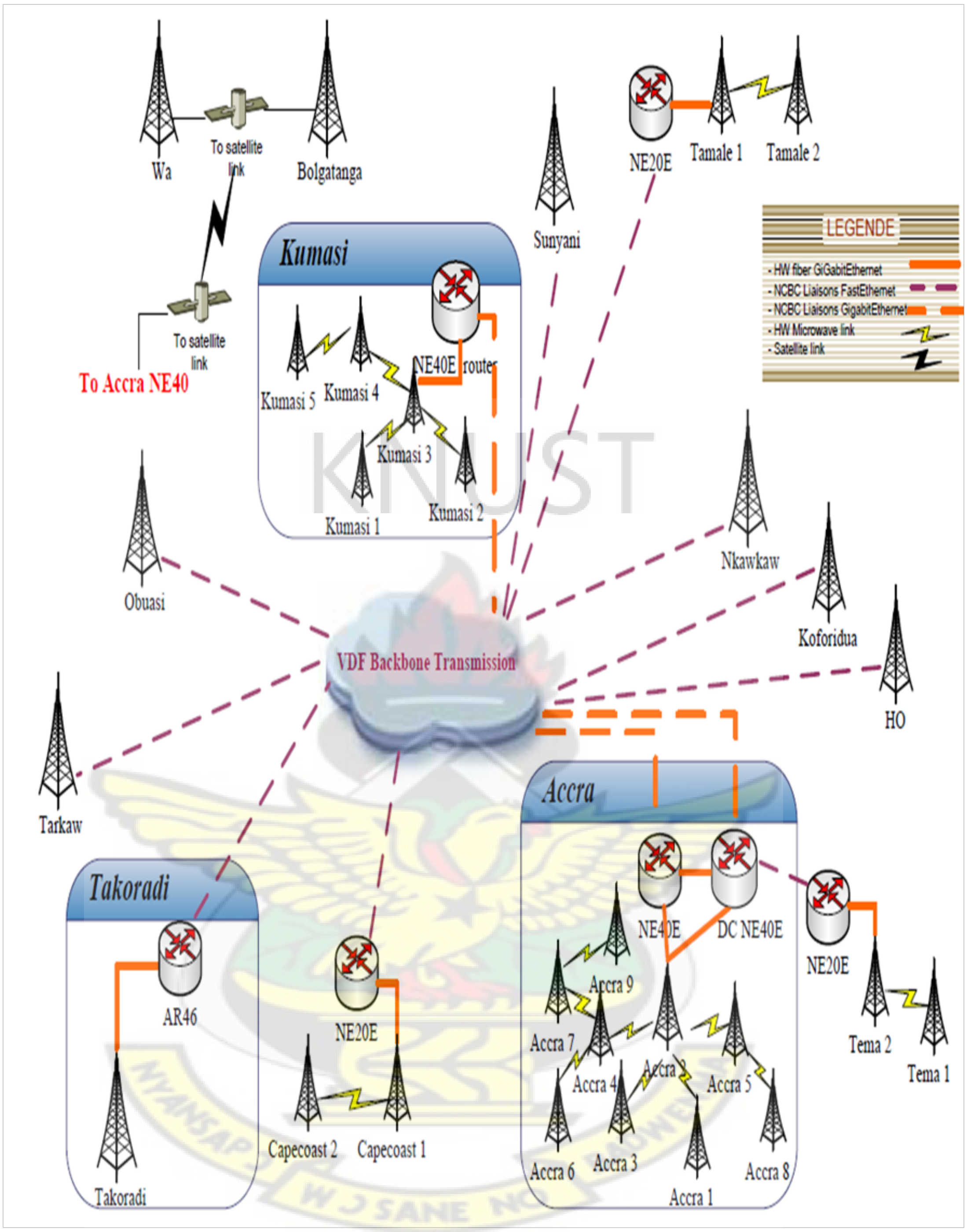

Figure 6.3: Proposed Network Architecture for Countrywide WiMAX deployment

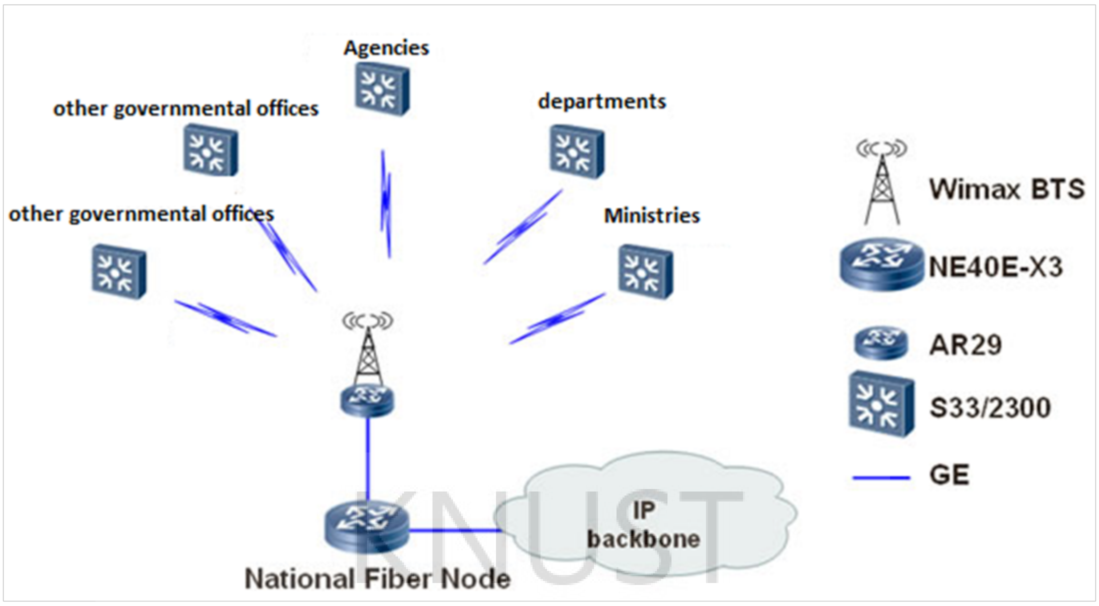

Figure 6.4: Connectivity service network for the e-Government Network

In order to determine the pilot WiMAX network under evaluation's ability to provide broadband access to implement the proposed model, mapping for the distribution of Government agencies and CPEs in the network has been done and is shown in Figure 6.5.

The distribution of governmental agencies on the network, shown in Figure 6.5 comprises some key agencies like the Regional Coordinating Council, the Audit Service, Controller and Account General's Department, Parliament house, the Data Center and Policy Evaluation Department. CPEs in the network will comprise fixed users (offices) and mobile users (who are mostly in the form of police and military patrol vans, IRS tax collectors).

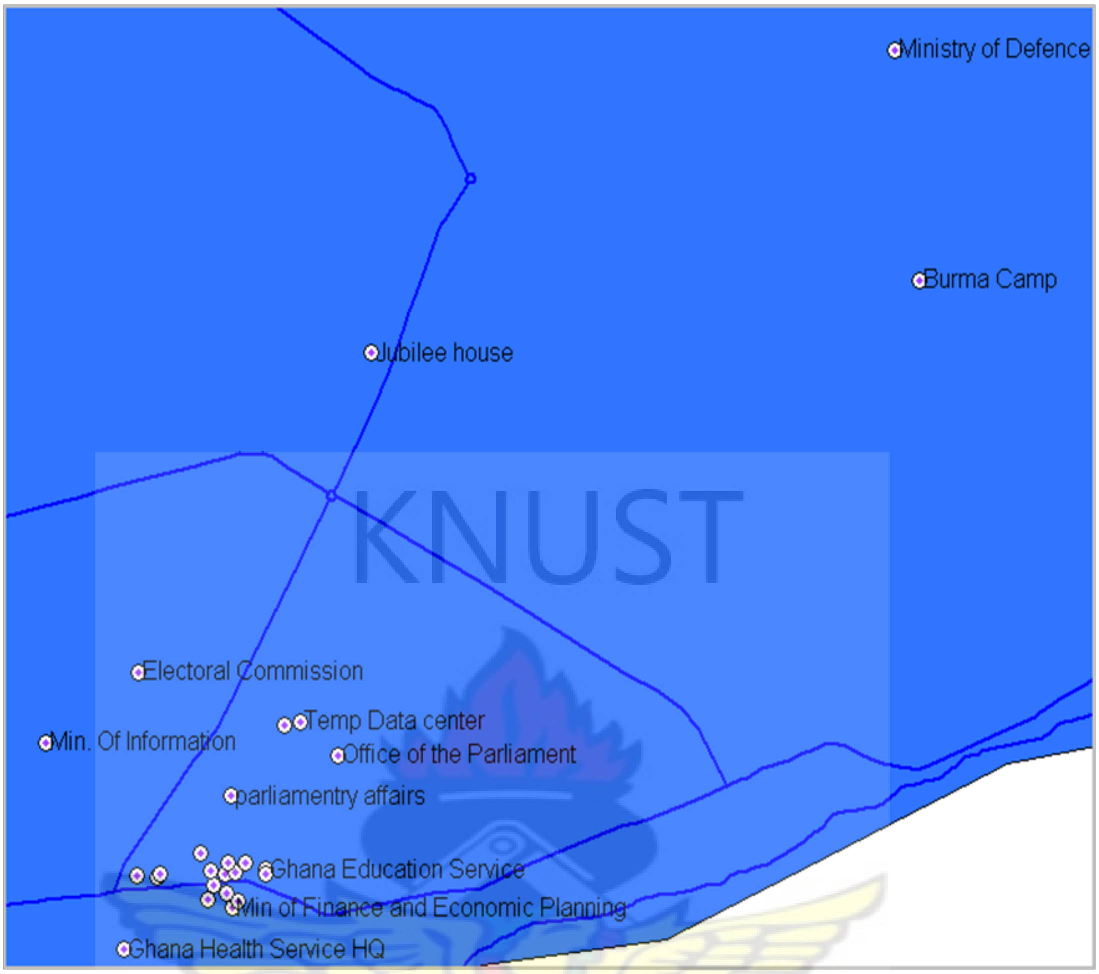

Figure 6.5: MDAs in the Pilot Area

6.2.3 Traffic Measurement

The traffic from four departments in the pilot area within a four months period (February-May, 2012) was measured prior to deploying the WiMAX network. The results of the measurements are shown in Figures 6.6-6.9. The inbound and outbound rates denote the downlink and uplink throughputs respectively.

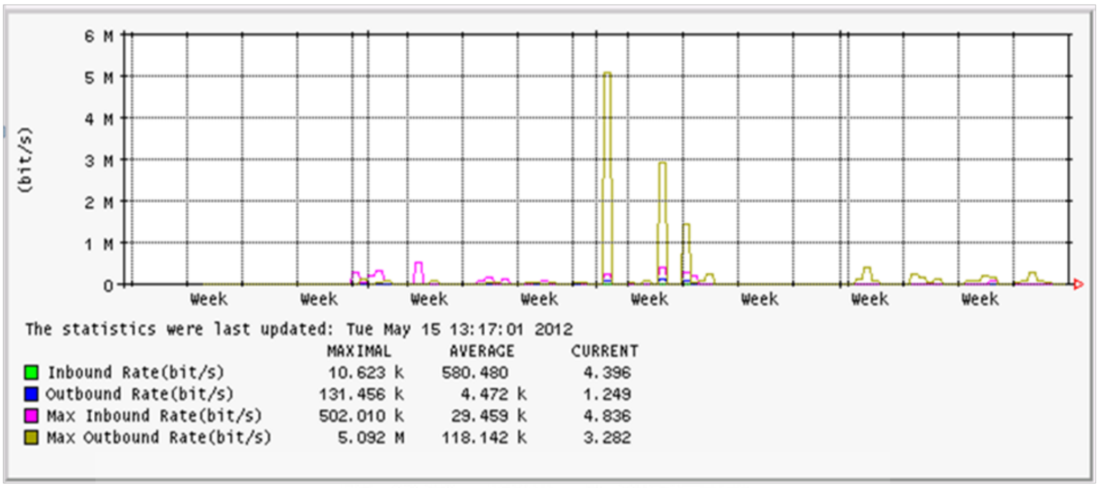

Figure 6.6: Traffic generation from the Regional Coordinating Council

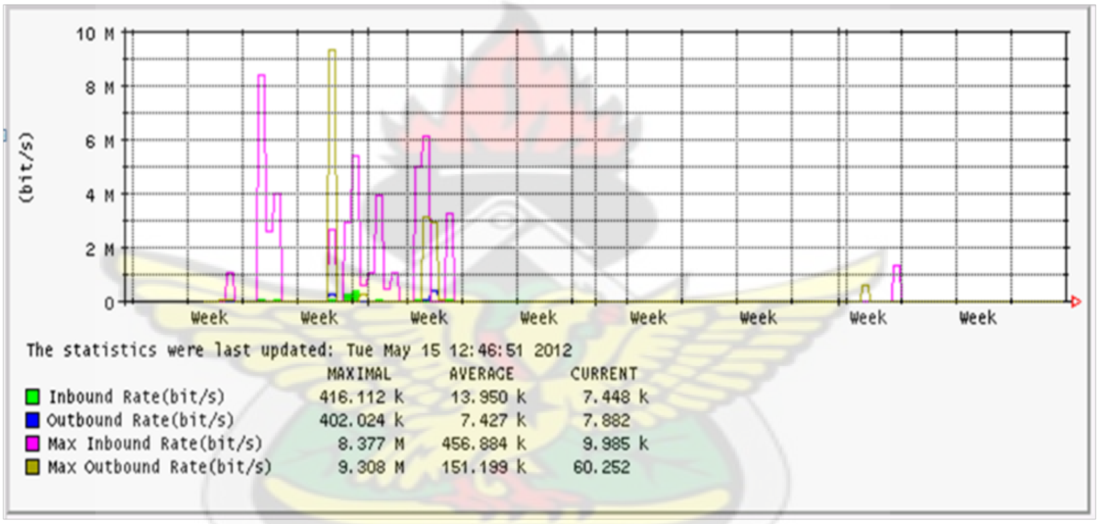

Figure 6.7: Traffic generation from the Data Center

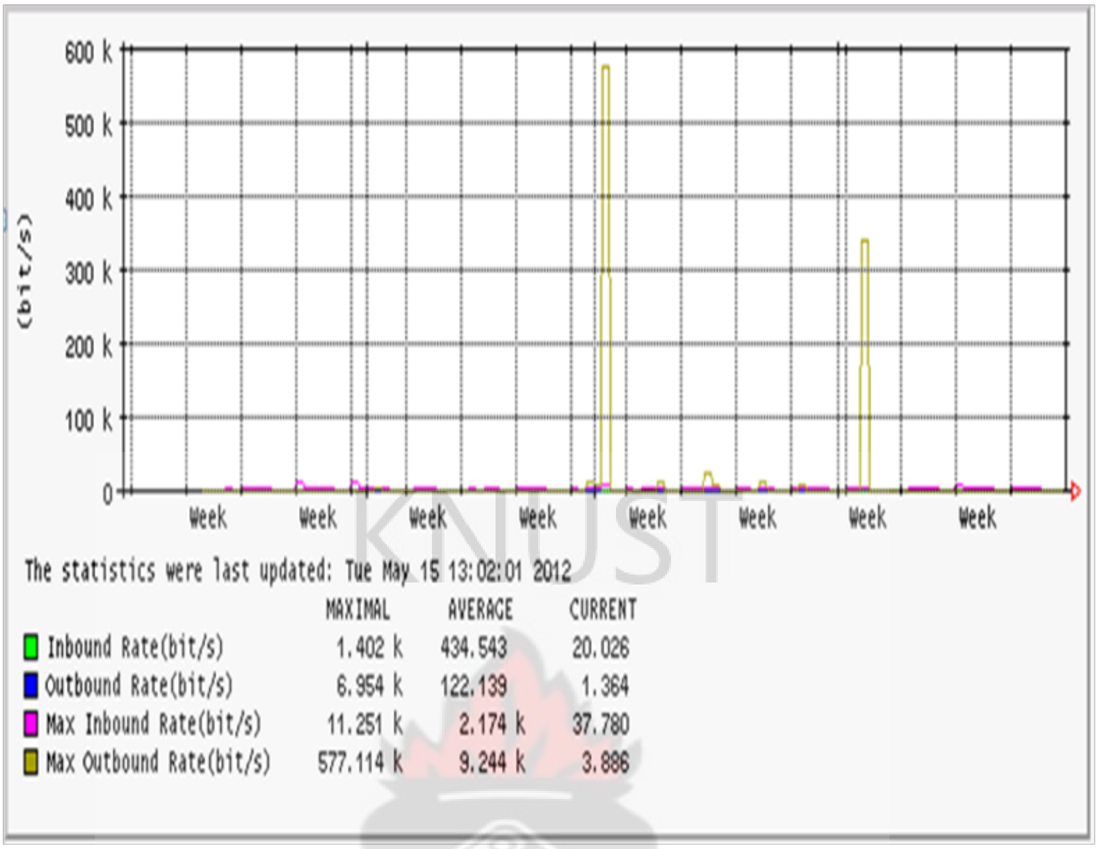

Figure 6.8: Traffic generation from the Audit Center

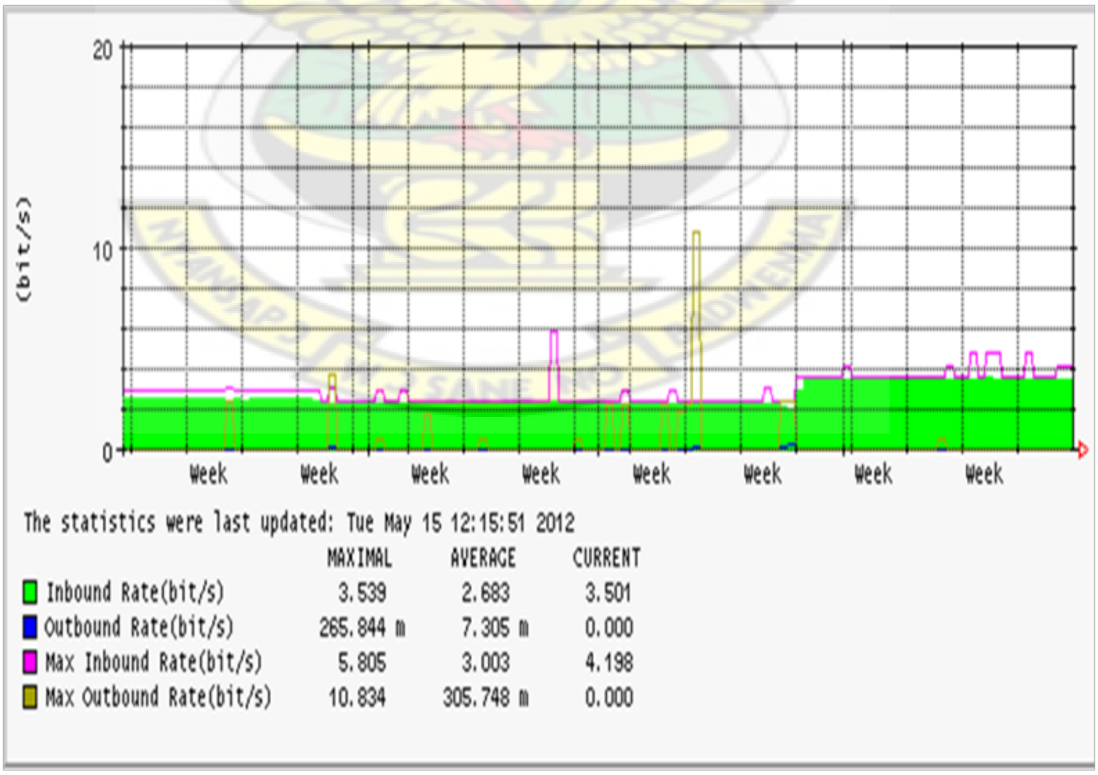

Figure 6.9: Traffic generation from the Brand Center

From the traffic measurements in Figures 6.6-6.9, it can be seen that the highest traffic generation came from the data center with a maximum outbound traffic of 9.308Mbps, Regional Coordinating Council with 5.092Mbps and Brand Ghana having the least maximum outbound traffic of 10.834kbps. From the network evaluation done in this research, the maximum measured average throughput per sector of 9.62Mbps in site 2 is enough to cater for the bandwidth utilization by the Data Center in site 2.

Based on the success of the pilot network, a nationwide deployment of WiMAX network can be done using the wide area connectivity plan described in this case study. This will enable the government to implement applications like:

- Integrated Payroll and Personnel Database for government workers by the controller and Accountant General?s department
- Integrated Financial Management Information System by the Ministry of Finance and Economic planning
- online TAX returns by the Internal Revenue Service
- Biometric Passport applications by the Ghana Immigration Service
- National Identification application processing by the National Identification Authority.

With WiMAX promising high bandwidth gains and longer distance of coverage for the e-Government network as have been presented in sections 5.1 and 5.3 , it is highly expected that WiMAX will help remove the geographic barrier which retards rural development and dissemination of Government policies to the rural areas in Ghana.

6.3 MOBILE TELEMEDICINE IMPLEMENTATION

Telemedicine has become an effective means of delivering quality healthcare in the world. Across the African continent, Telemedicine is increasingly being recognized as a way of improving access to quality healthcare. The use of technology to deliver quality healthcare has been demonstrated as an effective way of overcoming geographic barriers to healthcare in pilot Telemedicine projects in certain parts of Kumasi, Ghana. However because of poor network connectivity of the pilot projects, the success of the pilot network could not be extended to cover the whole city of Kumasi and other surrounding remote Villages. Fortunately, recent deployment of WiMAX in Ghana has delivered higher data rates at longer distances with improved network connectivity. This case study examines the feasibility of using WiMAX in deploying a city wide Mobile Telemedicine solution. Five WiMAX Base Stations have been suggested to give ubiquitous coverage to the proposed Mobile Telemedicine vans in the network using adaptive 4x4 MIMO antenna configurations.

6.3.1 Overview

Telemedicine involves the delivery of healthcare and related information over long distances by combining biomedical signals with information technology and means of communication [13]. The use of wireless technology to deliver health information has been demonstrated as an effective way of overcoming certain barriers to healthcare, particularly for communities located in rural and remote areas. Telemedicine has helped to bridge the gap in providing crucial care for those who are underserved, mainly due to inadequate health personnel [14]. Mobile Telemedicine is an improved form of Telemedicine, in which advanced wireless communication systems are used to deliver the biomedical signals of patients anywhere and anytime [15].

Mobile Telemedicine uses high capacity mobile communication systems such as 3G+, WiMAX and LTE to deliver protected health information over long distances. This capability of mobile Telemedicine has made it possible to deliver improved medical services such as emergency ambulance service [16], mobile hospital [17], general healthcare and early warning systems for diseases [18].

Ghana currently has a doctor to patient ratio of 1: 10,380 and 1:23, 456 in the urban and rural areas respectively [19]. This is a major challenge in delivering quality healthcare especially in the rural areas. In order to provide quality healthcare to the rural areas, the government of Ghana is striving to use the advances in healthcare delivery to provide quality healthcare to its citizenry. As part of project works at University of California Berkeley and Intel Research, a pilot Teleconsult based on experiences and reports from similar applications implemented in developing countries reported in [20] was implemented for selected health centers in Ghana [21]. Other pilot Telemedicine projects have also been implemented as part of the Millennium Villages Project in about 23 remote villages to help deliver affordable and accessible healthcare to the deprived communities.

The major setback to a nationwide implementation of these pilot Telemedicine projects was found to be inadequate bandwidth to support these Telemedicine applications. The 256 kbps provided by the existing 3G networks in outdoor locations is inadequate to support the major Telemedicine applications as specified in [22]. The government in its quest to deploy a reliable Telemedicine system has decided to use its recently deployed WiMAX network in several cities in the country to provide improved network connectivity to the existing Pilot Telemedicine projects. The selected cities for Telemedicine implementation is shown in Figure 6.10.

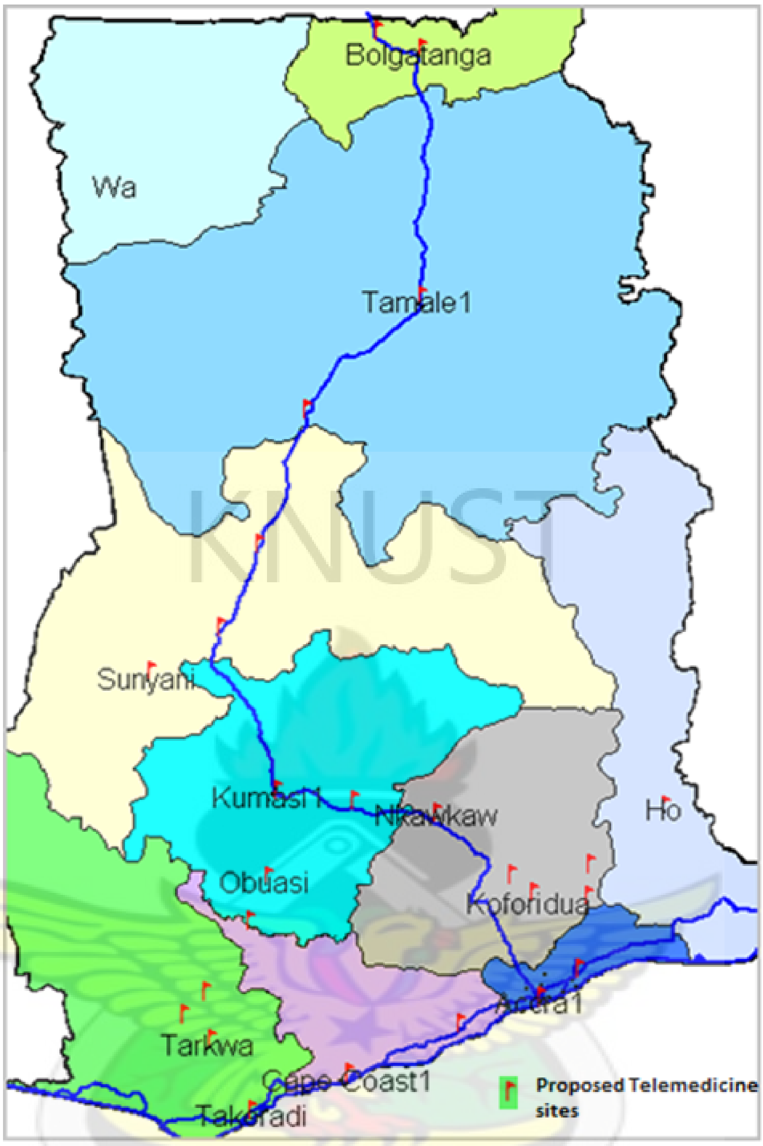

Figure 6.10: Proposed nationwide Telemedicine sites

This case study evaluates the existing Telemedicine systems in Kumasi and examines the possibility of a citywide deployment using WiMAX to develop a mobile Telemedicine system with multi-communication links for the city of Kumasi.

6.3.2 Deployed WiMAX Network Architecture

The proposed WiMAX network which will be deployed by the National Information Technology Agency (NITA) in Kumasi to provide wireless access for implementing an Electronic Governance system in Kumasi is shown in Figure

6.11. The proposed network architecture for the e-Government model will ensure that remote government Ministries, Departments and Agencies in Kumasi can access affordable and stable broadband internet services.

Flat network architecture and five (5) distributed Base Stations have been suggested to serve the MDAs, shown in Figure 6.12, in and around the city.

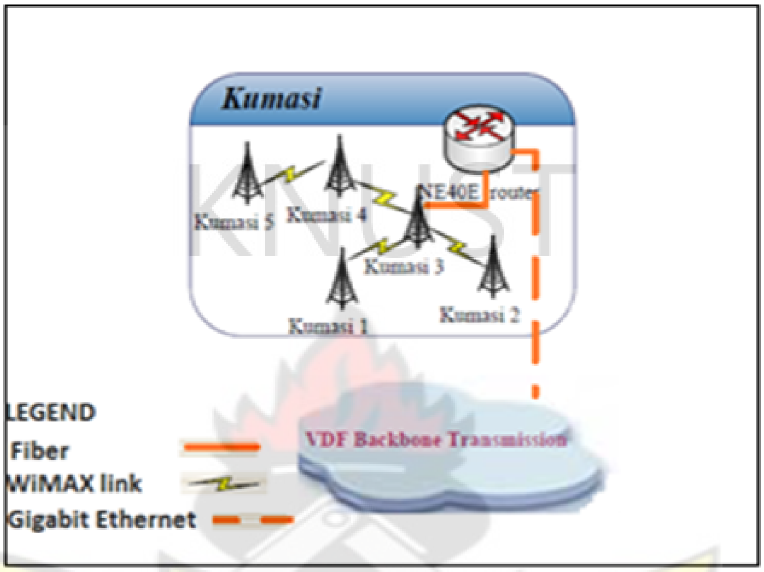

Figure 6.11: E-Government model

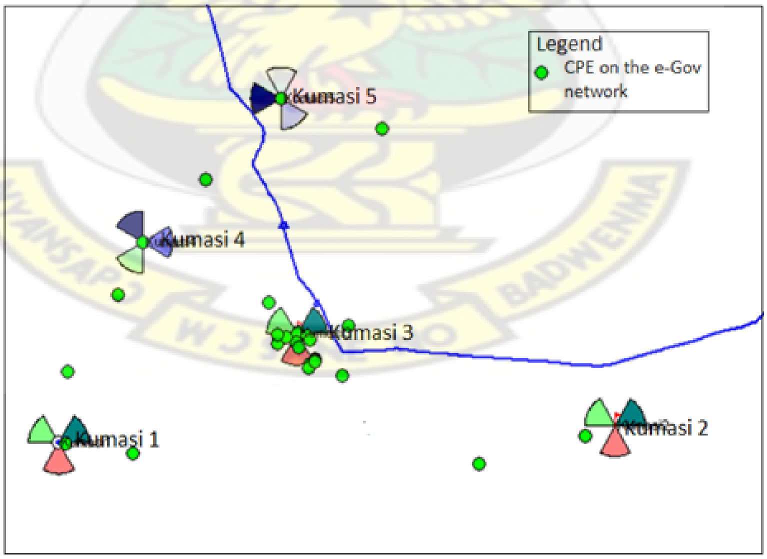

Figure 6.12: Proposed WiMAX site model

The WiMAX sites have been chosen using the estimated coverage range of the adaptive 4x4 MIMO configuration to provide coverage for the whole Kumasi metropolis.

6.3.3 Existing Telemedicine Applications

One of the more significant developments over the past decades has been the emergence and pilot usage of information and communication technologies in healthcare delivery in Ghana. There are several pilot Telemedicine applications in Ghana. These Telemedicine applications are focused on diagnostics and consultation. These systems have also been used for other healthcare service applications and have been considered to be particularly useful in many remote areas in the Millennium Villages Project. While Telemedicine systems in developed countries can have different goals, the basic objective of the existing systems in Ghana has to be scalable, ranging from establishment of basic Telemedicine services, and later upgraded to advanced up to date functionalities. The basic concepts that the existing systems are based on, include creating the necessary basic Medical Information Systems (MISs) in hospitals and developing a framework and interfaces where various multiplatform MISs could interconnect in an integrated MIS. This is more evident in pilot project implementation at Komfo Anokye Teaching Hospital (KATH) and Kwame Nkrumah University Hospital to enable medical students at Kwame Nkrumah University of Science and Technology (KNUST) learn and Teleconsult on the University campus.

Because of poor network connectivity, many existing Telemedicine systems in Ghana have not been able to go beyond the development of the framework and interfaces where various multiplatform management information systems (MISs) have been interconnected in an integrated MIS. This is mainly because of the non-existent modern telecommunication technologies to support connection of the integrated MIS to enable provision of advanced medical services at remote locations in the country. This limits the use of the integrated MIS for various Telemedicine applications such as sharing knowledge, experience and expertise among physicians in different hospitals even within the Kumasi metropolis.

6.3.4 Proposed Mobile Telemedicine Network

The Ministry of health in conjunction with the National Road Safety Commission has deployed emergency ambulance service on pilot basis in major cities and highways over the country. These emergency response ambulance services have played an important role in reducing the number of deaths caused by car accidents and other medical emergencies in Kumasi. With the current system, voice communications over a mobile phone is used between the paramedics and the emergency ward physician to provide relevant pre-hospital medical care. To effectively promote the possibility of future recovery, better medical care should be provided between the time at which paramedics arrive at an accident or emergency scene and before an ambulance arrives at a hospital. With the improved network connectivity WiMAX deployment in the country will offer, it will now be possible to carry out voice and video interactions for pre-hospital medical care in the ambulance.

Documented results in implemented mobile Telemedicine services suggests that real-time video distributed over a reliable high speed internet connections is a valuable aid in diagnosing and improving treatment in the case of suspected stroke victims in [23, 24]. As such, a mobile telemedicine system which will coexist with current telemedicine systems in two major hospitals in Kumasi, KNUST Hospital and KATH, using WiMAX technology is proposed in this thesis. The proposed mobile telemedicine network is shown in Figure 6.13.

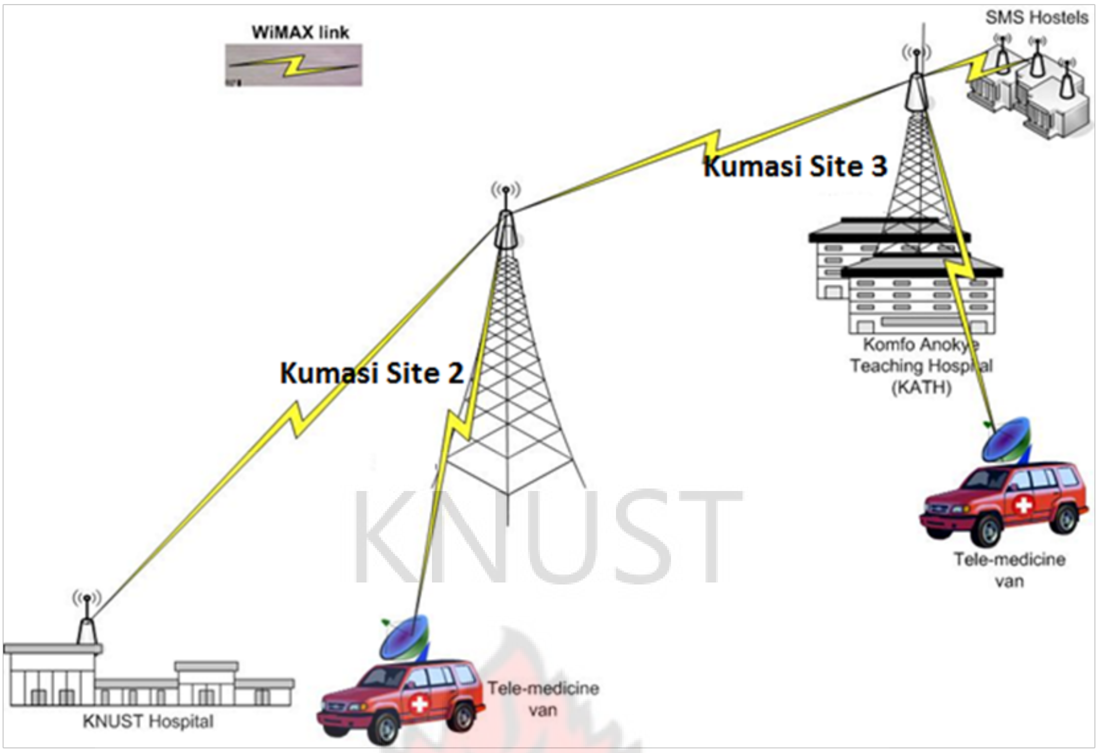

Figure 6.13: Proposed Mobile Telemedicine network layout

In designing the proposed Mobile telemedicine network, the transmission platform and transmission speed were considered. WiMAX was chosen as the microwave access system on the basis of factors such as real-time operation, transmission reliability, interference and system bandwidth. Initial field measurement of the deployed WiMAX network indicates WiMAX ability to deliver on all the factors necessary for implementing an effective Mobile Telemedicine system in Kumasi. The framework of the model is shown in Figure 6.14.

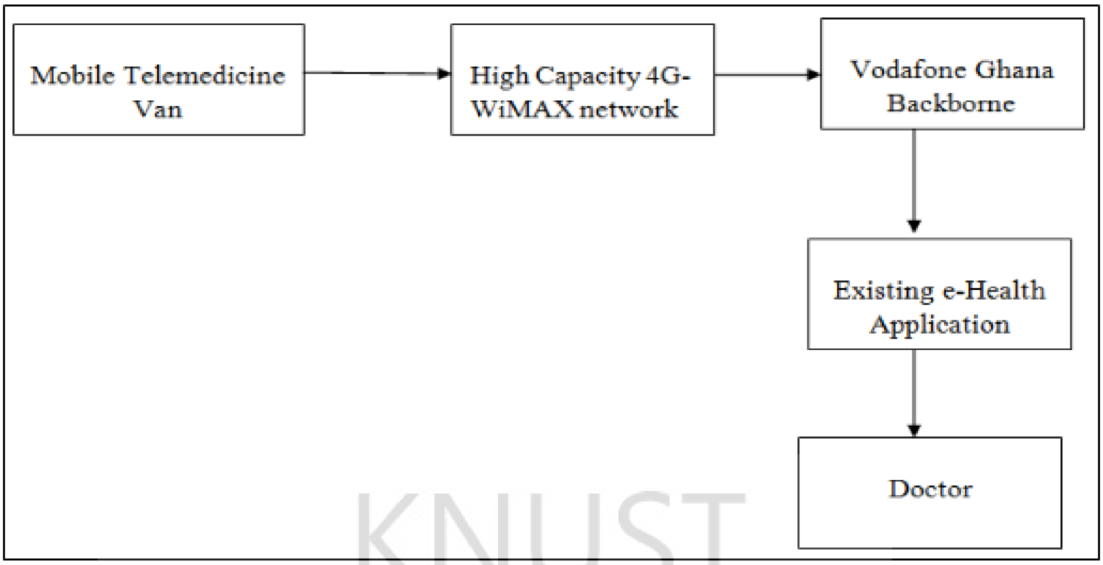

Figure 6.14: Layout of proposed design

The 4G-WiMAX network and Vodafone Ghana backbone transmission in the proposed network design will be the major block of the system network architecture. These two transmission systems will help link the various existing Telemedicine centres to the Mobile Telemedicine Vans located in other parts of the city.

The distribution of the Customer Premise Equipment which is on the Electronic Government system and the stochastic distribution of the existing Emergency Ambulance service in the city are shown in Figure 6.15.

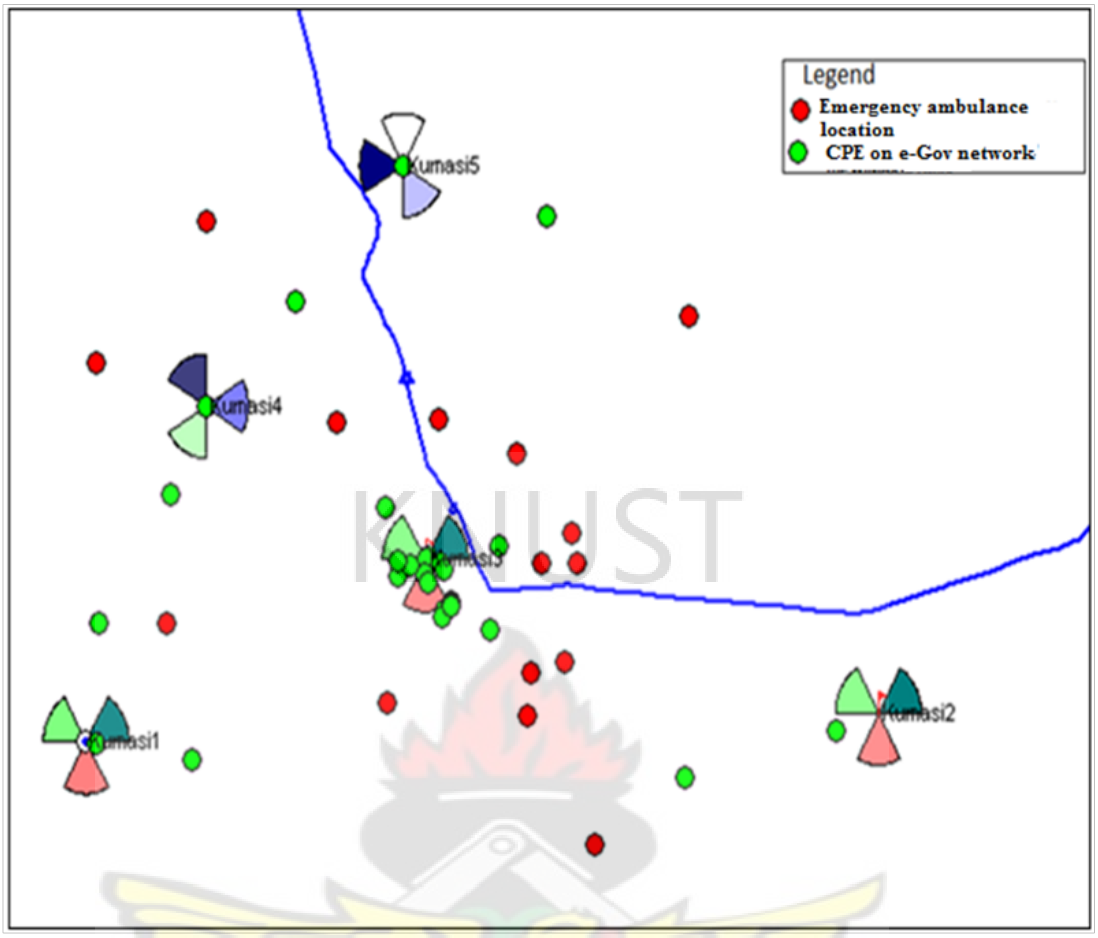

Figure 6.15: Distribution of CPE and ambulances in the existing network

From the mapping results of the ambulances in Kumasi, it can be seen that, the locations of the ambulance service lies within the existing WiMAX network. In order to be sure that the existing WiMAX can provide ubiquitous coverage for the Mobile Vans, coverage simulation and an estimation of the hand-off threshold of the network has been done. The coverage prediction for the deployed network is based on a realistic distribution of BS, CPEs on the e-Government network and the proposed mobile Telemedicine Vans as shown in Figure 6.15. The network parameters for the simulation and coverage range results are summarized in Tables 6.1 and 6.2 respectively. The recommended 4x4 MIMO configuration has been used to simulate the final radio plan in Figure 6.16.

Genex-Unet has been used to simulate the final radio network plan using an adaptive 4x4 MIMO antenna configuration. The final network plan is shown in Figure 6.16.

Table 6.1: Simulation Parameters

Resource frequency	2.5-2.53GHz
Channel Bandwidth	10MHz
MIMO Antenna Configuration	Adaptive 4x4 MIMO
Speed	80 km/h
Average users per sector	10
Fast Fourier Transform (FFT) Size	1024
Subcarrier spacing	10.93 kHz
Useful symbol time	91.4 μs
Guard time	11.4 μs
OFDMA symbol time	102.8 μs
Modulation	QPSK, 16-QAM, 64-QAM
Antenna frequency Range	2.3-2.7GHz
VSWR	$\leq$1.5
Input Impedance	50Ω
Gain	18dBi
Horizontal Beamwidth (3dB)	60°
Vertical Beamwidth (3dB)	7°
Electrical downtilt	2°
CPE antenna configuration	2T2R
Maximum power (dBm)	43
Antenna height	42m

Table 6.2: Coverage Range Simulation results in the network

CPE type	Morphology	Coverage range (km)
Indoor	Dense Urban	0.6 – 0.7
	Urban	1.0 – 1.5
	Sub urban	2.3 – 2.5
	Rural	4.8 – 5.5
Outdoor	Dense Urban	3.8 - 4.5
	Urban	4.6 – 5.2
	Sub urban	7.8 – 9.3
	Rural	13.5 – 18.5

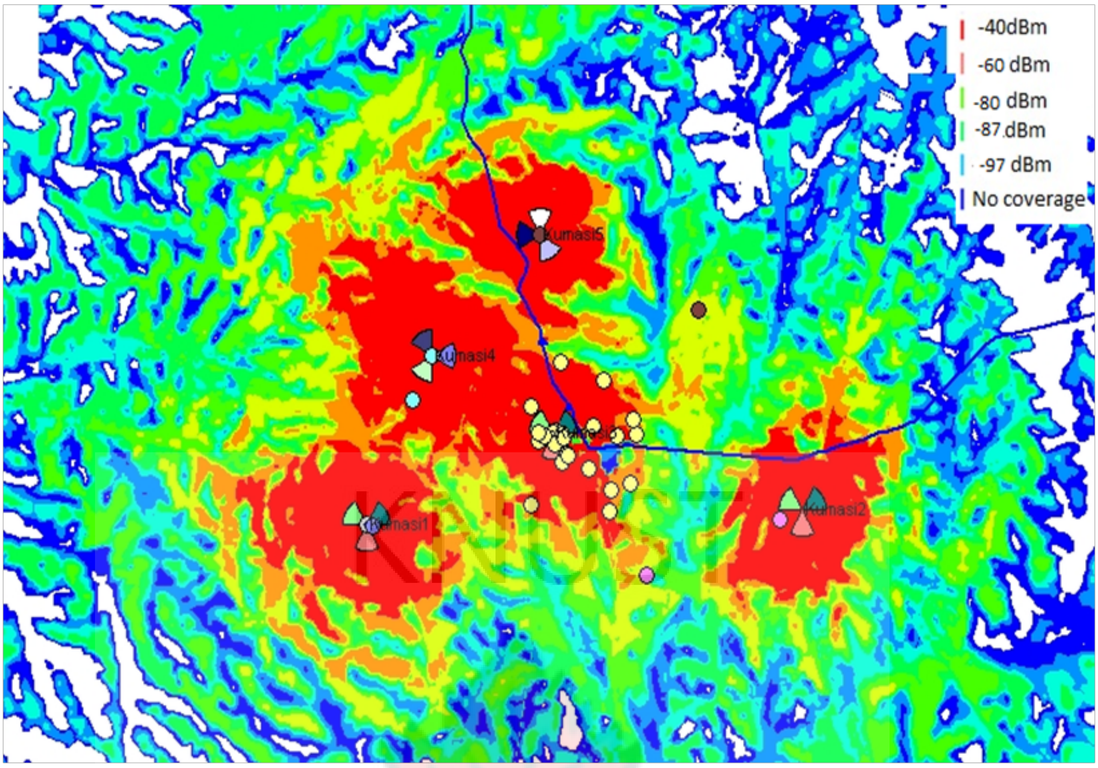

Figure 6.16: Coverage Simulation for the proposed Kumasi WiMAX network

The adaptive 4x4 MIMO antenna configuration has been seen to give a 3 dB increase in downlink/uplink coverage which reduces the number of Base Station. A simulated center and cell edge Received Signal Strength (RSS) values of -40dBm and -80dBm respectively was obtained. In order to be able to determine whether the network would be able to provide total coverage with no issues of drop in connection, the hand-off threshold of the Network was simulated with MATLAB and is shown in Figure 6.17.

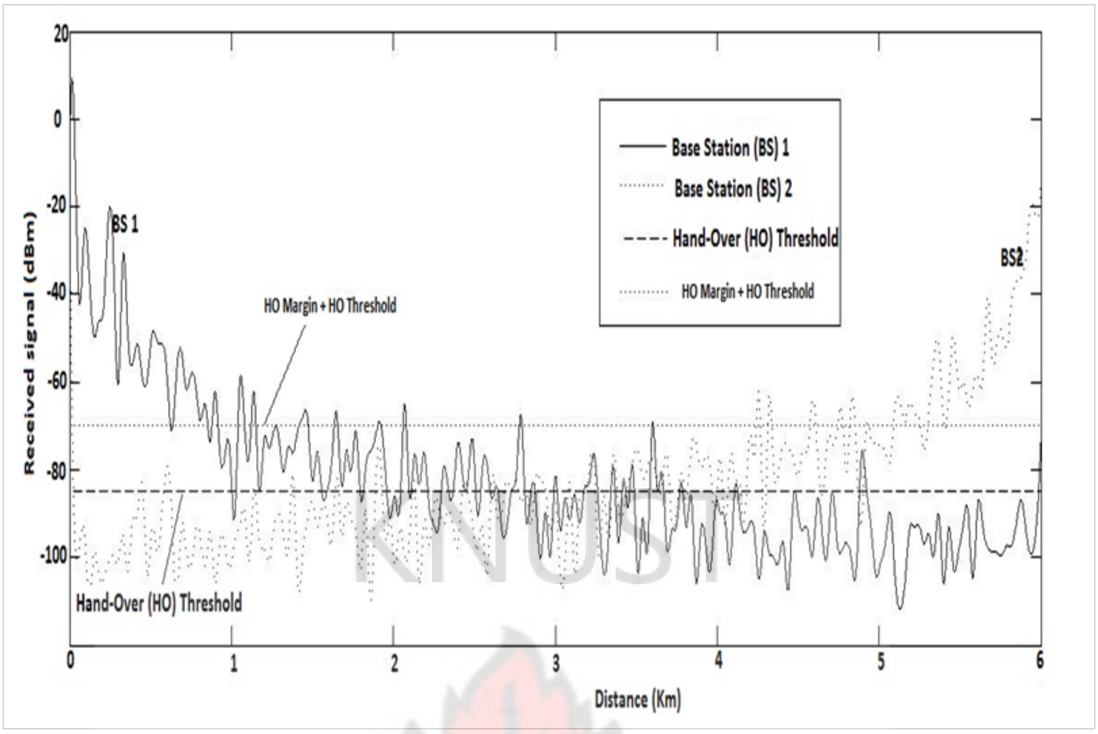

Figure 6.17: Hand-off threshold simulation

The Mobile Telemedicine Van is assumed to be travelling within Two Bases Stations, BS 1 and BS 2, which are 6 km apart. A simulated Hand-off threshold of -82dBm was obtained. The simulated cell edge RSS value of -80dBm is adequate to serve the mobile vans as they move within the WiMAX network. This value is high above the Hand-off threshold of -82dBm. This will prevent drastic BS changes and its resulting drop in network connection as the mobile Vans move in between sites. From the coverage simulation, the existing WiMAX service will offer ubiquitous coverage to the Mobile Vans in the network within Kumasi. Since the network has been designed to provide for future expansion, the WiMAX network will guarantee reliable network connection for an efficient Mobile Telemedicine system implementation.

6.4 CONCLUSION

Mobile Telemedicine services generally aim at facilitating and improving healthcare provision. The proposed Mobile Telemedicine solution in this case study is expected to help in coping with some major challenges faced by the national and regional health systems as a consequence of demographic, epidemiological and socio-cultural changes.

The proposed system design is useful and economically viable to build, deploy and operate alongside the existing pilot Telemedicine services in Kumasi. Since the design will use reliable existing nationwide WiMAX infrastructure, it will help immensely in increasing response times in cases of medical emergencies and also deliver quality healthcare to complement the efforts of the limited health professionals in the country.

REFERENCES

[1] E.T. Tchao, W.K. Ofosu, and K. Diawuo. A performance case study of electronic governance implementation in ghana with WiMAX technology. *International Journal of Computer Applications*, 71:36–42, 2013.

[2] E. T. Tchao, K. Diawuo, W. K. Ofosu, and I. Ghansah. A proposed secure network model for implementing smart grid applications in ghana with WiMAX technology. *Journal of Computer Science and Telecommunications*, 4:42–48, 2013.

[3] E.T. Tchao, W.K. Ofosu, K. Diawuo, and R. Ansah. Proposed network design for implementing mobile telemedicine in kumasi with WiMAX technology. In *IEEE International Humanitarian Technology Conference (IEEE IHTC 2014) Accepted*, 2014.

[4] K. Chaudhari, U. Dalal, and R. Jha. E-governance in rural india: Need of broadband connectivity using wireless technology. *Wireless Engineering and Technology*, 2:212–220, 2011.

[5] Ghana. A country profile. online:http:// www.accraexpat.com /pdfs/Ghana_ country_profile.pdf? accessed on 2/05/2013, 05 2013.

[6] H. S. Kumara. ICT Driven E-Governance Public Service Delivery Mechanism

in Rural Areas: A Case of Rural Digital Services (NEMMADI) Project in Karnataka, India. *Journal of Computing and ICT Research*, 4:37–45, 2011.

[7] Medium-term national development policy framework. Ghana shared growth and development agenda (GSGDA), 2010-2013. In *policy framework final draft*, 2011.

[8] The Singapore E-government Action Plan. United nations publication. online:http://unpan1.un.org, 04 2013.

[9] K. J. Bwalya and M. Healy. Harnessing e-government adoption in the SADC region: a conceptual underpinning. *Electronic Journal of e-Government*, 8: 23–32, 2010.

[10] S. Shingare, P. Shinde, D. Sarkar, P. Uttarwar, and R. Dusane. E-Governance at village level administration in rural india. In *World conference on Agricultural Information and IT, IAALD AFITA*, 2008.

[11] G. Z. Islam. Developing a model of e-governance for urban and rural areas of bangladesh. In *11th International Conference on Computer and Information Technology ICCIT*, pages 587 – 592, 2008.

[12] E-Governance. Its prospectives, opportunities and threats in nepal. In *International Conference on Computer and Information Technology*, 2008.

[13] E. Kyriacou, S. Voskarides, M. S. Pattichis, C. S. Pattichis, and R. Istepanian. Wireless telemedicine systems: An overview. *IEEE Antennas Propag. Mag*, 41:143–153, 2002.

[14] K. Shimizu, K. Yamamoto, T. Mikami, N.Hoshimiya, H. Murakami, and K. Kondo. Telemedicine using mobile satellite communication. *IEEE Trans. Biomed. Eng*, 41:488–497, 1994.

[15] V. T. Salcedo, E. M. Sanchez, H. F. Rashvand, and D. Iliescu. Ubiquitous wireless telemedicine. *IET Commun*, 2:237–254, 2008.

[16] J. Y. Chen, R. H. Shiu, C.F. Lin, and S. H. Chang. A Ka band WCDMA based LEO transport architecture in mobile telemedicine. In *In: Martinez, L., and Gomez, C. (Eds.), Telemedicine in the 21st Century*, pages 187–201, 2008.

[17] S. Laxminarayan, C. S. Pattichis, and R. S. H. Istepanian. Emerging mobile health systems. In *New York: Springer*, 2006.

[18] C. F. Lin and H. W Lee. Wireless multimedia communication toward mobile telemedicine. In *Proceedings of the 9th WSEAS International Conference*, pages 232–237, 2009.

[19] Ghana Health Service. 2012 annual report. accessed online: www.ghanahealthservice.org on 20/06/2013, 01 2013.

[20] M. Demmer, B. Du, M. Ho, M. Kam, S.Nedevschi, J. Pal, R. Patra, S. Surana, E. Brewer, and K Fall. The case for technology in developing regions. *IEEE Computer Applications*, 38:25–38, 2005.

[21] R. L. M. Ho and P. M. Aoki. Applying user-centered design to telemedicine in africa. *Journal of Telemedicine*, 6:177–182, 2002.

[22] H.S. Angela, M. Canales, J. Javier, V. Antonio, J. R. Gallego, and F. N. Julin. Performance analysis of multiplexed medical data transmission for mobile emergency care over the UMTS channel. *IEEE Trans. Inf. Technol. Biomed.*, 38:13–22, 2005.

[23] P. Hu, D. Gagliano, M. N. Bahmouth, R. D. Gunawardane, C. F. Mackenzie, W. R. Gaasch, M. P. LaMonte, Y. Xiao, and J. Cullen. TELEBAT: Shortening time to stroke treatment using ambulance telemedicine. *Journal of Stroke*, 26:67–73, 2004.

[24] M. P. LaMonte, P. Hu, W. Gaasch, R. Gunawadane, Y. Xiao, D. Gagliano, and C. Mackenzie. Design and evaluation of a real-time mobile telemedicine

system for ambulance transport. *Journal of High Speed Networks*, 32:47–56, 2008.

CHAPTER 7

CONCLUSION

In communication networks deployment, a major task is the design and optimization of the system parameters to achieve the purpose of setting up the network. The design and optimization process can be divided into:

- Choosing the system parameters: these parameters include antenna type, physical layer interface, modulation schemes, frequency range, bandwidth, number of carriers and deployment configuration.
- System performance evaluation: Once the system parameters are determined, the system performance can then be assessed in terms of error rates, outage probabilities or data throughputs, which are all inter-related.
- Optimization: Based on the system performance, some parameters might be adjusted to improve the system performance. The base station deployment can then be optimized based on the system performance obtained for each deployment/configuration.

This research has adopted formal evaluation methods to evaluate the network performance of a newly deployed WiMAX network based on the three stages stated above.

First, an initial feasibility study in the deployment area was done as part of the evaluation process. The study showed that during the initial planning processes for deploying the network with 2x2 MIMO configurations in the study area, which covers MDAs in the central parts of Accra and Tema, the effects of some key performance indicators such as Bit Error Rate, Received Total Wideband Power and Throughput were not carefully considered. These key performance indicators were used to model the effect of the different MIMO configurations on system capacity, interference and coverage as part of the configuration optimization process.

A simple step function which was derived as part of the optimization process showed that an antenna with a high number of elements and low angular spread achieves a higher directivity and greater coverage. It was discussed that, in order to reduce the initial cost of network deployment, an antenna with an optimal sidelobe suppression value greater than -30dB and 720 elements were efficient for the network deployments. These values were derived using a simple step function and was suggested as an operational guideline tool which can be used by any regulating body to specify added isolation factors to reduce overall network interference.

Furthermore, the BER performance of the configurations in the presence of multiple interfering BS was done with the adaptive 4x4 MIMO configuration which show promising performance than the deployed 2x2 configuration. An appropriate network striping technique was proposed for mitigating the low BER performance of the deployed adaptive 2x2 MIMO antenna configuration in the presence of multiple interfering sources. Even though the concept of successive cancellation is not new, the results of the proposed successive cancellation technique with an extension on MIMO systems with partial band interference was novel. The results presented by the decoding technique showed an impressive BER performance of 2x2 MIMO configurations once the acceptable Interference to Noise Ratio was exceeded. This was as a result of the virtually created wide bandwidth by the striping technique. The results indicate the possibility of the victim and the interfering Base Stations co-existing in the virtually created wide bandwidth to improve the MIMO antenna configuration performance.

Finally, a range of measurements done in the network confirmed the performance promised by WiMAX by delivering an average sector capacity of 9.62Mbps with a modulation scheme of 64-QAM. This measured average sector capacity could help support any broadband application deployment in Ghana. With WiMAX being a technology originally aimed at Line of sight (LOS) and near line of sight (NLOS) service with high modulation and the possibility of using fixed high gain directional antennas, the most impressive performance of WiMAX was realized under the study area, Ghana and hence by extension to the Sub- Saharan African environments.

7.1 MAJOR CONTRIBUTIONS

A growth in the demand for Wireless Broadband Access (WBA) technology has been seen in Ghana in the last few years. The reason for this growth can be attributed to the emergence of the use of multimedia applications, demands for ubiquitous high-speed internet connectivity, the massive growth in the wireless and mobile communications sector, and the deregulation in the telecommunications industry. WiMAX is currently being deployed in the 2,500-2,690 MHz band to help serve the ever increasing needs of broadband internet subscribers in the country. This thesis has presented analytical, simulation and field trial measurements results for a newly deployed 4G-WiMAX network in a typical dense urban Sub-Saharan African environment. The major contributions of the thesis include;

- An Interference to Noise Ratio parameter (INR) has been introduced to optimize the BER estimation model used in Section 4.4 in the presence of noise. The INR parameter was used to fit the BER results and then subsequently optimized in a striped case to create a wide virtual bandwidth in Section 4.6. The fitting INR parameter helped to improve the BER performance of the deployed 2x2MIMO configuration once the threshold of the INR was exceeded. This result is novel since the principle of successive decoding has not been extended to MIMO systems to partial band interference under the assumption of a common receive correlation matrix.

- A model for evaluating the effect of antenna radiation patterns in a practical network deployment scenario was presented. This simple step function can be used by a regulating body as a policy guideline and operational tool. The derived sidelobe level suppression values and the number of antenna elements will give network planners an idea of what practical antenna parameter values to choose. For example, a network planner could decide to choose an antenna with optimal sidelobe suppression technique with less number of elements, or an antenna with greater number of elements with adequate sidelobe suppression technique.

- An optimized radio network plan with considerations based on co-channel interference, transmission power, antenna tilt, polarization, beamwidth, and frequency reuse schemes has been presented as part of the MIMO configurations optimization process. Information on the outdoor performance of WiMAX systems in the sub region has also been provided. As at the time of writing this thesis, there has been little information on the performance of WiMAX systems under the Sub-Saharan African terrain conditions. The results produced in the evaluation may therefore serve as a guide for choosing system configurations for future network deployments in Ghana and other Sub-Saharan African countries.

- The provision of network architectures for case applications implementation; The proposed architectures when implemented will improve the efficiency of power generation and distribution, accessibility to healthcare for those in remote parts of the country and the way citizens access information.

- The analytical models and system configuration performance outcomes presented will provide radio engineers and system planners an understanding of the outdoor performance of MIMO configurations used in deploying WiMAX networks under the Sub-Saharan African environments; and be a guide for future network dimensioning and system optimization of

WiMAX networks deployed under similar environmental conditions.

7.2 RECOMMENDATION FOR FUTURE WORK

There are plans to deploy Long Term Evolution networks in the 2.6 GHz band on pilot basis in areas within the coverage areas of the deployed WiMAX systems. Since WiMAX and LTE are all OFDM-based networks, there is the need for studying spectrum sharing and coexistence scenarios of these 4G networks in the 2.6 GHz band. The impact of the Sub-Saharan environmental conditions in the deployment morphology should be studied in the modeling process. Interferences from Long Term Evolution (LTE) to Worldwide Interoperability for Microwave Access (WiMAX) systems and vice versa must be carefully investigated. Studies into the dimensioning of co-location and coexistence requirements in terms of separation requirements to specify additional isolations can be also be done.

Furthermore, the use of smaller cells was suggested as one of the means to mitigate the high levels of interference measured at some of the sites. The effect of the recommended Base Station densification on the capacity and coverage performance of MIMO configurations can be studied. The use of Pico and Femto cells as a means to mitigate the recorded high levels of interference is an emerging area of interest to radio planning engineers in the country.

A study into the effect of implementing appropriate extended intercell interference cancellation techniques on MIMO system performance for the OFDM-Based network is highly recommended in the cells which recorded higher RTWP. The effects of harmonics, downtilt and BS antenna height on the MIMO configurations can also be studied as and when a prototype is built on campus.

APPENDIX

LIST OF PUBLICATIONS FROM THE RESEARCH

[1] E. T. Tchao, W. K. Ofosu, and K. Diawuo. Radio planning and field trial measurement of a deployed 4g WiMAX network in an urban sub-saharan african environment. *In proceedings of IEEE Wireless Telecommunications Symposium, Phoenix, Arizona, April 2013. An extended version also appeared in International Journal of Interdisciplinary Telecommunications and Networking*, 5:1–10, 2013.

[2] Eric Tutu Tchao, Kwasi Diawuo, and W.K. Ofosu. On the comparison analysis of two 4G-WiMAX base stations in an urban sub-saharan african environment. *Journal of Communication and Computer*, 54:863–872, 2013.

[3] W.K. Ofosu and Eric Tutu Tchao. From the environment to the classroom: A sub-saharan african scenario. In *In Proceedings of IEEE International Conference on Teaching, Assessment, and Learning for Engineering 2014*, 2014.

[4] E. T. Tchao, W. K. Ofosu, and K. Diawuo. A performance case study of electronic governance implementation in ghana with WiMAX technology. *International Journal of Computer Applications*, 71:1–5, 2013.

[5] E. T. Tchao, W. K. Ofosu, K. Diawuo, E. Affum, and Kwame Agyekum. Interference simulation and measurements for a deployed 4G-WiMAX network in an urban sub-saharan african environment. *International Journal of Computer Applications*, 71:6–10, 2013.

[6] E. T. Tchao, W. K. Ofosu, K. Diawuo, and E. Affum. Analysis of MIMO systems used in planning a 4G-WiMAX network in ghana. *International*

Journal of Advanced Computer Science and Applications (IJACSA), 4:37–43, 2013.

[7] E. T. Tchao, K. Diawuo, W. K. Ofosu, and I. Ghansah. A proposed secure network model for implementing smart grid applications in ghana with WiMAX technology. *International Journal of Computer Science and Telecommunications*, 4:14–19, 2013.

[8] E. Affum, E.T. Tchao, K. Diawuo, and K. Agyekum. Wideband parameters analysis and validation for indoor radio channel at 60/70/80GHz for gigabit wireless communication employing isotropic, horn and omni directional antenna. *International Journal of Advanced Computer Science and Applications*, 4:292–297, 2013.

[9] E.T. Tchao, W.K. Ofosu, K. Diawuo, and R. Ansah. A proposed network design for implementing mobile telemedicine in kumasi with WiMAX technology. In *Abstract accepted. Full paper currently under review, IEEE International Humanitarian Technology Conference (IEEE IHTC), Montreal, Canada*, 2014.

	400m				500m				600m				700m				800m				900m				1km			
	location1				location 2				location 3				location 4				location 5				location 6				location 7			
	packet1	packet2	packet3	packet	packet1	packet2	packet3	packet4	packet1	packet2	packet3	packet4	packet1	packet2	packet3	packet4	packet1	packet2	packet3	packet4	packet1	packet2	packet3	packet4	packet1	packet2	packet3	packet4
Average RTT (msec)	123	171	182	251.5	133	106	106	234	340.5	240	220.5	220	124	156	206	198	154	143	128	124	154	164	169	405	132	175	220	172
Latency (msec)	61.5	85.5	91	125.8	66.5	53	53	117	170.25	120	110.25	110	62	78	103	99	77	71.5	64	62	77	82	84.5	202.5	66	87.5	110	86
Average Latency (msec)	90.9375				72.375				127.625				85.5				68.625				111.5				87.375			
Jitter (msec)	29.4375	5.4375	0.0625	34.81	5.875	19.375	19.375	44.625	42.625	7.625	17.375	17.625	23.5	7.5	17.5	13.5	8.375	2.875	4.625	6.625	34.5	29.5	27	91	21.375	0.125	22.625	1.375
Average Jitter (msec)	17.4375				22.3125				21.3125				15.5				5.625				45.5				11.375			
Throughput (Mbps)	9.62	6.71	3.4	9.02	3.2	4.1	5.5	5.1	4.8	4.12	1.2	3.11	5.3	3.45	4.6	4.71	4.1	2.34	1.4	7.6	4.02	2.11	3.11	2.08	4.65	5.6	6.7	5.9
Average Throughput (Mb	7.1875				4.475				3.3075				4.515				3.86				2.83				5.7125			
RSS (dBm)	-43	-44	-43	-42	-45	-46	-47	-46	-47	-47	-48	-48	-49	-49	-50	-50	-51	-52	-51	-52	-52	-53	-52	-54	-55	-55	-56	-58
	location 8 = 1.2km				location 9 = 1.3km				location 10 = 1.4km				location 11 = 1.5 km				location 12 = 1.6km				location 13 = 1.7km				location 14 = 1.8km			
	packet1	packet2	packet3	packet4																								
Average RTT (msec)	737	149	243.5	322.5	595.5	413	534.5	440	715.5	95	94	107	448	173.5	227.5	157.5	456	500	590	566	616.5	566.5	624	550.5	922	455.5	475	427.5
Latency (msec)	368.5	74.5	121.75	161.3	297.75	206.5	267.25	220	357.75	47.5	47	53.5	224	86.75	113.75	78.75	228	250	295	283	308.25	283.25	312	275.25	461	227.75	237.5	213.75
Average Latency (msec)	181.5				247.875				126.4375				125.8125				264				294.6875				285			
Jitter (msec)	187	107	59.75	20.25	49.875	41.375	19.375	27.875	231.3125	78.9375	79.4375	72.9375	98.1875	39.0625	12.0625	47.0625	36	14	31	19	13.5625	11.4375	17.3125	19.438	176	57.25	47.5	71.25
Average Jitter (msec)	93.5				34.625				115.6563				49.09375				25				15.4375				88			
Throughput (Mbps)	5.23	6.12	5.6	4.3	8.2	3.2	7.21	4.11	6.78	3.5	3.1	3.1	4.2	3.1	3.5	3.7	4.35	2.5	2.3	4.6	3.11	2.11	6.02	1.2	3.4	4.6	2.4	5.9
Average Throughput (Mb	5.3125				5.68				4.12				3.625				3.4375				3.11				4.075			
RSS (dBm)	-59	-60	-61	-61	-62	-63	-62	-63	-63	-64	-65	-66	-67	-67	-67	-68	-68	-68	-69	-70	-72	-71	-72	-73	-74	-74	-75	-76
	location 15 = 1.9km				location 16 = 2.0km				location 17 = 2.1km				location 18 = 2.2km				location 19 = 2.3km				location 20 = 2.4km				location 21 = 2.5km			
	packet1	packet2	packet3	packet4																								
Average RTT (msec)	456	169	169	173.5	769.5	699.5	732.5	709.5	898	663.5	952.5	635	227	789	643	317.5	1193.5	533.5	187.5	202	206.5	1093	698.5	507.5	1987	887.5	996.5	1611
Latency (msec)	228	84.5	84.5	86.75	384.75	349.75	366.25	354.75	449	331.75	476.25	317.5	113.5	394.5	321.5	158.75	596.75	266.75	93.75	101	103.25	546.5	349.25	253.75	993.5	443.75	498.25	805.5
Average Latency (msec)	120.9375				363.875				393.625				247.0625				264.5625				313.1875				685.25			
Jitter (msec)	107.0625	36.4375	36.4375	34.19	20.875	14.125	2.375	9.125	55.375	61.875	82.625	76.125	133.5625	147.4375	74.4375	88.3125	332.1875	2.1875	170.8125	163.56	209.9375	233.3125	36.0625	59.438	308.25	241.5	187	120.25
Average Jitter (msec)	53.53125				11.625				69				110.9375				167.1875				134.6875				214.25			
Throughput (Mbps)	3.2	1.11	3.1	2.1	3.4	2.23	3.2	1.62	1.32	1.89	1.65	1.74	1.65	1.83	1.43	2.05	2.05	2.01	1.89	2.11	1.95	1.65	1.89	1.89	1.67	1.11	1.02	1.34
Average Throughput (Mb	2.3775				2.6125				1.65				1.74				2.015				1.845				1.285			
RSS (dBm)	-77	-78	-79	-77	-77	-78	-79	-80	-80	-81	-82	-82	-84	-84	-85	-84	-83	-84	-85	-84	-85	-86	-87	-87	-88	-87	-87	-88
	location 22 = 2.6km				location 23 = 2.7km				location 24 = 2.8km				location 25 = 2.9km				location 26 = 3.2 km				location 27 = 3.5km				location 28 = 4.0km			
	packet1	packet2	packet3	packet4																								
Average RTT (msec)	348.5	156	156	153.5	427	271.5	300	575.5	377.5	191	180	191	527	463.5	299	393.5	368.5	167	171.5	161	281	165	165.5	171	682	568.5	473.5	463
Latency (msec)	174.25	78	78	76.75	213.5	135.75	150	287.75	188.75	95.5	90	95.5	263.5	231.75	149.5	196.75	184.25	83.5	85.75	80.5	140.5	82.5	82.75	85.5	341	284.25	236.75	231.5
Average Latency (msec)	101.75				196.75				117.4375				210.375				108.5				97.8125				273.375			
Jitter (msec)	72.5	23.75	23.75	25	16.75	61	46.75	91	71.3125	21.9375	27.4375	21.9375	53.125	21.375	60.875	13.625	75.75	25	22.75	28	42.6875	15.3125	15.0625	12.313	67.625	10.875	36.625	41.875
Average Jitter (msec)	36.25				53.875				35.65625				37.25				37.875				21.34375				39.25			
Throughput (Mbps)	1.11	1.34	1.43	1.02	0.599	0.942	0.853	0.444	0.678	1.34	1.42	1.34	0.867	0.785	0.9	0.867	0.694	0.764	0.563	0.742	0.5	0.502	0.532	0.423	0.375	0.3	0.41	0.302
Average Throughput (Mb	1.225				0.7095				1.1945				0.85475				0.69075				0.48925				0.34675			
RSS (dBm)	-88	-87	-88	-88	-87	-88	-87	-88	-89	-92	-90	-91	-94	-93	-92	-94	-95	-96	-97	-95	-99	-100	-99	-100	-102	-100	-103	-102

Figure 7.1: SAMPLE FIELD PARAMETER MEASUREMENTS DATA